2/81 | CMCRCZ 10 (2), 125-204 (1981)

ΧΗΜΙΚΑ ΧΡΟΝΙΚΑ

ΝΕΑ ΣΕΙΡΑ

CHIMIKA CHRONIKA

NEW SERIES

AN INTERNATIONAL EDITION OF THE GREEK CHEMISTS ASSOCIATION

CHIMICA CHRONIKA, NEW SERIES Volume 10, No 2, pp. 125-204 , June 1981

CHIMIKA CHRONIKA /NEW SERIES
Published by the Greek Chemists' Association
27, Kaningos Street, Athens (147), Greece

Correspondence, submission of papers, subscriptions, renewals and changes of address should be sent to Chimika Chronica, New Series, 27 Kaningos street, Athens, Greece. The Guide to Authors is published in the first issue of each volume, or sent by request. Subscriptions are taken by volume at 500, drachmas for members and 1.000 drachmas for Corporations in Greece and 28U.S. dollars to all other countries except Cyprus, where sybscriptions are made on request.
Printed in Greece by FOTOKIMENO E.P.E.
Υπεύθυνος σύμφωνα μέ τό νόμο: Παναγιώτης Ξυθάλης Κάννιγγος 27, Αθήνα (147)

CONTENTS

Chimika Chronika, New Series, 10, 127-142 (1981)

THE CONDUCTANCE BEHAVIOUR OF 1-NAPHTHALENE SULFONIC ACID POTASSIUM SALT IN DIOXANE-WATER MIXTURES

D. A. JANNAKOUDAKIS. D.K. PANOPOULOS
Laboratory of Physical Chemistry, Faculty of Physics & Mathematics, University of Thessaloniki, Greece.

(Received January 25. 1979)

Summary

Conductance measurements are reported for 1-Naphthalene sulfonic acid potassium salt in dioxane-water mixtures at 25°C in dioxane-rich region covering the range of dielectric constant $12.37 \leqslant D \leqslant 24.01$. The experimental results were analysed by means of Fuoss-Onsager-Skinner (FOS) and Graham-Kell-Cordon equations for associated electrolytes using the "y-x" method. The (FOS) equation reproduces the data with a random patern of $\Delta\Lambda$'s and the resulting values of Λ_o, K_A, $\mathring{a}_L$ and $\mathring{a}_K$ parameters are reported. The Walden product of the salt decreases with increasing dioxane content of the solvent. This hydrodynamic behaviour has been investigated by means of Fuoss-Boyd-Zwanzig theories. The $R^+_\infty + R^-_\infty$ distance (Fuoss empirical equation) is not in satisfactory agreement with $\mathring{a}_L$ and $\mathring{a}_K$ values. The failure is discussed. Zwanzig equation reproduces the walden products of the anion with an identical intercept-slope value of $\mathring{r}$ parameter, in the case of perfect sticking. In what it concerns the K^+, the two Zwanzig radii agree poorly in both cases ("stick" and "slip"). As a probable explanation, this discrepancy may be attributed to solvent microscopic structure properties and to specific ion-solvent interactions. Dioxane-Water intermolecular complexes -hydrogen bonded- form a solvation sheath around the cation, the existence of which is ignored by Zwanzig continuum model.

Key words: Equivalent conductance, association constant, Zwanzig, 1-Naphthalene sulfonic acid Potassium salt, Dioxane, Water.

Introduction

Experimental evidence from conductometric study of suitable systems has repeatedly shown that, although many properties of electrolyte solutions can be interpreted in terms of a continuum model for the solvent, others cannot. Attempts

have been made to relate association constants and ion mobilities to properties of the solvent and the solute, but all are limited in their application and can only be used under restricted conditions if the results are to have any meaning.

Association behaviour and ion mobilities are most complicated in systems where a protonic component is present and it is evident that adequate knowledge of the properties of the solvent mixtures is necessary for a meaningful discussion of the behaviour of the solution.

In this paper, we report on the conductance data of 1-Naphthalene sulfonic acid Potassium salt in Dioxane-Water mixtures over the range of dielectric constant $12.37 \leqslant D \leqslant 24.01$.

It is a part of our investigation on the conductance behaviour of sulfonic compounds -our interest being stimulated by the fact that their molecule gives a large organic ion and the lack of systematic conductometric data reported on them- in a series of mixtures of a given polar and protic solvent with a nonpolar aprotic solvent in low dielectric constants.

Unfortunately, solubility problems for this salt in Methanol prevented the extension of the measurements in Dioxane-Methanol, and Benzene-Methanol mixtures.

Dioxane-water system contains a polar hydrogen-bonding solvent and a non-polar component. It therefore presents an excellent opportunity to study ionic association and mobilities, to test the model and also to illustrate the methods of applying the theoretical analysis to conductance data. In Dioxane-rich region of the mixtures (low dielectric constant range) the calculation of the distance parameter can be obtained by three distinct methods.

While the continuum model serves to describe the electrostatic effects, however, it is found to be inadequate for the hydrodynamic properties. In our case, the Walden product, $\Lambda_0\eta$, is not constant but decreases with increasing dioxane in the mixed solvent. In such studies it is important to know if the changes observed in these properties, as dioxane is added to water, are due to the decreasing dielectric constant, to a relaxation field between ions and solvent dipoles, or to a change in solvent-ion or solvent-solvent interactions, since an inevitable weakness of any continuum theory is its inability to account for structural features. The key to understanding is to be sought in specific structural effects. A detailed picture of ion-solvent and solvent-solvent interactions is an essential prerequisite.

The date were analysed by means of Fuoss-Onsager-Skinner (FOS), Graham-Kell-Cordon (GKC), Fuoss (empirical) and Fuoss-Boyd Zwanzig (FBZ) equations. All symbols used, have their usual meaning.

Experimental Technique

1-Naphthalene sulfonic acid Potassium salt (PFALTZ and BAUER, INC. Assay-97-99%, typical) was dissolved in conductance water, filtrated to remove

insoluble impurities, recrystallized three times and dried at 115°C under reduced pressure. It was stored over phosphorous pentoxide in an evacuated desiccator.

Reagent grade 1.4-dioxane (RPE, Acs-Carlo Erba) was refluxed over metallic sodium for 12 hours. It was distilled under nitrogen through a 60-cm column; b.p. 101.1–101.3 °C; density at 25°C ranged from 1.02790–1.02809 g/ml which compares well with the best value reported by Lind and Fuoss[1].

Conductivity water was prepared by distillation of double-distilled water in an all-Pyrex-glass set. Specific conductance was less than $2 \cdot 10^{-7}$ mho/cm.

All conductance measurements were made at 25°C using an oil-filled thermostat of Leeds and Northrup Co., with an accuracy of 0.002°C.

Resistances were measured at 3000 c/sec on a Beckman conductivity bridge Type RC-18A. The cell constant, 0.027 cm^{-1} was determined by the method of Lind, Zwolenik, and Fuoss[2] and rechecked repeatedly during the work. For the measurements of dielectric constants of the various dioxane-rich mixtures a Dipolmeter WTW type DM 01, was used. Densities were measured in a Sprengel pycnometer and viscosities with an Ubbelohde-type viscometer taking the viscosity of water at 25°C as 0.008903 poise. The apparatus used for conductometric measurements permitted the solvent and solutions to be kept in an all glass completely closed system in an inert gas atmosphere at all times.

Conductance runs were made by dilution within the cell of a definite volume of the most concentrated solution. After immersion in the thermostat for 10 minutes the content of the cell was shaken to eliminate the effects of temperature gradients within the solution and left in the thermostat until resistance readings were constant. This usually required 20–25 minutes more. The measured resistances for all runs were in the range of 550–3.100 Ohms which is a convenient range of resistance for precise electrical measurements.

Data treatment, results and discussion

The properties of the dioxane-water mixtures used as solvents are given in Table I. The data were analysed on a DIEHL — Alphatronic Computer by means

TABLE I. *Properties of solvent mixtures at 25°C.*

System N°	Wt % Dioxane	mole-% Dioxane	d (g/ml)	$10^2\eta$ (poise)	D
1.	64.33	26.94	1.0369	1.9406	24.01
2.	69.40	31.68	1.0371	1.8988	19.84
3.	74.33	37.19	1.0363	1.8175	16.11
4.	79.28	43.89	1.0358	1.7108	12.37

of Fuoss-Onsager-Skinner (FOS)[3] three-parameter conductance equation for an associated salt.

$$\Lambda=\Lambda_O—S\ c^{1/2}\ \gamma^{1/2} + E'\ c\ \gamma\ \ln\ (6E_1'\ c\ \gamma) + L\ c\gamma—K_A'\ c\gamma\ f^2\ \Lambda \quad (1)$$

which symbolically may be written as

$$\Lambda=\Lambda_O—\Delta_S-|\Delta_E| + \Delta_L—\Delta_K \qquad (1,a)$$

Where Δ_S is the decrease in conductance due to the limiting Onsager terms. Δ_E is the decrease due to the transcendental terms of order clnc from the relaxation field. Δ_L is the increase due to linear terms from the same source and Δ_K is the decrease due to ionic association. For analysis of association we have adopted the "y-x" method. because association is marked. and K_A can be determined to good precision by this method.

Equation (1) can be rearranged[4] to give

$$\Lambda'=\Lambda-\Lambda_O + S\ c^{1/2}\ \gamma^{1/2}—E'c\gamma\ \ln\ (6\ E_1'\ c\gamma \qquad (2)$$

$$\Lambda'/c\gamma = L-K_A\ f^2\ \Lambda \qquad (3)$$

$$y=\Lambda'/c\gamma \qquad (4)$$

$$x=f^2\ \Lambda \qquad (5)$$

$$y=L-K_A\ x \qquad (6)$$

Assuming $y=\Lambda'/c\gamma$ to be a linear function of $x=f^2\Lambda$, the $L_{(a)}$ and K_A can then be evaluated from (6). a form which is of course amenable to treatment by the method of least squares. The computer first evaluates an approximate. γ, from[4]

$$\gamma=\Lambda/[\Lambda_O—S\ (\Lambda/\Lambda_O)^{1/2}\ c^{1/2}] \qquad (7)$$

using a Λ_O estimated from the phoreogram .

It then operates on equations (2-6) and does a least squares treatment on (6) calculating the $L_{(a)}$ and K_A. It finds new γ using the equation.

$$\gamma=\Lambda/[\Lambda_O — S\ c^{1/2}\ \gamma^{1/2} + E'c\gamma\ln\ (6E_1'\ c\gamma)+L\ c\gamma] \qquad (8)$$

This process is iterated until the condition

$$|\gamma_{in} — \gamma_{out}| < 5\cdot10^{-5}$$

is satisfied. The computer perfoms this series of calculations for a set of Λ_O values calculating and printing the correlation coefficient $r_{x,y}$ of the "y-x" line for each Λ_O, originally using I or 2 Λ_O unit increments. By means of correlation coefficient and "y-x" plots we select the Λ_O value which gives the best fit and we repeat the whole calculation with increments 0.01 Λ_O units. At this point machine calculates, also, $\Lambda_{(calcd)}$ obtained from eq.(1) on substituting the given concentrations and the values of the three constants which were obtained from the computer analysis of the data, $\Delta\Lambda = [\Lambda_{(obsd)} — \Lambda_{(calcd)}]$ and the standard deviation of $\Delta\Lambda$'s

$$\sigma_\Lambda^2 = \Sigma\ [\Delta\Lambda i\ —\ \Delta\Lambda]^2\ /\ (n-3) \qquad (9)$$

selects Λ_O, L, K_A which minimize the standard deviation printing the original (C,Λ) input, Λ_O, L, $\mathring{a}_L$, K_A, x, y values, $r_{x,y}$, σ_Λ, γ and f for each concentration, the limits

of K_A and $\mathring{a}_L$ and the terms Δ, of eq (1) or (1,a) for graphical purposes which are useful in certain cases.

The data were analysed, also, by the equation

$$\Lambda/F = \Lambda_O - (K_A/\Lambda_O) \cdot (f^2c\ \Lambda^2/F^2) \qquad (10)$$

suggested by Graham, Kell and Cordon[4,5] a-g

Equation (10) can be rearranged to give

$$y = \Lambda/F \qquad (11)$$

$$x = f^2c\ \Lambda^2/F^2 \qquad (12)$$

$$y = \Lambda_O - (K_A/\Lambda_O)x \qquad (13)$$

Eq. (13) is amenable to treatment by the method of least squares giving the values of Λ_O directly as the intercept and K_A from the slope K_A/Λ_O. The computer first evaluates an approximate γ, from (7) using a Λ_O estimated from the phoreogram. It then operates on eq. (11-13) and does a least squares treatment on (13) calculating Λ_O and K_A. The computer repeats the calculation with each new value of Λo obtained several times until the same value of Λ_O, K_A are obtained. At this point machine prints Λ_O, K_A, x, y values and the correlation coefficient $r_{x,y}$ of the "y-x" line.

Conductance data for the various systems studied and $\Delta\Lambda = [\Lambda_{(obsb)} - \Lambda_{(calcd)}]$, the difference between the measured Λ and that calculated from the theoretical equation (1), are summarised in Table II.

TABLE II. *Equivalent conductance of 1-Naphthalene sulfonic acid Potassium salt in Dioxane-Water mixtures at 25°C.*

(c: moles/l ; Λ : Ohm^{-1}cm^{2}equiv^{-1})

10^4c	Λ	$10^3\Delta\Lambda$	10^4c	Λ	$10^3\Delta\Lambda$
	D= 24.01			D= 19.84	
6.0714	34.1845	24	5.0000	30.8748	1
7.0833	33.7593	—19	7.0833	29.7945	—14
8.0952	33.4081	—13	8.0952	29.3574	— 1
8.9474	33.1209	—20	8.9474	29.0284	24
10.0000	32.8008	—14	10.0000	28.6335	32
10.9677	32.5458	15	10.9677	28.2280	—46
12.1429	32.2414	34	12.1429	27.8516	—32
13.0769	31.9886	19	13.0769	27.6159	36
14.7826	31.5425	—24			
	D=16.11			D=12.37	
7.0833	24.2997	—11	5.0000	17.6603	
8.0952	23.6991	18	6.0714	16.7611	
8.9474	23.2189	4	7.0833	16.0604	
10.0000	22.6871	1	8.0952	15.4440	——
10.9677	22.2392	— 7	8.9474	14.9983	
12.1429	21.7364	—28	10.0000	14.5365	
13.0769	21.4103	24	10.9677	14.1201	

In Fig. 1., the ratio Λ/Λ_o (reduced conductance) is plotted against $\kappa = (c/D)^{1/2}$, the Debye-Hückel parameter. The corresponding limiting tangents, Fig. 1. (a, b, c, d), are given by the equation[6].

$$\Lambda/\Lambda_o = 1 - (54.7/D + 1.640/\Lambda o\eta)\,(10^{8}\kappa) \qquad (14)$$

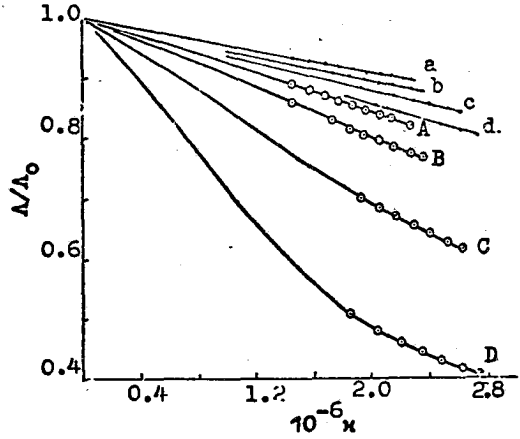

FIG. 1. *Normalized conductance curves and corresponding limiting tangents for* $C_{10}H_7SO_3K$ *in Dioxane-Water mixtures for the range* $12.37 \leqslant D \leqslant 24.01$.
(A,a : 24.01; B,b : 19,84; C,c : 16,11; D,d : 12,37).

Negative deviations from the limiting law of the conductance mean that, ion association is sufficient to pull each curve below its corresponding limiting tangent; with the decrease of dielectric constant, the curves become progressively steeper e.g. equivalent conductance decreases steadily more rapidly with increasing concentration. This means that association of the ions to pairs increases rapidly once the dielectric constant of the solvent drops.

Fig. 2. shows y vs.x plots for this Λ_o value which minimizes the standard deviation

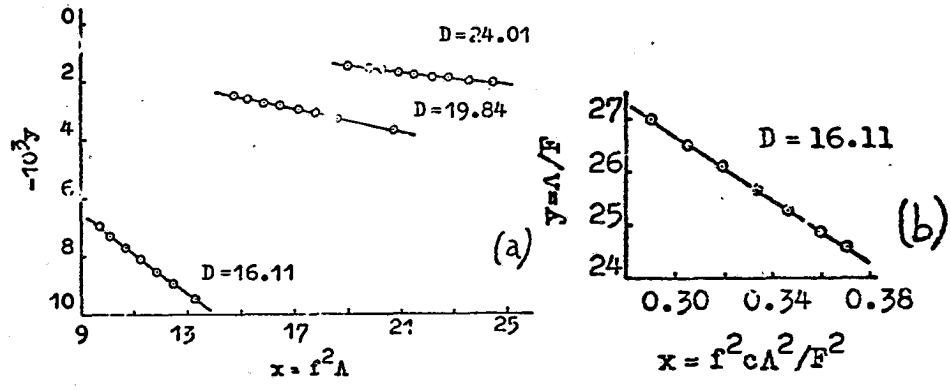

FIG. 2. *Application of "y-x" method to* $C_{10}H_7SO_3K$ *in Dioxane-Water mixtures [a : Eq.(1); b : Eq.(10)].*

of $\Delta\Lambda$'s in each mixture and we can see that the slopes increase with decreasing dielectric constant. Generally, as the dielectric constant increases, the "y-x" plot becomes increasingly sensitive to the trial value of Λo and simultaneously becomes nearly horizontal as K_A decreases. The sensitivity to experimental error is also considerably increased[4].

The conductance parameters derived for both equations (1) and (10) are summarised in Table III in which are also given the standard deviations, σ_Λ, of

TABLE III. *Derived conductance parameters for 1-Naphthalene sulfonic acid Potassium salt in Dioxane-Water mixtures at 25°C.*

Λ_O: Ohm^{-1}cm^{2}equiv.$^{-1}$; K_A: ml.mole^{-1}; $\mathring{a}$: $\mathring{A}$ $\Lambda_O\eta$: Ohm^{-1}.cm^{2}equiv.$^{-1}$P)

D	Λ_O	K_A	$\mathring{a}_L$	σ_Λ	$\Lambda_O\eta$	$r_{x,y}$	Eq.
24.01	38.41	104.73±10.28	4.54±0.98	0.0265	0.7454	—0.9907	(1)
	38.21	113.31			.7415	.9986	(10)
19.84	35.94	192.69±12.48	4.06±0.59	.0358	.6824	.9967	(1)
	35.91	253.34			.6819	.9993	(10)
16.11	34.62	717.86±15.37	4.03±0.30	.0223	.6292	.9997	(1)
	35.51	1,048.52			.6454	.9996	(10)
12.37	———	———	———	———	———	———	(1)
	34.78	5,129.82			.5950	.9994	(10)

$\Delta\Lambda$'s $\Lambda_O\eta$ products, the correlation coefficient $r_{x,y}$ of the "y-x" line for this Λ_O value which minimizes the standard deviation of $\Delta\Lambda$'s.

Figure 3 (a,b,c) shows the dependence on dielectric constant of the various terms, Δ, in the conductance equation (1) or (1,a). These curves serve to illustrate the transition from the case of moderate to pronounced association and also to show the shift in control from long range to short range interionic forces as the dielectric constant is decreased. All the Δ- terms increase numerically but Δ_K - term increases at a far more rapid rate, crosses Δ_S - term and finishes by controlling the course of the conductance-concentration curve in the usual range of concentration. In Fig. 3 (c), (D = 16.11), the difference between Δ_E and Δ_T is small with respect to Δ_K so that a completely satisfactory value of K_A could have been obtained by simultaneous neglect both of these higher terms. So, the dirived conductance parameters by eq. (10) for D, 16.11 and 12.37 could be more realistic.

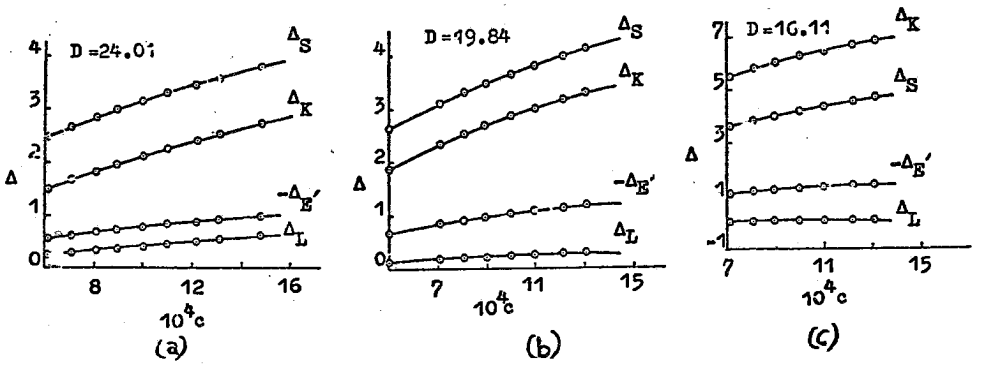

FIG. 3. *Dependence on dielectric constant of the various terms in the conductance equation (FOS).*

As the dielectric constant is lowered by adding dioxane to the solvent, the association constant increases approximately exponentially with reciprocal dielectric constant as shown in Fig. 4. in which the point for D = 12.37 is omitted

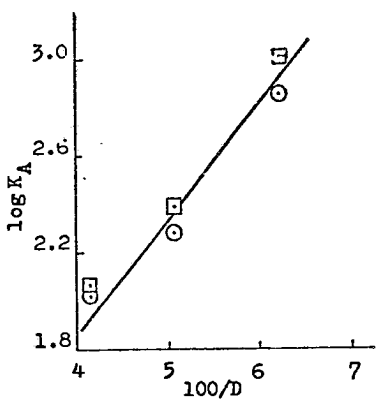

FIG. 4. *Dependence of association constant, K_A, on dielectric constant.*
○ = *values of logK_A obtained by analysing the data by Eq.(1).*
□ = *data obtained by the approximate Eq.(10).*

because it falls out of the experimental curve. Eventually, at this sufficiently low dielectric constant, the effects of association higher than pairwise must be included in the analysis. In order to obtain another experimental value of the distance parameter, from the slope of the logK_A - 1/D plot we consider the points with K_A estimated by eq.(1) for D values 24.01 and 19.84 and by eq.(10) for D value 16.11. The result is $\mathring{a}_k$ = 4.89 a value somewhat larger than those obtained from the values of L(a) derived by the "y-x" plots. It is a satisfactory agreement for the center-to-center distance of the ions taking in account that the L-values become uncertain

when association is marked as in our case. So, we can say that the system $C_{10}H_7SO_3K$ - dioxane- water is described by the (FOS) approach.

Over the D range covered, the Walden product, $\Lambda_o\eta$, (Table III) decreases as dioxane-content increases; That is, there appear to be a correlation between the Walden product and the dielectric constant. The decrease in the mobility of some ions produced by the addition of organic solvents to water has been attributed to a solvent relaxation effect. A moving ion orients the solvent dipoles around it, and these can relax again into a random distribution only after the ion has passed. Such a re-orientation requires a finite relaxation time (τ) of the order of 10^{-11}s. during the course of which the attendant electrostatic field in the medium opposes the ion's movement. This phenomenon of solvent-dipole relaxation was originally described by Born[7]. Fuoss[8] later noticed the dependence of the Walden product, $\Lambda_o\eta$, on the dielectric constant and in a heuristic argument suggested a semi-empirical expression from which the classical Stokes' radius, R, may be derived

$$R = R_\infty + s/D \qquad (15)$$

$$RD = s + R_\infty D \qquad (15\alpha)$$

where, S is an empirical constant for a given ion-solvent system, and R_∞ is the hydrodynamic radius of the ion in an hypothetical medium of infinite dielectric constant (where the electrostatic forces vanish). Boyd[9] showed that the effect of dielectric relaxation on ionic motion can be treated theoretically. Zwanzig[10] in a more rigorous derivation, taking into account the fact that some of the solvent near the ion is dragged along by viscous forces and does not need to be oriented, calculated the dielectric force which must be added to that produced by viscous drag.

Rearranging terms in his theoretical equation, it gives[11,12].

$$\frac{z^2eF}{\lambda_o\eta} = A_U\pi r + \frac{A_D z^2}{r^3}\cdot\frac{e^2(\varepsilon_o - \varepsilon_\infty)}{\varepsilon_o(2\varepsilon_o+1)}\cdot\frac{\tau}{\eta} \qquad (16)$$

With $A_U = 6$ and $A_D = \frac{3}{8}$ for perfect sticking

and $A_U = 4$ and $A_D = \frac{3}{4}$ for perfect slipping

Inserting numerical constants and r in Å it becomes

$$\frac{15.459}{\lambda_o \eta} = 18.84 \overset{o}{r} + \frac{8.64}{\overset{o}{r}^3} \cdot \frac{10^{12}(\varepsilon_o - \varepsilon_\infty)}{\varepsilon_o(2\varepsilon_o + 1)} \cdot \frac{\tau}{\eta} \qquad (17)$$

or $$L^* = 18.84 \overset{o}{r} + \frac{8.64}{\overset{o}{r}^3} \cdot P^* \qquad (17\alpha)$$

for perfect sticking and

$$\frac{15.459}{\lambda_o \eta} = 12.56 \overset{o}{r} + \frac{17.28}{\overset{o}{r}^3} \cdot \frac{10^{12}(\varepsilon_o - \varepsilon_\infty)}{\varepsilon_o(2\varepsilon_o + 1)} \cdot \frac{\tau}{\eta} \qquad (18)$$

or $$L^* = 12.56 \overset{o}{r} + \frac{17.28}{\overset{o}{r}^3} P^* \,, \qquad (18\alpha)$$

for perfect slipping, where:

τ: is the dielectric relaxation time for the solvent dipoles and

$\varepsilon_o, \varepsilon_\infty$ are static and limiting high-frequency dielectric constants of the solvent respectively.

Plots of L* versus the solvent function P* must be linear[10,b] and some hydrodynamic radius can be calculated from both intercept and slope. A quantitative test of eq.(16) may be obtained by comparing the value of $\overset{o}{r}$ from the slope and intercept of the straight line by a least squares treatment. The ionic conductance at infinite dilution[13] in pure water at 25°C $\lambda_o(K^+) = 73.50$. Λ_o of $C_{10}H_7SO_3K$ in pure water at 25°C has been found by us to be 114.8. From these values the transport numbers are $t_{K^+} = 0.640$, $t_{C_{10}H_7SO_3^-} = 0.360$. If we assume that the transport number is independent of composition in dioxane-water mixtures (probably the weakest assumption), $\lambda\overset{+}{o}\eta$ and $\lambda\bar{o}\eta$ can be calculated for these mixtures and Stokes radii R^+, R^- can be calculated from the values of $\Lambda_o\eta$. These values are summarised in Table IV. A test of eq.(15) is shown in Fig. 5 where R^+D

TABLE IV. *Limiting single ion conductance-viscosity products and Hydrodynamic Radii of the salt ions in Dioxane-Water mixtures.*

D	$\lambda_o^+ \eta_o$	$\lambda_o^- \eta_o$	R^+	R^-	R^+_{calcd}	R^-_{calcd}	Eq
24.01	0.477	0.268	1.718	3.058	1.730	3.076	(1)
19.84	0.437	0.246	1.875	3.331	1.847	3.285	(1)
16.11	0.413	0.232	1.984	3.532	2.003	3.562	(10)

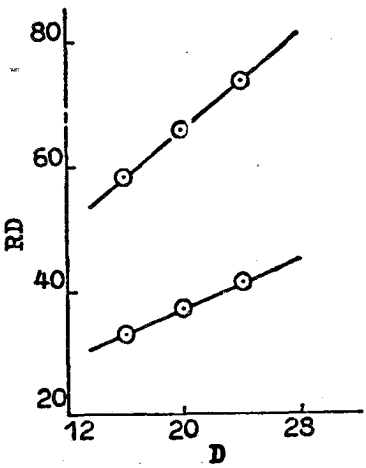

FIG. 5. *Dependence of classical Stokes radius on dielectric constant (anion: upper plot; cation: lower plot).*

and R^-D are plotted against D. The plots are linear and R^+, R- can be reproduced by the equations

$$R^+ = 1.17 + \frac{13.39}{D} \quad \text{and} \quad R^- = 2.09 + \frac{23.80}{D}$$

as shown by the values of $R^+_{(calcd)}$ and $R^-_{(calcd)}$ given in the last columns of Table IV. The center-to-center distance of the ions is $\mathring{a}_\Lambda = R^+_\infty + R^-_\infty = 3.26$ Å . This value is not in a satisfactory agreement with $\mathring{\alpha}_L$, $\mathring{\alpha}_K$ values. We have to recall that the polar component of our solvent mixtures introduces the complication of solvent composition near an ion and thus makes impossible any estimate of $\mathring{\alpha}$ by extrapolation of hydrodynamic radius to infinite dielectric constant. R_∞ is the radius of the sphere hydrodynamically equivalent to the ion if Stokes' model were valid and hydrodynamic friction were the only force to be overcome by the external field in order to produce ionic migration.

It was considered of interest to examine the applicability of Zwanzig's equation to dioxane-water mixtures, to investigate the retarding effect resulting from the relaxation of solvent dipoles around a moving ion. The necessary solvent parameters, which are interpolated values from data of G. Atkinson and Y. Mori[10,b] are summarised in Table V. Fig. 6. shows the Zwanzig plot for both cation and anion. Both plots are good straight lines. The linearity in both figures 5 and 6 means that solvent behaves like an ordinary liquid over the range of dielectric constant used[14] showing, also, a drag on the ions due to relaxation of solvent dielectric as ions move through it.

TABLE V. *Water-Dioxane Parameters (25°C)*

Wt% Dioxane	ε_o	ε_∞	$10^{12}\tau\eta$	$10^2\eta$	$P^* = \frac{10^{12}\tau D}{\eta}$	$\frac{\varepsilon_o-\varepsilon_\infty}{\varepsilon_o(2\varepsilon_o+1)}$
64.33	24.01	3.298	23.113	1.941	20.955	
69.40	19.84	3.141	23.916	1.899	26.057	
74.33	16.11	3.009	23.628	1.818	31.816	

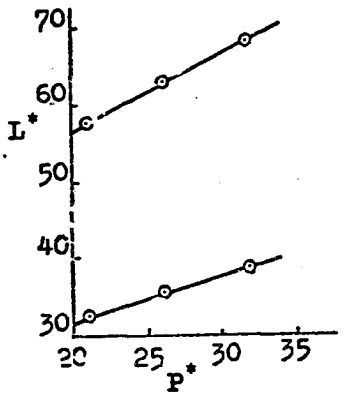

FIG. 6. *A plot of L* for both anion and cation versus the solvent function P*. (anion: upper plot; cation: lower plot).*

Table VI gives the resulting radii of both ions for the cases of perfect sticking and slipping, by a least squares treatment of eqs.(17,a), (18,a) respectively.

TABLE VI. *Radii Comparison (A°)*

Ion	Perfect sticking $\overset{o}{r}$ (intercept)	$\overset{o}{r}$ (slope)	Perfect slipping $\overset{o}{r}$ (intercept)	$\overset{o}{r}$ (slope)
$C_{10}H_7SO_3^-$	2.17	2.19	3.25	2.76
K^+	1.22	2.66	1.83	3.35

For the $C_{10}H_7SO_3^-$ anion the slope and intercept radii values are in very good agreement for the case of perfect sticking; With this $\mathring{r}$ value eq. (17) reproduces the $\lambda_0^- \eta$ experimental products of Table IV. In the case of perfect slipping $\mathring{r}$ slope-intercept values are close enough to each other. For their greater values compared with those of perfect sticking case we recall that the perfect slipping boundary condition allows greater relative motion between the ion and the surrounding solvent and thus increases the extent of dielectric friction. Dielectric friction is smaller in the case of perfect sticking since the solvent dipoles in the immediate neighborhood of the ion move together with it.

For the K^+ ion the two radii (intercept-slope) agree poorly in both cases (perfect "stick" and "slip"). It is recalled that in most cases the two radii are far from equal, indicating that the theory does not account quantitatively for mobility changes. Zwanzig theory is most successful for large organic ions in aprotic media where solvation is likely to be minimal and where viscous friction predominates over that caused by dielectric relaxation. The descrepancies become more striking the smaller the ionic radius is and the theory breaks down whenever the relaxation term becomes large i.e. for solvents of high P*[11] Limitations in continuum theory have led to the thought that the key to understanding is to be sought in specific structural effects. An inevitable weakness of any continuum theory is its inability to account for structural features.

Infrared and nuclear magnetic resonance studies[15,16] indicate that water and dioxane interact strongly. The non-aqueous component, 1,4-dioxane, contains two separated hydrogen-bonding sites; because of the inductive effect of the methylene groups the negatine charge on an oxygen atom is greater in the dioxane molecule than in water molecule, and further, a dioxane molecule can induce in a water molecule, hydrogen-bonded to it, an increased negative charge on the oxygen atom and a decreased positive charge on the hydrogen atoms[12]. Generally, mixtures of dioxane and water appear to form intermolecular hydrogen-bonded complexes of various possible structure[17,18,19].

Whatever the case may be in our mixtures, we shall find these intermolecular complexes immobilized to a considerable extent around the K^+ cations with the oxygen atoms (with increased negative charge) pointing inward causing an increased primary solvation, the existence of which Zwanzig-theory ignores. Consequently the difference between $\mathring{r}$ (slope) and $\mathring{r}$ (intercept) is not too disturbing; that is, the discrepancy between the two (intercept-slope) radii of K^+ could be attributed (as a probable explanation of this divergencies) to a solvation sheath due to specific solvent microscopic properties. This solvation leads to smaller dielectric friction and enhanced mobility[20] as it is shown in Fig. 7. where the failure of Zwanzig-continuum model to predict the dependence of mobility on solvent dielectric properties is obvious. Experimental K^+ mobility for D = 24.01 is much higher than this predicted by the theory for a crystal radius value of 1.33 Å (Pauling) or 1.49 Å (x-rays). In short, it is the case where Zwanzig-theory may be reminding that the concept of an ion radius in a hydrogen bonding solvent and where solvation is present is not an easily defined parameter.

Conversely, around the anions, we shall find intermolecular complexes

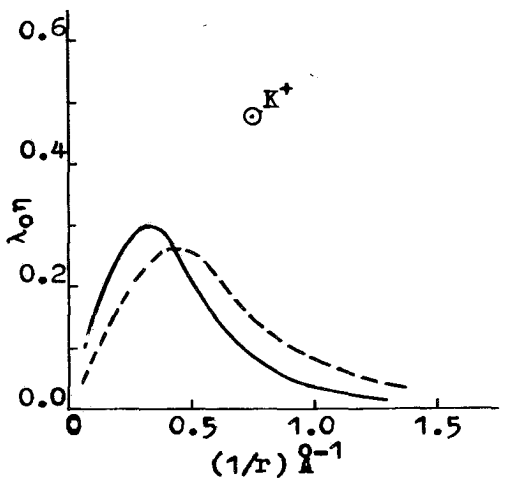

FIG. 7. *Ion mobilities in Dioxane-Water mixture of* ε_o*=24.01 against reciprocal crystal radius. Mobilities calculated are represented by the full curve (eq. 18.*$\hat{d}$*-slipping) and the dashed curve (eq. 17.*$\hat{d}$*-sticking).*

oriented with their hydrogen atoms (with decreased positive charge) adjacent to the anions and the primary solvation of the anions is likely to be minimal. Also, in the case of bulky anions viscous friction predominates over that caused by dielectric relaxation.

Although Zwanzig seems to assume that the $\hat{r}$ value of his equation is identical with the ion radius, "it would be very startling if this turned out to be true[14].

It has been suggested that this $\hat{r}$ parameter could be interpreted as a distance beyond which the solvent is no longer affected by the ion field[10,b].

Fuoss-Boyd-Zwanzig theory although relates the deviations from the Walden rule to the independently measurable solvent parameters and also introduces the concept of a hydrodynamic character to the solvent whose properties are affected by the presence of ions, it is based on a continuum model for the solvent using its macroscopic properties to describe an effect that has its origin in the microscopic nature of the solvent near the ions. Also, this theory completely ignores the possibility for a change in the size of the moving ion owing to changes in solvation. The ion is treated as a rigid sphere of radius r moving with a steady state velocity through a viscous incompressible dielectric continuum. Evidently, further developments of the Zwanzig equation are desirable and the next step of the problem is set for the theoretician: to include in the theory the discrete structure of the solvent and to calculate the distribution of a mixed solvent around ions dissolved in it; it has become clear that the sphere-in-continuum model has reached the limits of its developments. On continuum theory, 'specific ion-solvent

Περίληψη

Ἀγωγιμομετρική συμπεριφορά τοῦ 1-Ναφλαλινο-σουλφονικοῦ Καλίου σέ ὑδατο-διοξανικά διαλύματα.

Μελετήθηκε ἡ ἀγωγιμομετρική συμπεριφορά τοῦ 1-Ναφθαλινο-σουλφονικοῦ Καλίου σέ ὑδατοδιοξανικά διαλύματα στούς 25°C στήν περιοχή διηλεκτρικῆς σταθερᾶς $12.37 \leqslant D \leqslant 24.01$ καί παρέχονται οἱ φυσικές ἰδιότητες τοῦ διαλυτικοῦ μέσου γιά τήν περιοχή αὐτή τῆς διηλεκτρικῆς σταθερᾶς.

Τά πειραματικά δεδομένα ἀναλύθηκαν μέ τίς ἀγωγιμομετρικές ἐξισώσεις Fuoss-Onsager-Skinner (FOS) καί Graham-Kell-Cordon. Βρέθηκαν οἱ τιμές τῶν ἀγωγιμομετρικῶν παραμέτρων: ἰσοδύναμης ἀγωγιμότητας σέ ἄπειρη ἀραίωση, Λ_0 καί τῆς σταθερᾶς συζεύξεως, K_A, τοῦ ἄλατος. Τά πειραματικά ἀγωγιμομετρικά δεδομένα ἀναπαράγονται μέ ἱκανοποιητική ἀκρίβεια ἀπό τήν ἐξίσωση (FOS). Ἡ ἰονική παράμετρος, $\mathring{a}$, προσδιορίζεται ἀπό τήν ἐξίσωση (FOS) καί ἀπό τήν κλίση τῆς γραμμικῆς σχέσεως $\log K_A$—1/D. Οἱ δύο τιμές $\mathring{a}_L$, $\mathring{a}_K$ βρίσκονται σέ ἱκανοποιητική συμφωνία μεταξύ τους. Τό ἄθροισμα τῶν ἀκτίνων Stokes τῶν ἰόντων, $R^+_\infty + R^-_\infty$ βρίσκεται σέ ἀσυμφωνία μέ τίς τιμές $a°_L$. $a°_K$. Ἡ ἀσυμφωνία αὐτή συζητεῖται μέ ἱκανοποιητικό τρόπο.

Παρατηρήθηκε ὅτι τό γινόμενο Walden ἐλαττώνεται μέ τήν αὔξηση τῆς περιεκτικότητας τοῦ διαλύτη μέ διοξάνιο. Ἡ ὑδροδυναμική αὐτή συμπεριφορά τοῦ ἄλατος μελετήθηκε σύμφωνα μέ τίς θεωρητικές ἀπόψεις καί ἐξισώσεις τῶν Fuoss-Boyd-Zwanzig προκειμένου νά διαπιστωθεῖ ἡ ἐπίδραση τοῦ φαινομένου Born-Fuoss-Boyd-Zwanzig (τῆς διηλεκτρικῆς τριβῆς τῶν διπόλων τοῦ διαλύτη) στήν κίνηση τῶν ἰόντων. Διαπιστώθηκε ὅτι γιά τό ἀνιόν τοῦ ἄλατος ἡ ἐξίσωση Zwanzig-perfect sticking δίνει τήν ἴδια τιμή τῆς παραμέτρου $\mathring{r}$ τόσο ἀπό τήν κλίση ὅσο καί ἀπό τήν τεταγμένη ἐπί τήν ἀρχή τῆς εὐθείας πού παριστάνει καί ἡ ἐξίσωση ἀναπαράγει τά πειραματικά γινόμενα Walden τοῦ ἀνιόντος μέ μεγάλη ἀκρίβεια· ἐνῶ γιά τό κατιόν τοῦ K παρατηρεῖται μεγάλη ἀσυμφωνία. Ἡ ἀσυμφωνία αὐτή ὀφείλεται πιθανῶς στήν ἔντονη ἐπιδιαλύτωση τῶν κατιόντων τοῦ K ἀπό τά σχηματιζόμενα μέ δεσμούς ὑδρογόνου ἐνδομοριακά συζεύγματα τῶν μορίων τοῦ μικτοῦ διαλύτη. Ὑπενθυμίζεται ὅτι ἡ θεωρία Zwanzig ἀγνοεῖ τήν μεταβολή τῆς ἀκτίνας τῶν ἰόντων λόγω ἐπιδιαλυτώσεως.

References

1. Lind J.E., J.R., and Fuoss R.M.: *J. Phys. Chem.*, **65**, 999 (1961).
2. Lind J.E., J.R., Zwolenik J.J. and Fuoss R.M.: *J. Phys. Chem.*, **81**, 1557 (1959).
3. Fuoss R.M., Onsager L., Skinner J.F.: *J. Phys. Chem.*, **69**, 2581 (1965).
4. Fuoss and Accascina: *Electrolytic Conductance* Chapters XVI-XVII Interscience. New York (1959).
5. a) Fuoss R.M. and Kraus C.A.: *J. Am. Chem. Soc.*, **55**, 476 (1933);
   b) Fuoss R.M: *Chem. Rev.*, **17**, 27 (1935); (C) 4;
   d) Graham J.R., Kell G.S. and Gordon A.R.: *J. Am. Chem. Soc.*, **79**, 2352 (1957);
   e) Fuoss R.M. and Kraus C.A.: *J. Am. Chem. Soc.*, **80**, 3163 (1958);

f) D'Aprano A. and Fuoss R.M.: *J. Phys. Chem.*, **67**, 1871 (1963);
g) Accascina F., D'Aprano A. and Triolo R.: *J. Phys. Chem.*, **71**, 3469 (1967).
6) Fuoss R.M.: *Electrochemistry second Australian Conference* Melburne (1968).
7. Born M.: *Z. Physik*, **1** 221 (1920).
8. Fuoss R.M.: *Proc. Nat. Acad. Sci. (U.S.)*, **45**, 807 (1959);
Sadek H. and Fuoss R.M.: *J. Am. Chem. Soc.*, **81**, 4507 (1959).
9. Boyd R.H.: *J. Chem. Phys.*, **35**, 1281 (1961); **39**, 2376 (1963).
10. a) Zwanzig R.: *J. Chem. Phys.*, **38**, 1603, 1605 (1963); **52**, 3625 (1970);
b) Atkinson G. and Mori Y.: *J. Phys. Chem.*, **71**, 3523 (1967).
11. Covington A.K. and Dickinson T.: *"Physical Chemistry of Organic Solvent Systems"* (Plenum Press, New York 1973) p. 647.
12. Covington A.K. and Jones P.: *"Hydrogen-Bonded solvent systems"* (Taylor and Francis, London 1968) p.p. 241, 250.
13. Robinson R.A. and Stokes R.H.: *"Electrolyte solutions"* (Butterworths, London 1959) p. 463.
14. Fabry T. and Fuoss R.M.: *J. Phys. Chem.*, **68**, 971 (1964).
15. Greinacher E., Luttke W. and Mecke R.: *Z. Electrochem.* **59**, 23 (1955).
16. Fratiello A. and Luongo J. P.: *J. Am. Chem. Soc.*, **85**, 3072 (1963).
17. Hammes G. and Knoche W.: *J. Chem. Phys.*, **45**, 4041 (1966).
18. Jannakoudakis D., Papanastasiou G. and Moumtzis J.: *Chimika Chronika, New Series*, **2**, 73 (1973)
19. Jannakoudakis D., Papanastasiou G. and Mavridis P.: *J. Chim. Phys.*, **73**, 156 (1976).
20. Fernádez-Prini R. and Atkinson G.: *J. Phys. Chem.*, **75**, 239 (1971).

Chimika Chronika, New Series, 10, 143-153 (1981)

IONIZATION OF METHYL ORANGE AND TAUTOMERIC EQUILIBRIUM OF ITS MONOPROTONATED FORMS IN AQUEOUS SOLUTIONS

D. JANNAKOUDAKIS, E. THEODORIDOU AND L. MOUMTZIS
Laboratory of Physical Chemistry, the Faculty of Physics and Mathematics, University of Thessaloniki, Greece.

(Received April 7, 1979)

Summary

The behavior of 4-dimethylaminoazobenzene-4′-sulfonic acid natrium salt (methyl orange) in acidic aqueous solutions is investigated. Monoprotonation of methyl orange (in pH region 2,5 - 4,5) gives an equilibrium mixture of the azonium and the ammonium ions, in which the former is predominant. In strong acidic solutions there is an equilibrium between the azonium and the biprotonated form, whereas in concentrated sulfuric acid, methyl orange exists exclusively as biprotonated. The ionization constants of the mono- and the biprotonated forms, as well as the partial pK values of the azonium and the ammonium form and the tautomeric equilibrium constant K_T between them, are estimated by a spectrophotometric process, which seems to give more accurate results in comparison to those up to now employed for the study of similar azobenzene derivatives.

Key words: methyl orange, mono- and biprotonated form, azonium and ammonium form tautomeric equilibrium, dissociation constants, partial pKs, tautomeric equilibrium constant.

Introduction

Several divergent views have been expressed by many authors on the behavior of p-aminoazobenzene derivatives in acidic solutions. In such solutions these compounds are mono- or biprotonated, and the electron density at their azo-linkage is more or less associated with their carcinogenetic activity[1].

Some previous authors have assigned the ammonium structure III (scheme I) as the exclusive structure of the monoprotonated form of the above aminoazoben-

zene derivatives[2-4]. Other authors on the other hand have concluded that the monoprotonated form has the azonium quinoid structure II, with the proton attached to the β-azo nitrogen atom[5,6]. It is clear however from careful examination of the UV spectra in solutions of different acidities, that the conjugate acid of IV is an equilibrium mixture of II and III containing substantial amounts of both tautomers [1,7-13].

The equilibrium diagram between the possible protonated forms of a p-aminoazobenzene derivative is given in Scheme I.

Scheme I

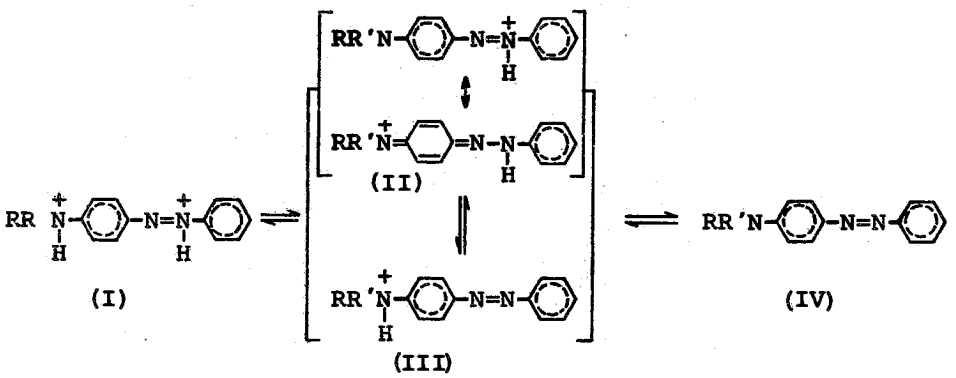

The two tautomers exhibit in the UV spectrum markedly different absorption bands; the azonium ions in the 500 nm region and the ammonium ions in the 320 nm region. Azobenzene derivatives which are protonated exclusively at the azo-linkage (e.g. 4,4′-azoanisole [11] and p-phenyl-aminoazobenzene [11,14] have only the 500 nm band, whereas the derivatives protonated only at the amino group (e.g. 4-dimethylamino-3-methyl-azobenzene[11], p-dimethylaminoazobenzenemethiodide[7] and p-phenylazotrimethylanilinium methylsulfate[10] have only a single band at 320 nm. Some authors have estimated the tautomeric equilibrium constant K_T between the azonium and the ammonium form of several aminoazobenzene derivatives by means of the relation[10,12,15].

$$K_T = \frac{C_2}{C_1} = \frac{\varepsilon_{mixt} - \varepsilon_1}{\varepsilon_2 - \varepsilon_{mixt}}$$

where C_1 and C_2 are the molar concentrations of the ammonium and the azonium form, ε_1 and ε_2 the respective molar extinction coefficients and ε_{mixt} the experimentally observed molar extinction coefficient of the equilibrium mixture at the same wave length.

Other authors [16,17] on the other hand have estimated the tautomeric

equilibrium constant by means of equation

$$K_T^{-1} = K_t = \frac{\varepsilon_c^{III} \cdot \varepsilon_a}{\varepsilon_a^{II} \cdot \varepsilon_c}$$

where ε_a, ε_c are the apparent extinction coefficients and ε_a^{II}, ε_c^{III} are the molar extinction coefficients of the ammonium and the azonium form at their absorption maxima respectively. In both cases the extinction coefficients of the pure tautomers could not be measured directly and were estimated from the spectral data of model compounds, which exist only in a single form.

S. Yamamoto and co-workers [17,18] have however determined the extinction coefficients of the two tautomeric forms ε_a^{II} and ε_c^{III} of the relation (2) of some p-aminoazobenzene derivatives by a graphical method in mixed solvents.

In some cases [12,16-18] the partial pK-values of the two tautomeric forms are also estimated by means of the K_T or K_t value, found from the equations (1) or (2).

In a previous paper [14] the behavior of p-aminoazobenzene-sulfonic acid and p-phenylaminoaminoazobenzene-sulfonic acid in acidic aqueous and aqueous-methanol solutions has been investigated, and has been found that in case of p-aminoazobenzene derivative the molar extinction coefficient of the azonium form could be directly measured from the spectra of this compound in strong acidic solutions. Based on this extinction coefficient a process has been followed, which permits the determination of the partial pKs of the azonium and ammonium form, whithout knowing the tautomeric equilibrium constant K_T between the two forms.

In order to have a further evidence for the application of the above mentioned process [14] to other aminoazobenzene derivatives the ionization steps of 4-dimethylaminoaminoazobenzene-4′-sulfonic acid natrium salt (methyl orange) in aqueous strong acidic and buffered solutions have been thoroughly investigated in tne present paper.

Experimental

Methyl orange (Fluka, puriss p.a.) was recrystallized from ethanol solutions. The buffer solutions were prepared according to Walpole Standarts [19]. The spectra were recorded using a Beckman DB-GT-spectrophotometer, the intensities of the solutions at a fixed wave length were measured by a Beckman ACTA-5-spectrophotometer. The pH-values of the buffer solutions were measured by a Knick pH-meter.

The concentrated sulfuric acid used for the preparation of the strong acidic solutions was puriss p.a. of the Fa.Fluka. The pH-values of these solutions were taken from the tables of Michaelis-Granick [20]. The methyl orange concentration was in all cases 2.10^{-5} M. All measurements were carried out at $25^0 \pm 0{,}01^0$C.

Results and Discussion

The absorption spectra of methyl orange in aqueous standard buffer solutions (pH range 2,5 - 4,5) as well as in acidic (0,1 N HCl) and alkaline (0,1 N NaOH) solutions are given in fig 1. The absorption band at 464 nm is due to the

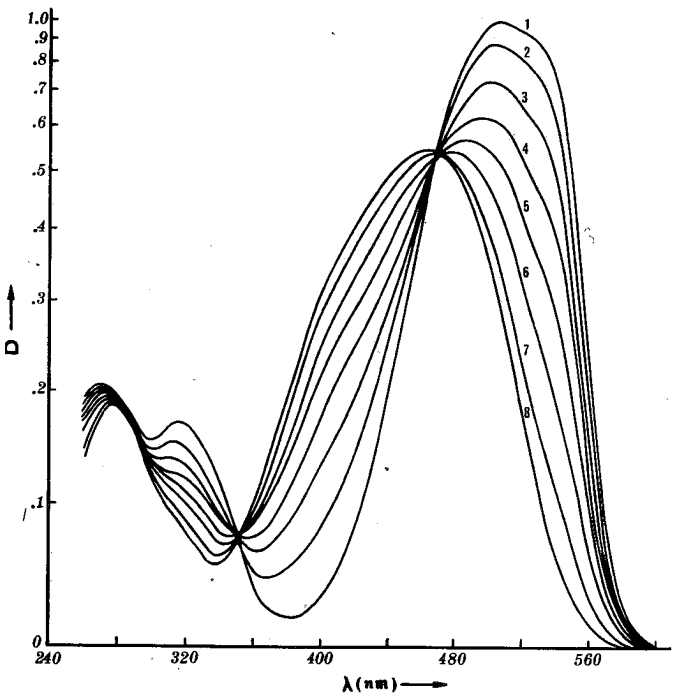

FIG. 1. *Spectra of methyl orange (2.10^{-5} M) in acidic, alkaline and buffered aqueous solutions at 25°C. (1) 0,1 N HCl, (2) pH 2,72, (3) pH 3,12, (4) pH 3,46, (5) pH 3,72, (6) pH 4,03, (7) pH 4,43, (8) 0,1 N NaOH.*

unprotonated indicator, while the absorptions at 508 and 317 nm are attributed to the azonium and the ammonium form respectively. The azonium ion is expected to absorb at a longer wave length because of its quinoid structure, whereas addition of the proton to the amino group shortens the chain of conjugation and causes a strong violet shift in the band of the unprotonated species [8d].

Scheme II

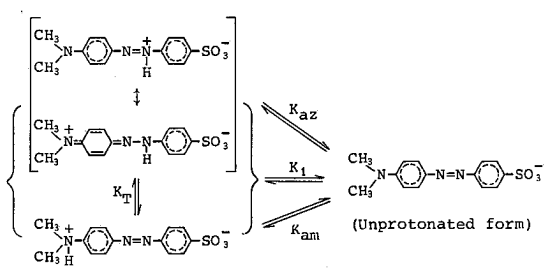

The band at about 275 nm is due to the unprotonated as well as to the azonium form - at this region both species show almost the same absorptivity –, while the ammonium form does not absorb at this wave length [7,8b] . This is more obvious in the spectra of methyl orange in strong acidic solutions (fig. 2).

On the basis of the intensities measured in buffer solutions at 420 nm - this wave length has been chosen instead of the absorption maximum at 464 nm in order to measure the absorbance of the remained unprotonated form far from the absorption band of the azonium form; on the other hand Beer's law has given very good linearity for alkaline solutions at 420 nm – the total pK_1-value (scheme II) for the dissociation of the monoprotonated form of methyl orange in general has been estimated by means of equation:

$$pK_1 = pH - \log \frac{D - D^{\circ}_{AH^+}}{D^{\circ}_{A} - D}$$

where D°_{A}, $D^{\circ}_{AH^+}$, and D are the optical densities of an alkaline (0,1 N NaOH), of an acidic (0,1 N HCl) and of a buffer solution of methyl orange at 420 nm.

In order to obtain the partial pKs of the azonium and the ammonium form the spectra of methyl orange in strong acidic solutions have been recorded and are given in figure 2. As it is shown in this figure the spectrum in 2 N H_2SO_4 (curve 1) is

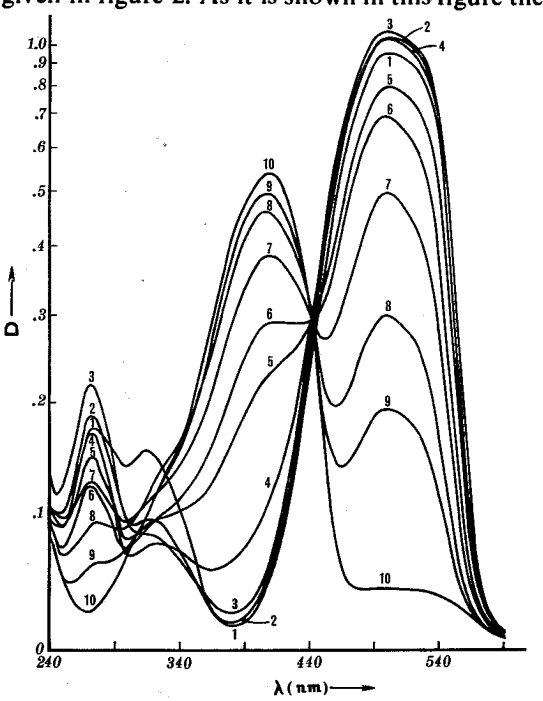

FIG. 2. *Spectra of methyl orange (2.10^{-5} M) in sulfuric acid aqueous solutions at 25°C. Sulfuric acid concentration: (1) 2 N, (2) 10 N, (3) 15,3 N, (4) 20,4 N, (5) 22,3 N, (6) 23,2 N, (7) 24 N, (8) 25 N, (9) 26 N, (10) 100 % H_2SO_4.*

similar to that in 0,1 N HCl (fig. 1, curve 1) with two absorption bands at 508 and 317 nm respectively. In a more acidic solution (10 N H_2SO_4) the intensity at 508 nm increases and at 317 nm decreases (fig. 2, curve 2). This fact is considered as a further evidence, that the two bands are due to two isomers in equilibrium. With increasing acidity (15,3 - 26 N H_2SO_4) the absorbance at 508 nm decreases, while a new absorption band appears at 406 nm, which is attributed to the biprotonated form of methyl orange (scheme III). In pure concentrated sulfuric acid (fig. 2, curve 10) the whole amount of the indicator is considered to be biprotonated. Because of the absence of the quinoid structure the biprotonated form absorbs at a shorter wave length than the azonium form. The absorption band at 317 nm almost disappears in the acidic solutions with a sulfuric acid concentration greater than 20 N, so that one can make the assumption that in these solutions only the biprotonated and the azonium form are in equilibrium.

From the optical density of the solution in pure sulfuric acid at 406 nm, the extinction coefficient of the biprotonated form at this wave length can be determined by means of Beer's law:

$$\varepsilon^{o}_{AH_2^{++}} = \frac{D^{o}_{406}}{C_o} \qquad (4)$$

and has been found equal to $2{,}76 \cdot 10^4$ $mole^{-1}.lit.cm^{-1}$. In equation (4) Co is the total concentration of methyl orange in the solution (2.10^{-5} M). In the strong acidic solutions the remained concentration of the biprotonated form can also be found from Beer's law at 406 nm:

$$C_{AH_2^{++}} = \frac{D_{406}}{\varepsilon^{o}_{AH_2^{++}}} \qquad (5)$$

Thus the concentration of the azonium form can be obtained each time from the difference

$$C_{AH^{+}(az)} = C_o - C_{AH_2^{++}} \qquad (6)$$

The extinction coefficient of the azonium form at 528 nm - chosen instead of the absorption maximun (508 nm) for the same reason as in case at 464 nm - has then been estimated from the relation.

$$\varepsilon^{o}_{AH^{+}(az)} = \frac{D_{528}}{C_{AH^{+}(az)}} \qquad (7)$$

and found $5{,}84 \cdot 10^4$ $mole^{-1}.lit.cm^{-1}$ (average value for five different strong acidic solutions).

The pK_2-value for the dissociation of the biprotonated to the monoprotonated form - in case of methyl orange K_2 corresponds to the dissociation of the

biprotonated to the azonium form

Scheme III

(Biprotonated) (Azonium form)

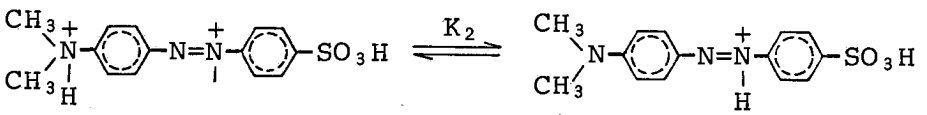

– can also be estimated – since the concentrations of the two forms are known – by means of the relation

$$pK_2 = pH - \log \frac{C_{AH^+(az)}}{C_{AH_2^{++}}} \qquad (8)$$

The calculated pK_2-values for some strong acidic solutions at 25°C are given in table I, together with the observed optical densities at 406 and 528 nm, the pH-values of the solutions and the calculated by means of equ. (5) and (6) concentrations of the biprotonated and the azonium form of methyl orange.

TABLE I. *Spectral data, concentration of the biprotonated and the azonium form and pK_2 values for methyl orange (Co = 2.10^{-5} M) in strong acidic aqueous solutions at 25°C.*

$N_{H_2SO_4}$	— pH	D_{406}	D_{528}	$C_{AH^+(az)}.10^5$	$C_{AH_2^{++}}.10^5$	— pK_2
20,4	5,52	0,097	0,863	1,649	0,351	6,19
22,3	6,05	0,215	0,697	1,221	0,779	6,25
23,2	6,31	0,290	0,553	0,949	1,051	6,27
24,0	6,54	0,368	0,398	0,667	1,333	6,24
25,0	6,82	0,444	0,252	0,391	1,609	6,21

The obtained average value for pK_2 is equal to -6,23(±0,04).

On the other hand the observed optical density of a buffer solution at 420 nm is equal to

$$D_{420} = \varepsilon_A \cdot C_A + \varepsilon_{AH^+}(C_o - C_A) \qquad (9)$$

where ε_A is the obtained by means of Beer's law extinction coefficient of alkaline solutions (0,1 N NaOH) at 420 nm ($\varepsilon_A = 2{,}04 \cdot 10^4$ mole^{-1}.lit.cm^{-1}) and ε_{AH+} is the extinction coefficient of acidic (0,1 N HCl) solutions found in the same way at the same wave length ($\varepsilon_{AH+} = 3{,}35 \cdot 10^3$ mole^{-1}.lit.cm^{-1}).

Finally the measured optical density of a buffer solution at 528 nm is equal to

$$D_{528} = \varepsilon^{o}_{AH^+(az)} \cdot C_{AH^+(az)} + \varepsilon'_A \cdot C_A \qquad (10)$$

Here ε'_A (= $6{,}13 \cdot 10^3$ $mole^{-1}.lit.cm^{-1}$ by means of Beer's law) is the extinction coefficient of alkaline solutions of methyl orange at 528 nm and C_A is the remained concentration of the unprotonated form, found by means of eq. (9). On the basis of eq. (10) the concentration of the azonium form can be estimated. Of course it is considered that the ammonium form shows no absorption at 528 nm. A similar assumption cannot be made for the azonium form at the absorption maximum of the ammonium form (at 317 nm), since as already mentioned the azonium form absorbs at 275 nm neighboring the ammonium form band.

The concentration of the ammonium form is then found from the difference

$$C_{AH^+(am)} = C_o - C_{AH^+(az)} - C_A \quad , \qquad (11)$$

without using the absorbance at 317 nm.

The known concentrations of the two tautomers permit now the calculation of the partial pK-values as well as of the tautomeric equilibrium constant K_T between them (scheme II) by means of the relations

$$pK_{az} = pH - \log \frac{C_A}{C_{AH^+(az)}} \quad , \quad pK_{am} = pH - \log \frac{C_A}{C_{AH^+(am)}} \qquad (12)$$

and

$$K_T = \frac{C_{AH^+(az)}}{C_{AH^+(am)}} \qquad (13)$$

These values are given in table II, together with the calculated by means of eq.(3) total pK_1-values, the measured optical densities at 420 nm and 528 nm and the pH-values of the standard aqueous buffered solutions at 25°C.

TABLE II. *Spectral data, pK_1, pKaz, pKam and K_T values of methyl orange ($Co=2.10^{-5}$ M) in standard buffer aqueous solutions at 25°C.*

pH	D_{420}	D_{528}	pK_1	pKaz	pKam	K_T
2,46	0,100	0,793	3,43	3,30	2,85	2,85
2,73	0,124	0,739	3,42	3,30	2,84	2,83
3,12	0,181	0,613	3,42	3,29	2,84	2,78
3,37	0,228	0,511	3,41	3,28	2,84	2,77
3,46	0,248	0,467	3,40	3,27	2,83	2,75
3,59	0,275	0,408	3,39	3,26	2,83	2,72
3,72	0,299	0,356	3,38	3,26	2,82	2,71
3,90	0,325	0,301	3,40	3,27	2,83	2,74
4,03	0,340	0,258	3,41	3,26	----	----
4,23	0,359	0,212	3,44	3,26	----	----
4,43	0,374	0,180	3,45	3,25	----	----

The average values are: pK_1 = 3,41(±0,04), pK_{az} = 3,27(±0,03)
pK_{am} = 2,84(±0,02) and K_T = 2,77(±0.08),
and confirm very satisfactorily the following relation, resulting from the combination of the K-values:

$$K_1^{-1} = K_{az}^{-1} + K_{am}^{-1} \qquad (14)$$

The pK_1 value is in a very good agreement with that of De Ligny and co-workers [21] who have pointed out for pK_1 of p-dimethylaminoazobenzene-sulfonic acid in aqueous solutions the values 3,39 and 3,37. Furthermore the constancy of the pK values given in table II must be considered as an additional evidence concerning the applicability of the method employed.

Comparison of the above partial pKs with those obtained for p-aminoazo-benzene-sulfonic acid (pK_{az} = 2,23, pK_{am} = 2,72) [14] shows that pKaz is greater in case of methyl orange. This is attributed to the stronger electronegativity of the dimethylamino group compared to that of the animo group (Hammett constant σ for $-NH_2$ -0,660 [22,23], while for $-N(CH_3)_2$ -0,931, based on the half wave potentials of p-substituted azobenzene derivatives [24]. Therefore the proton is stronger attached to the azo nitrogen in the conjugate acid of methyl orange. The pKam values of both compounds are on the other hand almost equal. The two methyl groups cause a steric hindrance on the animo nitrogen, but this is probably refracted by the positive inductive (+I) effect of these groups.

It is obvious from all above mentioned that the followed in the present and in a previous [14] paper process permits the determination of the partial pKs of p-aminoazobenzene derivatives, without knowing the tautomeric equilibrium constant K_T between the two forms. It is justified to believe that these pK values are of greater accuracy in comparison to those given by some authors [12,16,17,18] found from K_T, which is taken by means of equations (1) or (2), because K_T is estimated from spectral data of model compounds and mainly because K_T depends strongly on the acidity of the solution [14,15]

On the other hand in case of p-aminoazobenzene derivatives the assumption that the azonium form does not absorb at 317 nm ($\varepsilon_2 = 0$ in eq. 1)[12] is not correct-because of its remarkable absorption at 275 nm - so that eq.(1) becomes inapplicable.

The calculated by means of eq.(2) - from spectral data obtained as mentioned by a graphical method in aqueous 50% ethanol solutions [17,18] - K_T value is considered to be more accurate, although the ratio $\varepsilon\alpha/\varepsilon c$ of eq.(2) is estimated only at one acidity (= 1 N HCl), so that the obtained K_T suits only to this acidity [25] and not to the whole acidity region, where both tautomers exist at various concentration ratio in equilibrium.

Περίληψη

Ἰονισμός τῆς ἡλιανθίνης καί ταυτομερής ἰσορροπία τῶν μονοπρωτονιωμένων μορφῶν της σέ ὑδατικά διαλύματα.

Μελετᾶται ἡ συμπεριφορά τοῦ ἄλατος μέ νάτριο τοῦ 4-διμεθυλαμινοαζωβενζολο-4′-σουλφονικοῦ ὀξέος (ἡλιανθίνη ἤ πορτοκαλλόχρουν τοῦ μεθυλίου) σέ ὄξινα ὑδατικά διαλύματα. Σέ ρυθμιστικά διαλύματα περιοχῆς pH 2,5 — 4,5 σχηματίζεται ταυτομερές μίγμα τῶν δύο μονοπρωτονιωμένων μορφῶν τῆς ἡλιανθίνης (scheme II), δηλαδή τῆς πρωτονιωμένης στήν ἀζωομάδα (ἀζωνιομορφή) καί τῆς πρωτονιωμένης στήν ἀμινοομάδα (ἀμμωνιομορφή). Οἱ δύο μορφές ἐμφανίζουν λόγω συντονισμοῦ διαφορετικά μέγιστα ἀπορροφήσεως στό φάσμα UV, ἡ ἀζωνιομορφή στά 508 nm καί ἡ ἀμμωνιομορφή στά 317 nm (fig. 1). Σέ ἰσχυρά ὄξινα μέ θεικό ὀξύ διαλύματα ὑφίσταται ἰσορροπία μεταξύ τῆς ἀζωνιο- καί τῆς ἐμφανιζόμενης μέ μέγιστο ἀπορροφήσεως στά 406 nm (fig. 2) διπρωτονιωμένης μορφῆς (scheme III), ἐνῶ ἡ ἀμμωνιομορφή ἔχει σχεδόν ἐξαφανισθεῖ. Τέλος σέ καθαρό θειικό ὀξύ ὅλη ἡ ποσότητα τῆς ἡλιανθίνης εἶναι διπρωτονιωμένη (fig. 2). Ἀπό τά φάσματα τῆς ἡλιανθίνης σέ ἰσχυρά ὄξινα διαλύματα προσδιορίζεται ὁ γραμμομοριακός συντελεστής ἀπορροφήσεως τῆς ἀζωνιομορφῆς, ἀπό τόν ὁποῖο καθώς καί τίς μετρούμενες ὀπτικές πυκνότητες τῶν διαλυμάτων τῆς ἡλιανθίνης στά διάφορα μέγιστα ἀπορροφήσεως ὑπολογίζονται οἱ ἐπιμέρους συγκεντρώσεις τῆς μή πρωτονιωμένης, τῆς ἀζωνιο— καί τῆς ἀμμωνιομορφῆς.

Ἀπό τίς σχέσεις (12) καί (13) προσδιορίζονται στή συνέχεια τά pK τῶν δύο ταυτομερῶν μορφῶν καθώς καί ἡ σταθερά ἰσορροπίας μεταξύ αὐτῶν καί βρίσκονται οἱ τιμές: pKaz = 3,27, pKam = 2,84 καί Kτ = 2,77. Τέλος ἀπό τή σχέση (3) βρίσκεται τό pK τῆς διαστάσεως τῆς μικτῆς μονοπρωτονιωμένης πρός μή πρωτονιωμένη μορφή (pK_1 = 3,41) καί ἀπό τή σχέση (8) τό pK τῆς διαστάσεως τῆς διπρωτονιωμένης πρός τήν ἀζωνιομορφή (pK_2 = —6,23). Ἡ μέθοδος πού ἀκολουθεῖται στήν ἐργασία αὐτή γιά τόν προσδιορισμό τῶν μερικῶν σταθερῶν διαστάσεως τῶν δύο ταυτομερῶν μορφῶν τῆς ἡλιανθίνης πιστεύεται ὅτι δίνει ἀκριβέστερα ἀποτελέσματα συγκριτικά μέ τίς μεθόδους πού ἔχουν μέχρι τώρα ἐφαρμοσθεῖ γιά παρόμοια παράγωγα τοῦ ἀζωβενζολίου. Στίς μεθόδους αὐτές χρησιμοποιεῖται ἀποκλειστικά γιά τόν προσδιορισμό τῶν μερικῶν σταθερῶν διαστάσεως τῶν δύο ταυτομερῶν μορφῶν ἡ σταθερά ἰσορροπίας Kτ μεταξύ αὐτῶν, ἡ ὁποία ὅμως ἀφενός βρίσκεται τίς περισσότερες φορές ἀπό γραμμομοριακούς συντελεστές ἀπορροφήσεως πρότυπων ἐνώσεων, πού ὑφίστανται μόνο ὑπό τήν ἀμμωνιο- ἤ τήν ἀζωνιομορφή καί ἀφετέρου ἐξαρτᾶται σημαντικά ἀπό τήν ὀξύτητα τοῦ διαλύματος.

References

1. Badger G.M., Buttery R.G. & Lewis G.E.: *J. Chem. Soc.*, 1888 (1954).
2. Klotz I.M., Fiess H.A., Chen Ho J.Y. & Mellody M.: *J. Am. Chem. Soc.*, **76**, 5136 (1954).
3. McGuire W.S., Izzo T.F. & Zuffanti S.: *J. Org. Chem.*, **21**, 632 (1956).
4. Pentimalli L.: *Tetrahedron*, **5**, 27 (1959).
5. Bury C.R.: *J. Am. Chem. Soc.*, **57**, 2115 (1935).
6. Rogers M.T., Campbell T.W. & Maatman R.W.: *J. Am. Chem. Soc.*, **73**, 5122 (1951).
7. Cilento G., Miller E.C. & Miller J.A.: *J. Am. Chem. Soc.*, **78**, 1718 (1956).
8. Sawicki E.: *J. Org. Chem.*, **21** 605 (1956); *J. Org. Chem.*, **22**, 365, 621, 1084 (1957).
9. Jaffé H.H. & Yeh Si-Yung: *J. Org. Chem.*, **22**, 1281 (1957).
10. Yeh Si-Yung & Jaffé H.H.: *J. Am. Chem. Soc.*, **81**, 3283 (1959).
11. Lewis G.E.: *Tetrahedron*, **10**, 129 (1960).
12. Reeves R.L.: *J. Am. Chem. Soc.*, **88**, 2240 (1966).
13. Patai S.: "*The Chemistry of the hydrazo, azo and azoxy groups*", Part 2, p. 844, John Wiley & Sons, London, 1975.
14. Jannakoudakis D., Theodoridou E. & Pelekourtsa A.: *Chimika Chronika, New Series*, **1**, 67 (1972).
15. Isaks M. & Jaffé H.H.: *J. Am. Chem. Soc.*, **86**, 2209 (1964).
16. Gerson F. & Heilbronner E.: *Helv. Chim. Acta*, **45**, 42 (1962).
17. Yamamoto S., Nishimura N. & Hasegawa S.: *Bull. Chem. Soc. Japan*, **46**, 194 (1973).
18. Yamamoto S.: *Bull. Chem. Soc. Japan*, **46**, 3139 (1973).
19. Britton H.T.S.: "*Hydrogen Ions*", p. 217, Chapman & Hall Ltd, London, 1932.
20. Michaelis L. & Granick S.: *J. Am. Chem. Soc.*, **64**, 1861 (1942).
21. De-Ligny C.L., Loriaux H. & Ruiter A.: *Recueil*, **80**, 725 (1961).
22. Jaffé H.H.: *Chem. Revs.*, **53**, 191 (1953).
23. Johnson C.D.: "*The Hammett Equation*", p. 3, University Press, Cambridge, 1973.
24. Jannakoudakis D. & Stalidis G.: *Chimika Chronika, N.S.*, **2**, 175 (1973).
25. Patai S.: "*The Chemistry of the hydrazo, azo and azoxy groups*", Part 2, p. 848, John Wiley & Sons, London, 1975.

Chimika Chronika, New Series, 10, 155-162 (1981)

POLAROGRAPHIC BEHAVIOR AND DISCONTINUITY OF THE ELECTROREDUCTION CURVES OF PHTHALALDEHYDE IN METHANOL

DIMITRIOS JANNAKOUDAKIS and GEORGE KOKKINIDIS
Laboratory of Physical Chemistry, University of Thessaloniki, Thessaloniki, Greece.
(Received November 28, 1979)

Summary

The polarographic curves obtained during the reduction of phthalaldehyde in methanol in the presence of carboxylic acids display discontinuity and hysteresis effects. The role of hemiacetals formation was taken into consideration for the interpretation of these effects. The change of the acid concentration in the vicinity of the dropping mercury electrode, caused by the hydrogen discharge, leads to alteration of the electrochemical process, which is responsible for the discontinuity and hysteresis effects.

Key words: Hysteresis of the polarographic wave, hemiacetal formation, proton donors, hydrogen discharge, catalytic hydrogen wave.

Introduction

In the course of our studies on the polarographic behavior of carbonyl compounds[1-4] in methanol, we found that the polarographic curves obtained during the reduction of phthalaldehyde in the presence of carboxylic acids, present discontinuity as well as hysteresis effects. It is well known that oxygen containing anions, such as nitrates[5,6], iodates and bromates[7,8] give polarographic curves with the same characteristic properties during their reduction in the presence of tri— and tetra—valent cations. However, other organic depolarizers showing a similar behavior have not yet been cited in the literature so far. Therefore, an investigation regarding to the probable explanation of the discontinuity occuring during the reduction of phthalaldehyde was considered necessary for our further research interests.

Experimental

Polarographic curves and cyclic voltammetric i — E curves at a H.M.D.E. were obtained as discribed previously(4). The potential was measured relatively to the aqueous calomel electrode (SCE) saturated with KCl. The experiments were carried out at constant temperature 25 + 0,1 C.

The reagents were methanol "zur analyse" from Merck, lithium chloride R.P. from Carlo-Erba and phthalaldehyde "puriss p.a." from Fluka. The other substances were also of high grades obtained commercially.

Results and Discussion

The polarographic curves of phthalaldehyde in methanol in the absence as well as in the presence of benzoic acid are given in Fig. 1. The reduction mechanism of phthalaldehyde in the absence of any proton donor was discussed previously(3). The first wave is due to the reduction of the free aldehyde and it possesses kinetic character; the second wave corresponds to the reduction of monohemiacetal followed by the reduction of 2-hydroxymethyl-benzaldehyde formed in the first step according to the reactions:

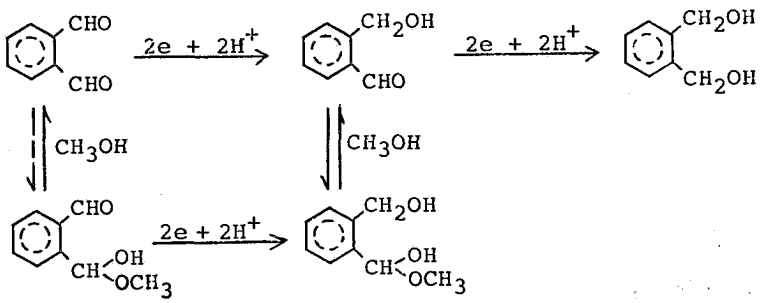

In the presence of benzoic acid a discontinuous increase of current to the maximum limiting value is observed and the polarographic curves obtained do not have the usual exponential form (Fig. 1, curve 2). A further anomaly in connection with the discontinuity is the hysteresis of the reduction wave.

The potential of discontinuity (the potential at which the discontinuous increase of current occurs) is affected by the following factors.

1. The concentration of acid. Fig. 2 demonstrates the fact that by increasing gradually the concentration of benzoic acid the potential of discontinuity is displaced at more negative values. Other acids also present a similar behavior.

2. The strength of acids. For stronger acids, the potential of discontinuity is shifted to more positive values. This has been detected by using a series of acetic acid derivatives (Fig. 3) as well as a series of benzoic acid derivatives. In the presence of even stronger acids (i.e. CCl_3COOH, CF_3COOH) the polarographic curve of phthalaldehyde maintains its usual exponential form. In this case, a time dependent decrease of the height of the polarographic wave is obtained, which is

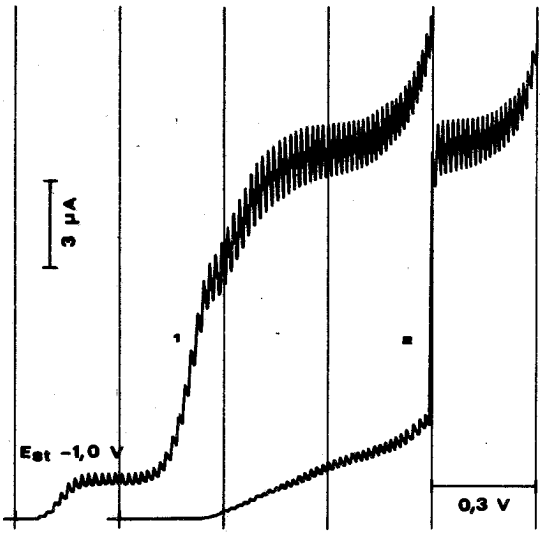

FIG. 1. *Polarograms of 10^{-3}M phthalaldehyde in methanol in the absence (curve 1) and in the presence of 10^{-3} M C_6H_5COOH (curve 2). Supporting electrolyte 0,1 M LiCl.*

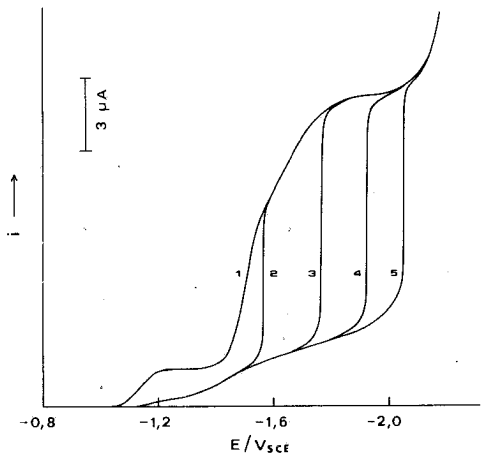

FIG. 2. Polarographic curves of 10^{-3} M *phthalaldehyde in methanol in the presence of varying amounts of* C_6H_5COOH: *1) Without* C_6H_5COOH, *2)* 5.10^{-4} M, *3)* $7,5.10^{-4}$ M, *4)* 10^{-3} M, *5)* 2.10^{-3} M C_6H_5COOH. *Supporting electrolyte 0,1 M LiCl.*

attributed to the formation of the non reducible acetal.

Comparing the polarographic curves of phthalaldehyde in the presence of acids with the polarographic curves obtained when phthalaldehyde is absent, we observe that the discontinuous increase of current takes place at the potential where the current of the hydrogen ions reduction wave approaches its limiting value. This is not evident in the case of CH_3COOH or C_6H_5COOH, because these acids do not form well defined hydrogen waves in methanol[9]; it becomes, however, obvious

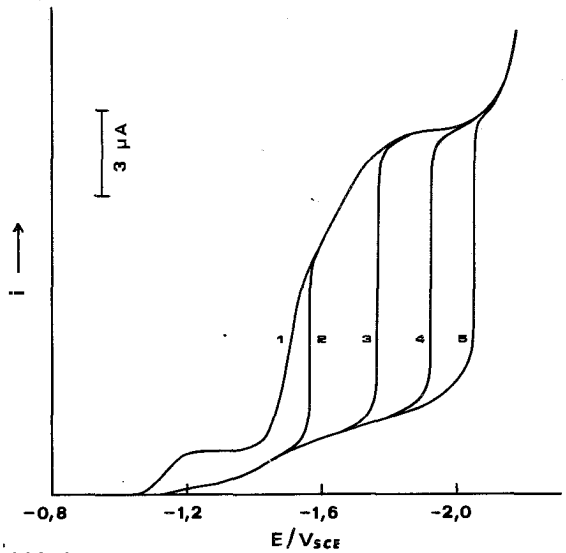

FIG. 3. *Polarographic curves of 10^{-3} M phthalaldehyde in methanol in the presence of different carboxylic acids: 1) Without any acid, 2) 10^{-3}* M $CH_2ClCOOH$, *3) 10^{-3}* M CH_2ClCH_2COOH, *4) 10^{-3}* M CH_3COOH, *5) 10^{-3}* M CH_3CH_2COOH. *Supporting electrolyte 0,1 M LiCl.*

with stronger acids ($CH_2ClCOOH$, $CHCl_2COOH$, salicylic acid), which form well defined hydrogen ions reduction waves (Fig. 4). Therefore, we infer that the potential of discontinuity must be related to the hydrogen ions reduction of the acids used.

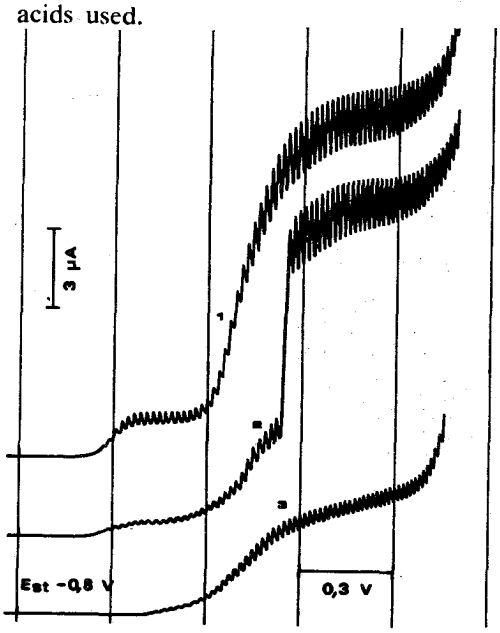

FIG. 4. *Polarograms of 10^{-3} M phthalaldehyde in methanol in the absence (curve 1) and in the presence of 10^{-3} M* $CH_2ClCOOH$ *(curve 2). Curve 3 presents the corresponding hydrogen wave of 10^{-3} M* $CH_2ClCOOH$. *Supporting electrolyte 0,1 M LiCl.*

3. The same conclusion can be drawn from the influence of substances which lower the hydrogen overvoltage. N,N-dimethyl-p-phenylendiamine[9,10] has been used for this purpose. It is evident from Fig. 5 that the discontinuity completely disappears and the wave acquires the usual exponential form, when a small quantity of catalyst is added to the solution. In the presence of catalyst the reduction potential of hydrogen ions is displaced to more positive values. The resulting catalytic hydrogen wave is also given in Fig. 5.

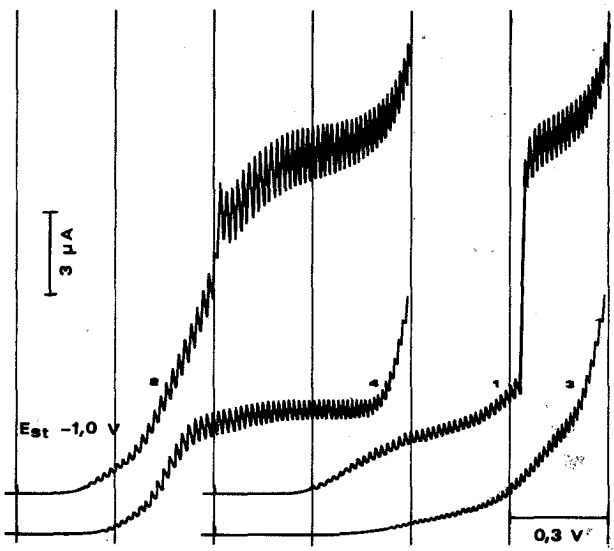

FIG. 5. *Polarograms of 10^{-3} M phthalaldehyde in methanol in the presence of 10^{-3} M CH_3COOH. 1) Without catalyst, 2) with 2.10^{-4} M N,N—dimethyl—p—phenylendiamine. Curves 3 and 4 present the corresponding hydrogen waves of 10^{-3} M CH_3COOH without catalyst (curve 3) and with 2.10^{-4} M N,N-dimethyl-p-phenylendiamine (curve 4). Supporting electrolyte 0,1 M LiC'*

4. The presence of oxygen. The potential of discontinuity is displaced to positive values when successive streams of oxygen are passed through a solution, which has been previously deaerated by a nitrogen stream. This can be explained by the assumption that the OH- – ions formed during the preceding reduction of oxygen neutralize the acid molecules in the vicinity of the dropping mercury electrode.

In order to gain additional experimental data about this behavior of phthalaldehyde, the method of cyclic voltammetry at a H.M.D.E. was also employed. The cyclic voltammetric behavior of phthalaldehyde in the absence as well as in the presence of benzoic acid is shown in Fig. 6. As it can be seen, in the presence of benzoic acid the double wave of phthalaldehyde disappears from the cyclic voltammogram. However, this wave appears again when the vicinity of the

electrode is sufficiently depleted of acid molecules, after holding the electrode at potential −2.0 Volt, where the hydrogen evolution takes place. This behavior is found to be in agreement with the aspect that the discontinuity and hysteresis effects appearing in the polarographic curves of phthalaldehyde are associated with the hydrogen ions reduction of the acids used.

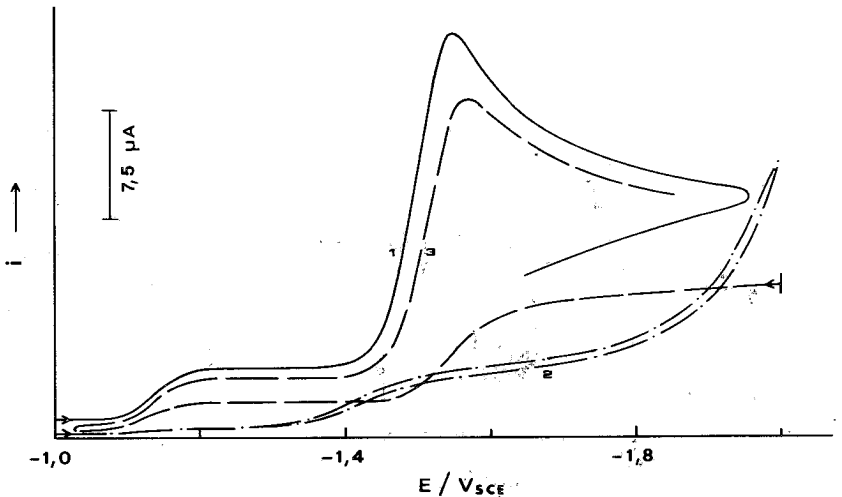

FIG. 6. *Cyclic voltammograms of 10^{-3} M phthalaldehyde in methanol in the absence (curve 1) and in the presence of 10^{-3} M C_6H_5COOH (curves 2 and 3). Curve 3 was recorded after holding the electrode at potential −2.0 Volt for 30 sec. Supporting electrolyte 0.1 M LiCl. Scan rate v=200mV/sec.*

Although the regular influence of weak acids (CH_3COOH, C_6H_5COOH) on the polarographic behavior of substituted benzaldehydes is manifested through the shift of the polarographic waves towards positive potentials[1,2], in the case of phthalaldehyde discontinuity and hysteresis effects are observed. It is worth enough to point out that phthalaldehyde in methanol forms hemiacetals, while in aqueous solutions it gives rise to the corresponding hydrates[11,12] to a considerable extent in both cases. The hemiacetalic forms are monohemiacetal (I), its cyclic form (II) and probable dihemiacetal (III). The last two forms are polarographically inactive. The case of acetal formation must be rejected, since acetals are formed only in the presence of strong acids[1-4].

Our interpretation is based upon the assumption that it is the existence of these forms itself, which is responsible for the discontinuity and hysteresis effects in the overall polarographic behavior of phthalaldehyde. In pure methanol the reducible

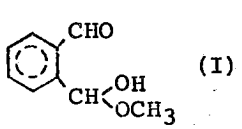

(I)

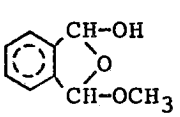

(II)

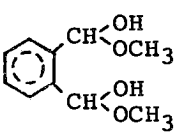

(III)

form of monohemiacetal predominates, while in the presence of weak acids we assume that the equilibrium is displaced to the non reducible forms. Concequently, the addition of acids causes the decrease or even the elimination of the reduction waves of phthalaldehyde. At the potential where the hydrogen discharge takes place, one would expect local changes in acid concentration on electrode surface. The vicinity of the dropping mercury electrode is depleted of acid molecules and the equilibrium is shifted towards the reducible form of monohemiacetal, which at this potential attains its limiting current. After the current has taken its limiting value, the acid molecules reaching the electrode surface do not give hydrogen discharge current, but act as proton donors for the reduction of phthalaldehyde. Therefore, it is the change of the electrochemical process itself, which is responsible for the appearance of the discontinuity in the polarographic curves obtained.

The polarographic behavior of phthalaldehyde in aqueous buffered solutions ([11], [12]) indicates also that changes in pH affect the equilibrium between the corresponding hydrated forms. The non reducible forms predominate at pH 3–5 where the heights of the polarographic waves are very small. This behavior is in agreement with our assumption that phthalaldehyde in methanol in the presence of weak acids mainly exists in its non reducible hemiacetalic forms.

One could expect that phthalaldehyde presents an analogous behavior in aqueous non buffered solutions in the presence of weak acids (i.e. CH_3COOH, C_6H_5COOH). However, discontinuity and hysteresis effects do not appear in the polarographic curves of this aldehyde in such a system. This is attributed to the fact that in aqueous solutions the hydrogen discharge takes place at a potential very close to that where the current of phthalaldehyde attains its limiting value.

Another interpretation of the discontinuity and hysteresis effects based on the assumption that a non reducible monohemiacetal–acid complex (IV) is formed – in a way similar to that of carboxylic acid dimers([13]) – seems to be reasonable, since at the potential of hydrogen discharge, free monohemiacatal is obtained on electrode surface. But it must be pointed out that there are certain reasons for which the

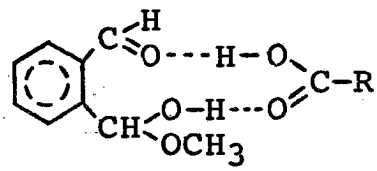

above mechanism fails to discribe the appearance of the discontinuity. It is unlike to believe that such a complex is polarographically inactive. The reduction of monohemiacetal would precede the hydrogen discharge, as far as it is reduced at more positive potentials. Such a mechanism could justify the appearance of a kinetic current and not a discontinuity of the polarographic wave. However, the main argument against this interpretation is the fact that discontinuity and hysteresis effects appear also in the presence of non carboxylic acids, as we observed with chlorophenols.

Περίληψη

Πολαρογραφική Συμπεριφορά καί Ἀσυνέχεια τῶν Καμπύλων Ἠλεκτροαναγωγῆς τῆς Φθαλαλδεΰδης σέ Μεθανολικά Διαλύματα.

Κατά τήν ἀναγωγή τῆς φθαλαλδεΰδης μέσα σέ μεθανόλη παρουσία ἀσθενῶν καρβοξυλικῶν ὀξέων παρατηρεῖται μία ἀσυνέχεια καί μία ὑστέρηση στά λαμβανόμενα πολαρογραφικά κύματα. Τά φαινόμενα αὐτά συνδέονται ἄμεσα μέ τό γεγονός ὅτι ἡ ἀλδεΰδη αὐτή μέσα στά μεθανολικά διαλύματα σχηματίζει σέ σημαντική ἔκταση ἡμιακετάλες. Ἡ μεταβολή τῆς συγκεντρώσεως τοῦ ὀξέος στήν περιοχή τοῦ σταγονικοῦ ἠλεκτροδίου, ἡ ὁποία προκαλεῖται ἀπό τήν ἀπόθεση τοῦ ὑδρογόνου, ἔχει σάν ἀποτέλεσμα τήν ἀπότομη ἀλλαγή τῆς ἠλεκτροχημικῆς δράσεως. Σ' αὐτή τήν ἀπότομη ἀλλαγή ἀποδίδονται ἡ ἀσυνέχεια καί ἡ ὑστέρηση στά λαμβανόμενα πολαρογραφικά κύματα τῆς φθαλαλδεΰδης.

References and Notes

1. Jannakoudakis, D., Kokkinidis, G. & Stalidis, G.: *Sci. Annals Fac. Phys. Mathem. Univ. Thessaloniki*, **11**, 523 (1971).
2. Jannakoudakis, D., Stalidis, G. & Kokkinidis, G.: *Chimika Chronika, New Ser.*, **5**, 313 (1976).
3. Jannakoudakis, D., & Kokkinidis, G.: *Chimika Chronika, New Ser.*, **6** 439 (1977).
4. Kokkinidis, G., Karabinas, P. & Jannakoudakis, *J. Electroanal. Chem.*, **91** 265 (1978).
5. Masek, J.: *Prec. Ist. Internat. Polarog. Congress, Prague (1951).* Vol. III p 382, 386, 390.
6. Frumkin, A.N. & Zhdanov, S.I.: *Dokl. Akad. nauk. SSSR*, **97**, 867 (1954).
7. Masek, J.: *Chem. Listy*, **46** 200 (1952).
8. Masek, J.: *Chem. Listy*, **46** 385 (1952). *Coll. Czech. Chem. Communs.*, **18**, 583 (1953).
9. Jannakoudakis, D., Wildenau, A. & Holleck, L.: *J. Electroanal. Chem.*, **15**, 83 (1967).
10. Holleck, L., Jannakoudakis, D., & Wildenau, A.: *Electrochimica Acta*, **12**, 1523 (1967).
11. Furman, N.H. & Norton, D.R.: *Anal. Chem.*, **26**, 1111 (1954).
12. Person, M., Meunier, J.M. & Beau, D.: *C.R., Acad. Sci., Ser. C.*, **275 (10)**, 527 (1972).
13. Vinogradov, S.N. & Linnell, R.H.:"*Hydrogen Bonding*" **8** Van Nostrand Reinhold Company. (1970) p. 264.

Chimika Chronika, New Series, 10, 163-174 (1981)

ΜΕΛΕΤΗ ΤΗΣ ΥΔΡΟΛΥΣΕΩΣ ΑΛΟΓΟΝΟ·Υ·ΠΟΚΑΤΕΣΤΗΜΕΝΩΝ ΥΔΡΑΖΙΔΙΩΝ ΤΟΥ ΒΕΝΖΟ·Ι·ΚΟΥ ΟΞΕΟΣ

ΔΗΜΗΤΡΙΟΣ Α. ΧΑΡΙΣΤΟΣ, ΛΕΑΝΔΡΟΣ Κ. ΤΖΑΒΕΛΛΑΣ καί ΓΕΩΡΓΙΟΣ Ε. ΜΑΝΟΥΣΑΚΗΣ.
Ἐργαστήριο Ἀνόργανης Χημείας Φυσικομαθηματικῆς Σχολῆς, Ἀριστοτελείου Πανεπιστημίου Θεσσαλονίκης.

(Received January 10, 1980)

Περίληψη

Μελετᾶται φασματοφωτομετρικῶς ἡ ὑδρόλυση τῶν ἀλογονοϋποκατεστημένων ὑδραζιδίων τοῦ βενζοϊκοῦ ὀξέος 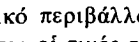 (ὅπου X = F, Cl, Br καί I σέ ο-, μ- καί π-θέση) σέ ἀλκαλικό περιβάλλον καί σέ περιοχή θερμοκρασιῶν 40-60 °C.

Ὑπολογίζονται οἱ τιμές τῶν σταθερῶν τῆς ταχύτητας τῶν ἀντιδράσεων ἐνολοποιήσεως (k_1) καί ὑδρολύσεως (k_2) πού εἶναι ἀντιστοίχως τῆς τάξεως 10^{-3} sec^{-1} καί 10^{-5} $mol^{-1}.lit.sec^{-1}$.

Ἀπό τήν ἐπεξεργασία τῶν ἀποτελεσμάτων προκύπτει ὅτι ἡ κινητική τῆς ἐνολοποιήσεως ἐλάχιστα ἐπηρεάζεται ἀπό τήν θερμοκρασία καί τόν ὑποκαταστάτη ἐνῶ διαπιστώνεται σημαντική ἐπίδραση τῆς θερμοκρασίας καθώς καί τῆς θέσεως καί τῆς φύσεως τοῦ ὑποκαταστάτη στήν κινητική ὑδρολύσεως.

Συντμήσεις: **HBAH** = ὑδραζίδιο βενζοϊκοῦ ὀξέος. **XBAH** = ἀλογονοϋποκατεστημένο στόν πυρήνα ὑδραζίδιο βενζοϊκοῦ ὀξέος. **Bac²** = ἀλκαλική ὑδρόλυση κατά τόν διμοριακό μηχανισμό.

Ὁρολογία: Κινητική, ταχύτητα, τάξη καί μηχανισμός ἀντιδράσεως ἀλογονοϋποκατεστημένο στόν πυρήνα ὑδραζίδιο βενζοϊκοῦ ὀξέος, ἀλκαλική ὑδρόλυση.

Εἰσαγωγή

Στήν ἐργασία αὐτή μελετᾶται ἡ ἐπίδραση τοῦ ὑποκαταστάτη ἐπί τῆς ὑδρολύσεως τῶν ὑδραζιδίων τοῦ βενζοϊκοῦ ὀξέος καί γενικώτερα ἡ διερεύνηση τοῦ μηχανισμοῦ τῆς ὑδρολύσεώς τους, ὑπό τήν ἐπίδραση τοῦ ἐπαγωγικοῦ καί τοῦ συζυγιακοῦ φαινομένου[1] πού εἰσάγεται ἀπό τό ἀλογόνο. Ἡ μελέτη αὐτή τῶν ὑδραζιδίων κρίθηκε ἀναγκαία προκειμένου νά χρησιμοποιηθοῦν σάν ἀναγωγικά σέ ἀντιδράσεις μεταφορᾶς ἠλεκτρονίου καί σέ συνθέσεις ὀργανομεταλλικῶν ἐνώσεων. Εἰδικώτερα στήν παρασκευή διθειοκαρβαμιδικῶν παραγώγων (ἐνώσεων) τά ὁποῖα βρίσκονται ὑπό μελέτη. Στό κείμενο, τά ὑδραζίδια ἀναφέρονται συντομογραφικά σάν XBAH ὅπου X ὁ ὑποκαταστάτης στόν πυρήνα.

Ἀξιοσημείωτες ἐργασίες ἐπί τῆς ὑδρολύσεως τῶν ὑδραζιδίων ἔγιναν ἀπό τόν A.P. Grekov[2,3] καί τούς συνεργάτες του, οἱ ὁποῖοι μελέτησαν τήν ὄξινη καί

βασική ὑδρόλυση τῶν ὑδραζιδίων, ($RCONHNH_2$), ὁρισμένων ἀλειφατικῶν καί ἀρωματικῶν ὀξέων. Μεταξύ αὐτῶν περιλαμβάνονται τά ὑδραζίδια τοῦ βενζοϊκοῦ καί τοῦ μ-χλωρο-βενζοϊκοῦ ὀξέος, τοῦ ὁποίου μελέτησαν μόνο τήν ὄξινη ὑδρόλυση.

Στά φάσματα UV τῶν ὑδραζιδίων γιά ὁρισμένες τιμές pH ἐμφανίζονται δύο ζῶνες ἀπορροφήσεως[4] (σχῆμα 1). Μιά στήν περιοχή 225—260 nm πού ἀποδίδεται στήν διέγερση π→π* καί μιά στήν περιοχή 270—290 nm πού ἀποδίδεται στήν διέγερση n→π*. Ἡ ἔνταση τῆς ζώνης 270—290 nm, ὅπως διαπιστώθηκε καί πειραματικά (σχῆμα 2) αὐξάνεται μέ τήν αὔξηση τῆς τιμῆς τοῦ pH καί ὀφείλεται στήν αὔξηση τῆς συγκεντρώσεως τῆς ἐνολικῆς μορφῆς. Ἐπίσης ἀπό τήν σύγκριση τῶν φασμάτων UV τοῦ π-Cl-BAH καί π-Cl-C_6H_4COOH φαίνεται γιατί ἐπελέγη στήν περιοχή 270-290 nm τό ἀναλυτικό μῆκος κύματος.

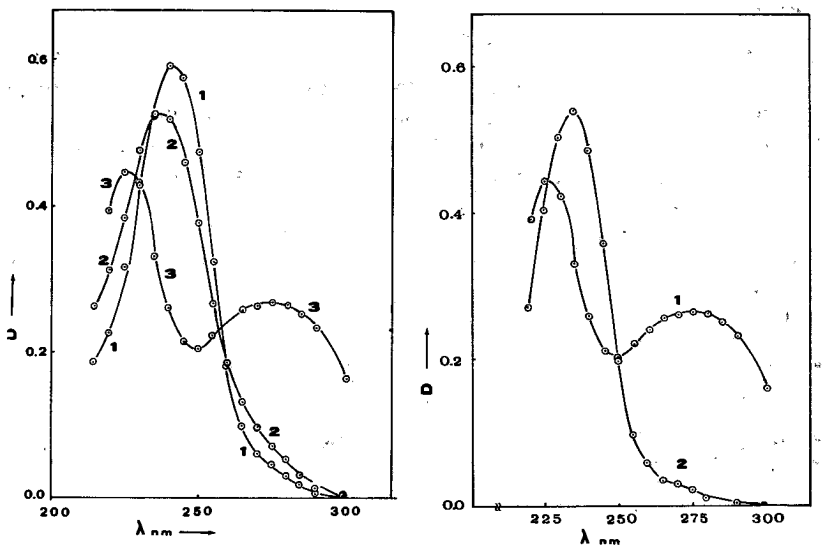

ΣΧΗΜΑ 1. *Ἐξάρτηση τῆς ὀπτικῆς πυκνότητας ἀπό τό μῆκος κύματος τῶν διαλυμάτων τοῦ π-Cl-BAH (C= 4×10^{-5} M) στήν θερμοκρασία τῶν 40 °C σέ 0,1 M HCl (1), σέ οὐδέτερο περιβάλλον (2) καί σέ 0,1 M KOH (3).*

ΣΧΗΜΑ 2. *Ἐξάρτηση τῆς ὀπτικῆς πυκνότητας ἀπό τό μῆκος κύματος τῶν διαλυμάτων τοῦ π-Cl-BAH (1), καί του π-Cl-C_6H_4-COOH (2), συγκεντρώσεων 4×10^{-5} M σέ 1,0 M KOH καί θερμοκρασία 40 °C.*

Πειραματικό μέρος

Ἀντιδραστήρια καί ὄργανα.

Τά ὑδραζίδια πού χρησιμοποιήθηκαν παρασκευάστηκαν σύμφωνα μέ

μέθοδο, πού ἀναφέρεται σέ προηγούμενη ἐργασία.[5] Τά διαλύματα τῶν ὑδραζιδίων παρασκευάστηκαν μέ διάλυση ἀκριβῶς ζυγισμένης ποσότητας μέσα σέ δίς ἀπεσταγμένο νερό. Γιά νά ἀποφύγουμε τήν ὀξειδωτική δράση τοῦ ἀτμοσφαιρικοῦ ὀξυγόνου πάνω στά ὑδραζίδια, τά διαλύματα ἀπαερώθηκαν μέ συνεχή διαβίβαση ἀργοῦ περιεκτικότητας σέ Ar > 99,995 %.

Τά διαλύματα τοῦ H_2SO_4 καί τοῦ KOH πού χρησιμοποιήθηκαν παρασκευάσθηκαν ἀπό ἀναλυτικῆς καθαρότητας ἀντιδραστήρια τοῦ οἴκου **Merck** καί τιτλοδοτήθηκαν μέ διαλύματα **Titrisol** HCl καί KOH τοῦ ἴδιου οἴκου. Γιά τά διαλύματα αὐτά χρησιμοποιήθηκε ἐπίσης δίς ἀπεσταγμένο νερό ἀπαερωμένο μέ ἀργό.

Οἱ μετρήσεις πάρθηκαν μέ φασματοφωτόμετρο **Karl Zeiss PMQ II** τό ὁποῖο εἶχε σύστημα θερμοστατήσεως τῶν κυψελίδων. Ἡ θερμοστάτηση τῶν ἀρχικῶν διαλυμάτων ἔγινε σέ ἀνεξάρτητη παράλληλη διάταξη καί στίς δύο περιπτώσεις χρησιμοποιήθηκαν θερμοστάτες ροῆς νεροῦ τύπου **Gebrüder Haake K.G. Typ. Fe.** Ἀκρίβεια θερμοστατήσεως $\pm$ 0,2 °C.

Οἱ ἀπαιτούμενες ποσότητες τῶν διαλυμάτων ἀναμιγνύονταν πρίν ἀπό τήν λήψη τῶν μετρήσεων μέ προσθήκη τοῦ H_2SO_4 ἤ τοῦ KOH στό διάλυμα τοῦ ὑδραζιδίου.

Ἡ μελέτη τῆς ὑδρολύσεως τῶν ὑδραζιδίων ἔγινε σέ θερμοκρασίες 40 ἕως 60 °C καί συγκεντρώσεις ὀξέος καί βάσεως μέχρι 2,0 N. Τά ὄξινα καθώς καί τά οὐδέτερα διαλύματα τῶν ὑδραζιδίων ἔδειξαν ἀξιοσημείωτη σταθερότητα τῆς ὀπτικῆς πυκνότητας σέ συνάρτηση μέ τό χρόνο σέ ὅλη τήν ἔκταση τοῦ φάσματος. Μεταβολές παρατηρήθηκαν μόνο σέ ἀλκαλικό περιβάλλον καί συγκεκριμένα σέ τιμές pH > 10.

Οἱ μετρήσεις τιμῶν τοῦ pH ἔγιναν μέ πεχάμετρο τοῦ οἴκου **L. Pusl Amt** 112 πού εἶχε ἠλεκτρόδια ὑάλου καί καλομέλανος. Οἱ μετρήσεις τοῦ pH τῶν διαλυμάτων ἔγιναν σέ σταθερή θερμοκρασία.

Καθορισμός τῶν προϊόντων τῆς ἀντιδράσεως.

Ὁ καθορισμός τῶν προϊόντων τῆς ἀντιδράσεως ἔγινε σέ πυκνότερα διαλύματα μέ συγκεντρώσεις ὑδραζιδίων περίπου δεκαπλάσιες τῶν χρησιμοποιηθέντων.

Μετά τήν ὀξίνιση τῶν διαλυμάτων ὑδραζιδίου—ὑδροξειδίου τοῦ καλίου ἐμφανίσθηκε λευκό στερεό. Ἀπό τό σημεῖο τήξεως καί ἀπό τό φάσμα I.R. τῆς οὐσίας ἀποδείχθηκε ὅτι εἶναι τό ἀντίστοιχο ἀρωματικό ὀξύ τοῦ ὑδραζιδίου.

Μετά τήν ἀπομάκρυνση τοῦ ἀρωματικοῦ ὀξέος μέ διήθηση, προστέθηκε στό διήθημα $KBrO_3$ σέ περίσσεια γιά τόν προσδιορισμό τῆς ὑδραζίνης. Μετά δεκαπεντάλεπτη παραμονή προστέθηκε στό διάλυμα ὁρισμένη ποσότητα KI καί τό I_2 πού ἀπελευθερώθηκε, ὀγκομετρήθηκε μέ πρότυπο διάλυμα $Na_2S_2O_3$[6].

Ἀποτελέσματα καί Συζήτηση

Ὁ καθορισμός τῆς τάξεως τῆς ἀντιδράσεως ἔγινε γραφικῶς ἀπό τό διάγραμμα τῆς μεταβολῆς τῆς τιμῆς τῆς παραστάσεως $\log(D_t - D_\infty)$ σέ

συνάρτηση μέ τόν χρόνο[7,8] (σχῆμα 3). Τά δύο εὐθύγραμμα τμήματα πού ὑπάρχουν σέ κάθε καμπύλη ὁδηγοῦν στήν ὑπόθεση ὅτι συμβαίνουν δύο διαδοχικές ἀντιδράσεις[9,10,11].

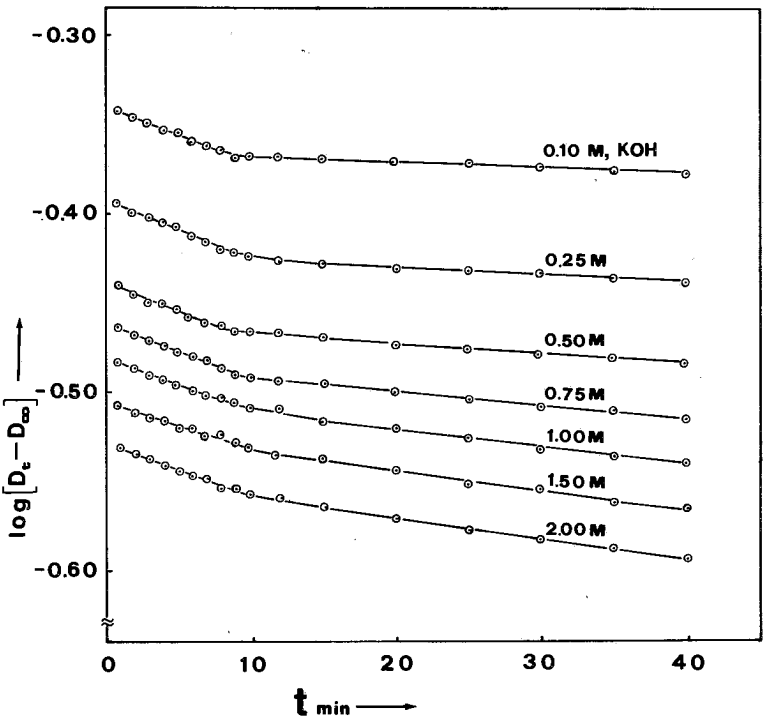

ΣΧΗΜΑ 3. *Ἐξάρτηση τοῦ log (Dt-D$_\infty$) ἀπό τό χρόνο γιά σταθερή συγκέντρωση π-Br-BAH (C=8×10^{-5} M) καί γιά διάφορες συγκεντρώσεις KOH. (Θ=50 ^{0}C, λ_{av}=280nm).*

Στήν ἀρχή, πρακτικά, γίνεται μόνο ἡ ταχύτερη ἀντίδραση ἐνῶ μετά τά 30 min συνεχίζεται ἡ βραδεία. Ἐπομένως ἡ ὀπτική πυκνότητα τοῦ προϊόντος τῆς πρώτης ἀντιδράσεως (D∞_1) θεωρεῖται ὅτι εἶναι ἡ ὀπτική πυκνότητα τοῦ ἀντιδρῶντος συστατικοῦ τῆς δεύτερης ἀντιδράσεως (D$_{02}$) σέ χρόνο μηδέν γιά τήν δεύτερη ἀντίδραση.

Ἡ D∞_1 ὑπολογίζεται μέ βάση τή σχέση

$$D_{\infty 1} = \frac{D_t^2 - D_{01} - D_{2t}}{2D_t - (D_{2t} + D_{01})}$$

όπου D_{01} εἶναι ἡ τιμή τῆς ὀπτικῆς πυκνότητας τοῦ ἀρχικοῦ συστατικοῦ σέ χρόνο μηδέν, D_t εἶναι ἡ τιμή τῆς ὀπτικῆς πυκνότητας σέ χρόνο t_1 κατά τήν πρώτη ἀντίδραση καί $D_{\infty 1}$ εἶναι ἡ τιμή τῆς ὀπτικῆς πυκνότητας τῆς ἴδιας ἀντιδράσεως σέ διπλάσιο χρόνο.

Ἡ σταθερά ταχύτητας τῆς πρώτης ἀντιδράσεως k_1 ὑπολογίζεται ἀπό τήν κινητική ἐξίσωση τῶν ἀντιδράσεων πρώτης τάξεως.

$$\log (D_t - D_{\infty 1}) = \log (D_{01} - D_{\infty 1}) - \frac{k_1}{2{,}303} t \qquad (2)$$

στήν ὁποία ὁ χρόνος t λαμβάνεται ἐπί τοῦ πρώτου εὐθύγραμμου τμήματος τοῦ σχήματος 3.

Ἡ k_2 ὑπολογίζεται ἀπό τήν κινητική ἐξίσωση τῶν διαδοχικῶν ἀντιδράσεων.

$$|B| = |A|_0 \frac{k_1}{k_2 - k_1} [e^{-k_1 t} - e^{-k_2 t}] \qquad (3)$$

όπου $|A|_0$ εἶναι ἡ ἀρχική συγκέντρωση τοῦ ὑδραζιδίου, $|B|$ εἶναι ἡ συγκέντρωση τοῦ προϊόντος τῆς πρώτης ἀντιδράσεως σέ χρόνο t. Ἡ $|B|$ ὑπολογίζεται ὡς ἑξῆς:

Σέ χρόνο κατά τόν ὁποῖο ἡ πρώτη ἀντίδραση θεωρεῖται ὅτι ἔχει τελειώσει θά ἰσχύει ἡ σχέση:

$$|B| + |\Gamma| = |XBAH| \qquad (4)$$

όπου $|\Gamma|$ εἶναι ἡ συγκέντρωση τοῦ τελικοῦ προϊόντος καί $|XBAH|$ εἶναι ἡ ἀρχική συγκέντρωση τοῦ ὑδραζιδίου.

Ἀπό τήν σχέση (4) προκύπτει

$$\frac{D_t(B)}{\varepsilon_B} + \frac{D_t(\Gamma)}{\varepsilon\Gamma} = |XBAH| \qquad (5)$$

όπου $D_{t(B)}$ καί $D_{t(\Gamma)}$ εἶναι οἱ ὀπτικές πυκνότητες τῶν συστατικῶν Β καί Γ σέ χρόνο t καί ε_B καί ε_Γ οἱ μοριακοί συντελεστές ἀποσβέσεως τῶν συστατικῶν Β καί Γ στό ἀναλυτικό μῆκος κύματος.

Στό ἀναλυτικό μῆκος κύματος ἡ ὀπτική πυκνότητα τοῦ προϊόντος Γ, δηλαδή τοῦ ἀρωματικοῦ ὀξέος, εἶναι ἀμελητέα, ἐπομένως ὁ μοριακός συντελεστής ἀποσβέσεως ε_B δίνεται ἀπό τήν σχέση:

$$\varepsilon^B = \frac{D_{\infty 1}}{|XBAH|} = \frac{D_{02}}{|XBAH|} \qquad (6)$$

Μέ τήν παραπάνω παραδοχή καί μέ συνδυασμό τῶν σχέσεων 5 καί 6 ὑπολογίζεται ἡ $D_{t(B)}$ ἀπό τήν ὁποία μπορεῖ νά ὑπολογισθεῖ ἡ συγκέντρωση τοῦ συστατικοῦ Β σέ χρόνο t, ἀπό τήν σχέση $\varepsilon_B / |B| = D_{t(B)}$ (7)

Γιά χρόνο $t > 2500$ sec ή τιμή τῆς παραστάσεως e^{-k_1} τῆς ἐξισώσεως 3 γίνεται πολύ μικρότερη ἀπό τήν e^{-k_2} ἔναντι τῆς ὁποίας μπορεῖ νά παραλειφθεῖ.

Ἐπομένως ἡ κινητική ἐξίσωση τῶν διαδοχικῶν ἀντιδράσεων μπορεῖ νά ἐφαρμοσθεῖ μέ τήν μορφή

$$e^{-ak_2} - \beta k_2 + \gamma = 0 \quad \text{ἤ} \qquad (8)$$

$$\frac{a^2k_2^2}{2} + (\beta-\alpha)k_2 + (1-\gamma) = 0 \qquad (9)$$

ὅπου α εἶναι ὁ χρόνος σέ sec, $\beta = \left[\frac{[B]}{[A]_o} \cdot \frac{1}{k_1}\right]$ καί $\gamma = \frac{[B]}{[A]_o}$

Ἡ ἐπίλυση τῆς ἐξισώσεως 9 δίνει δύο τιμές τῆς k_2 ἀπό τίς ὁποῖες μιά μόνον ἐπαληθεύει τό πείραμα.

Γιά τόν καθορισμό τοῦ μηχανισμοῦ τῆς ἀντιδράσεως μελετᾶται ἡ ἐπίδραση τῆς συγκεντρώσεως τοῦ KOH ἐπί τῆς ταχύτητας τῆς ἀντιδράσεως σέ σταθερή ἰονική ἰσχύ 2M, μέ KCl. Γιά τό σκοπό αὐτό μετρήθηκαν οἱ ὀπτικές πυκνότητες σέ συνάρτηση μέ τόν χρόνο, διαλυμάτων ὑδραζιδίων διαφόρων συγκεντρώσεων καί σέ διάφορες συγκεντρώσεις KOH. Οἱ τιμές τῶν συγκεντρώσεων αὐτῶν κυμαίνονταν γιά τά ὑδροζίδια ἀπό $0{,}8\times10^{-4}$ M ἕως $1{,}0\times10^{-4}$ καί τό KOH ἀπό 0,1 ἕως 2,0M. Τυπικά ἀποτελέσματα τῆς μελέτης αὐτῆς γιά τήν περίπτωση τοῦ π-Br-BAH δίδονται στόν πίνακα I.

ΠΙΝΑΚΑΣ I. *Τιμές τῶν* k_1 *καί* k_2 *γιά σταθερή συγκέντρωση π-Br-BAH* ($C=1{,}0\times10^{-4}$ *M) καί διάφορες συγκεντρώσεις KOH σέ* $\Theta=50\ ^0C$ *καί σταθερή ἰονική ἰσχύ 2,0 M.*

|KOH| mol.lit^{-1}	|OH^-|* mol.lit^{-1}	$k_1\times10^3$ sec^{-1}	$k_2.10^5$ mol^{-1}.lit.sec^{-1}
0,10	0,069	2,0	1,3
0,25	0,174	2,2	1,5
0,50	0,347	2,4	2,6
0,75	0,550	2,7	5,1
1,00	0,775	2,1	6,6
1,25		2,5	6,4
1,50		2,2	6,2
2,00		2,6	5,6

* Οἱ συγκεντρώσεις τῶν ἰόντων OH^- ὑπολογίζονται ἀπό τίς τιμές τοῦ pH.

'Από τά ἀποτελέσματα τῆς κινητικῆς μελέτης τῆς ὑδρολύσεως καί τῶν ὑπολοίπων ὑδραζιδίων, προκύπτει ὅτι ἡ k_1 εἶναι ἀνεξάρτητη τῆς συγκεντρώσεως τοῦ KOH, γιά τήν περιοχή συγκεντρώσεων KOH 0,1 ἕως 2M, (σχῆμα 4) ἐνῶ ἡ k_2 αὐξάνεται μέχρι περίπου τήν συγκέντρωση 1,0 M KOH (σχῆμα 5). Κατόπιν καί μέχρι τή συγκέντρωση 2,0 M KOH ἡ k_2 τείνει νά ἐλαττωθεῖ. 'Ανάλογη ἐπίδραση τῆς συγκεντρώσεως τῶν ἰόντων OH^- παρατηρήθηκε καί στήν κινητική ὑδρολύσεως τοῦ ο-ὑδροξυλαμινο-σουλφονικοῦ ὀξέος[12].

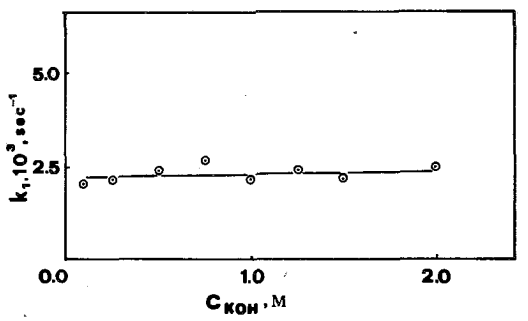

ΣΧΗΜΑ 4. *Συσχέτιση τῶν τιμῶν τῆς* k_1 *μέ τήν συγκέντρωση τοῦ KOH γιά τό π-Br-BAH σέ* Θ=50 °C, *(Cπ-Br-BAH= 1,0 × 10⁻⁴ M).*

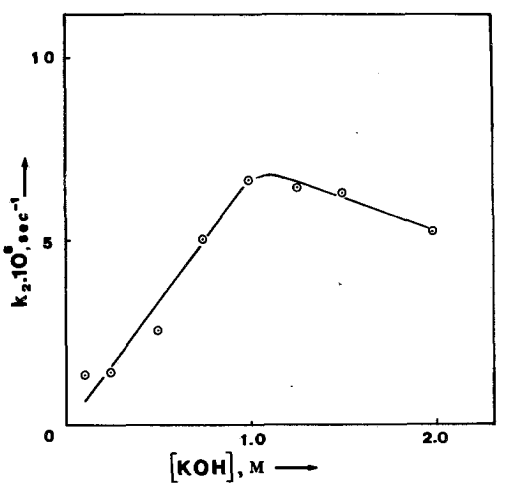

ΣΧΗΜΑ 5. *'Εξάρτηση τῆς* k_2 *ἀπό τήν συγκέντρωση τοῦ KOH διά τό π-Br-BAH σέ* Θ=50 °C, *(Cπ-Br-BAH=1,0×10⁻⁴ M).*

Η ταχύτητα τῆς ὅλης ἀντιδράσεως μπορεῖ νά ἀποδοθεῖ ἀπό τήν σχέση:

$$\upsilon = k_1 |XBAH| + k_2 |XBAH| |OH^-| \qquad (10)$$

ἡ ὁποία μετά ἀπό περίπου 30 min μπορεῖ μέ μεγάλη προσέγγιση, νά γραφεῖ ὡς ἑξῆς:

$$\upsilon = k_2 |XBAH| |OH^-| \qquad (11)$$

ἡ ὁποία ἀναλυτικά δίνεται μέ τήν μορφή

$$\upsilon = \{k_a|HK| + k_b |HE|\}|OH^-| \qquad (12)$$

ὅπου k_a εἶναι ἡ σταθερά ταχύτητας ὑδρολύσεως τῆς κετονικῆς μορφῆς HK, k_b εἶναι ἡ σταθερά ταχύτητας ὑδρολύσεως τῆς ἐνολικῆς μορφῆς HE, |HK| εἶναι ἡ συγκέντρωση τῆς κετονικῆς μορφῆς καί |HE| εἶναι ἡ συγκέντρωση τῆς ἐνολικῆς μορφῆς.

Εἶναι φανερό ὅτι $|XBAH|_{\text{ἀρχική}} = |HK| + |HE|$. Ἐπειδή ὅμως ὑπάρχει ἡ ἰσορροπία

$$|HK| + |OH^-| \rightarrow |HE| \qquad (13)$$

τελικά παίρνουμε τή σχέση

$$|HK| |OH^-| \rightleftarrows K|HE| \qquad (14)$$

Μέ συνδυασμό τῶν ἐξισώσεων (12) καί (14) προκύπτει ἡ σχέση

$$\upsilon = k_a K + k_b |OH^-| |HE| \qquad (15)$$

$$\text{ὅπου } k_a K + k_b |OH^-| = k_2 \qquad (16)$$

Οἱ τιμές $k_a K$ μποροῦν νά ὑπολογισθοῦν ἀπό τό διάγραμμα τῆς μεταβολῆς τῆς k_2 σέ συνάρτηση μέ τή συγκέντρωση τῶν ἰόντων OH^- γιά σταθερή συγκέντρωση ὑδραζιδίων. Στήν παρούσα μελέτη οἱ τιμές αὐτές εἶναι τῆς τάξεως 10^{-8} γιά τήν θερμοκρασία τῶν 50 °C.

Η τιμή τῆς k_1 γιά τήν περιοχή θερμοκρασιῶν 40-60 °C ἐλάχιστα ἐπηρεάζεται ἀπό τήν θερμοκρασία. Τό μή ὑποκατεστημένο ὑδραζίδιο ἐμφανίζει τήν μεγαλύτερη τιμή τῆς $k_1 = (3,4 + 0,4).10^{-3}$ sec^{-1} ἐνῶ ἡ εἰσαγωγή τοῦ ἀλογόνου προκαλεῖ ἐλάττωση τῆς σταθερᾶς ταχύτητας τῆς ἀντιδράσεως. Ἔτσι γιά τά π-ὑποκατεστημένα ὑδραζίδια λαμβάνεται τιμή $k_1 = (2,0 + 0,6).10^{-3} sec^{-1}$ καί γιά τά μ-ὑποκατεστημένα ἡ τιμή $k_1 = (1,3 + 0,3).10^{-3}$ sec^{-1}. Τά ο-ὑποκατεστημένα, πλήν τοῦ o-F-BAH ἐμφανίζουν ἀξιοσημείωτη σταθερότητα τῆς ὀπτικῆς πυκνότητας σέ συνάρτηση μέ τό χρόνο, ἐπί ἀρκετές ὧρες. Γιά τό o-F-BAH ἔχει βρεθεῖ ἡ τιμή $k_1 = (1,8 + 0,2).10^{-3}$ sec^{-1}. Οἱ ὑπολογιζόμενες τιμές τῆς ἐνέργειας ἐνεργοποιήσεως κυμαίνονται γενικά ἀπό 0,5 ἕως 2,0 kcal.mol $^{-1}$.

Στούς πίνακες II καί III δίνονται οἱ ὑπολογισθεῖσες τιμές τῆς k_2 καί τῆς ἐνέργειας ἐνεργοποιήσεως E_a ὅλων τῶν ὑδραζιδίων πού μελετήθηκαν.

ΠΙΝΑΚΑΣ ΙΙ. *Τιμές τῆς* k_2 *καί* Ea *ἀπό τήν κινητική μελέτη τῆς ὑδρολύσεως τοῦ HBAH.*

Θ °C.	$k_2.10^5$ mol $^{-1}$.lit.sec^{-1}	Ea kcal.mol^{-1}
60	8.5	
50	3.0	24.4
40	0.8	

Γιά τήν πρώτη ἀντίδραση γίνεται δεκτό ὅτι συμβαίνει ἐνολοποίηση τοῦ ὑδραζιδίου κατά τό σχῆμα

$$R - \overset{\overset{O}{\|}}{C} - NHNH_2 + KOH \rightleftharpoons R - \overset{O^-}{C} = NNH_2 + K^+ + H_2O \qquad (17)$$

Ἡ ἀντίδραση 17 σέ περίσσεια KOH εἶναι ποσοτική. Γιά συγκεντρώσεις ὅμως KOH ἀπό 0,1 M ἕως 2,0 M εἶναι πρώτης τάξεως καί ἀνεξάρτητη τῆς συγκεντρώσεως τοῦ KOH[13]. Τό ἰόν ὑδρογόνου προέρχεται ἀπό τήν ἰμινοομάδα γιατί τό ὑδρογόνο τῆς ἰμινοομάδας εἶναι πιό ὄξινο ἀπό τά ὑδρογόνα τῆς ἀμινοομάδας. Αὐτό ὀφείλεται στήν τάση σχηματισμοῦ συστήματος διπλῶν δεσμῶν διά τῆς μετατοπίσεως τῶν φορτίων ἀπό τό ἄζωτο τῆς ἀμινοομάδας πρός τά ἄτομα τοῦ ἄνθρακα καί τοῦ ὀξυγόνου[14].

Ἡ ἀπόσπαση τοῦ ἰόντος ὑδρογόνου σέ συνδυασμό μέ τήν δημιουργία sp^2 ὑβριδισμοῦ στό ἄτομο τοῦ ἀζώτου ἔχει σάν ἀποτέλεσμα τήν ἐμφάνιση τριῶν p ἀτομικῶν τροχιακῶν, ἑνός ἀπό κάθε ἄτομο O, C καί N. Τά p ἀτομικά τροχιακά ὑπό τήν ἐπίδραση τῶν ἰόντων OH^- ὑφίστανται ἰσχυρή πόλωση. Ἡ πόλωση αὐτή μπορεῖ νά ὁδηγήση σέ πυρηνόφιλη προσβολή πρός σχηματισμό (ἐνδιαμέσου) συστατικοῦ II.

$$R - \overset{\overset{O}{\|}}{C} - NHNH_2 \;(I) \quad + H_2O \underset{k_{-3}}{\overset{k_3}{\rightleftharpoons}} \left[R - \overset{\overset{O}{\|}}{C} - \overset{\curvearrowright}{N} - NH_2 \right] \;(II) \xrightarrow{k_4}$$

$$\longrightarrow R - \overset{\overset{O}{\|}}{\underset{\underset{OH}{|}}{C}} \;(III) + \overset{\curvearrowright}{N}HNH_2 \longrightarrow R - \overset{\overset{O}{\|}}{\underset{\underset{O^-}{|}}{C}} + H_2NNH_2 \qquad (18)$$

ΠΙΝΑΚΑΣ ΙΙΙ. *Τιμές τῆς* k_b *καί τῆς* Ea *ἀπό τήν κινητική μελέτη τῆς ἀλκαλικῆς ὑδρολύσεως τῶν ὑδραζιδίων.*

		ορθο		*μετα*		*παρα*	
Ὑδραζίδιο	Θ °C	$k_2.10^5$ $mol^{-1}.lit.sec^{-1}$	Ea kcal.mol^{-1}.	$k_2.10^5$ $mol^{-1}.lit.sec^{-1}$.	Ea kcal.mol.	$k_2.10^5$ $mol^{-1}.lit.sec^{-1}$	Ea kcal.mol.
F-BAH	60	6.2		20.2		2.8	
	50	3.7	11.8	14.2	7.9	2.2	4.2
	40	2.0		9.4		1.7	
Cl-BAH	60	—		10.2		11.6	
	50	—		5.6	13.6	6.7	13.3
	40	—		2.7		3.2	
Br-BAH	60	—		15.7		9.5	
	50	—		6.8	16.5	6.6	7.5
	40	—		3.2		4.6	
I-BAH	60	—		17.0		7.1	
	50	—		8.1	14.9	5.9	5.4
	40	—		4.0		4.2	

Τό βραδύ στάδιο τό ὁποῖο καθορίζει τήν ὁλική ταχύτητα ἀντιδράσεως ὑδρολύσεως εἶναι τό στάδιο μετατροπῆς τοῦ συστατικοῦ II πρός τό ἀντίστοιχο ὀξύ III καί τήν ὑδραζίνη [11,12,13].

Κατά τόν προτεινόμενο μηχανισμό ἡ σταθερά ταχύτητας τῆς ὅλης ἀντιδράσεως προκύπτει λαμβάνοντας ὑπ' ὄψη ὅτι ἡ ταχύτητα σχηματισμοῦ τοῦ συστατικοῦ II εἶναι ἴση μέ τήν ταχύτητα μετατροπῆς τοῦ (steady state approximation)[7], δηλαδή

$$\frac{d|II|}{dt} = k_3 |I| - \left[k_{-3} + k_4\right]|II| = 0 \qquad (19)$$

καί ἡ τιμή k_b (ἐξίσωση 16), δίνεται ἀπό τήν σχέση

$$k_b = \frac{k_3 k_4}{k_{-3}+k_4} \qquad (20)$$

Μέ συνδυασμό τῶν ἐξισώσεων 15 καί 20 προκύπτει ὅτι γιά συγκεντρώσεις KOH 0,1 — 1.0 ἰσχύει ἡ σχέση

$$\upsilon = k_a K + \frac{k_3 k_4}{k_{-3}+k_4} |OH| \quad |HE| \qquad (21)$$

Συμπεράσματα

Στό σύστημα ὑδραζιδίων —ΚΟΗ γίνονται διαδοχικές ἀντιδράσεις ταυτομερειώσεως καί ὑδρολύσεως. Ἡ ταχύτητα ταυτομερειώσεως γιά τήν περιοχή συγκεντρώσεων ΚΟΗ 0,1 — 2,0 Μ εἶναι ἀνεξάρτητη τῆς συγκεντρώσεως τοῦ ΚΟΗ.

Ἡ εἰσαγωγή τοῦ ἁλογόνου προκαλεῖ ἐλάττωση τῆς ταχύτητας τῆς ἀντιδράσεως ταυτομερειώσεως καί μάλιστα ἡ ἐλάττωση αὐτή βαίνει ἀντίθετα πρός τήν αὔξηση τῆς ἱκανότητας ἰονισμοῦ τοῦ ὑδραζιδίου. Τό —I ἐπαγωγικό φαινόμενο τό ὁποῖο εἰσάγει τό ἁλογόνο παρεμποδίζει τήν μετατόπιση φορτίων πρός τήν καρβονυλική ὁμάδα καί κάνει λιγώτερο ἠλεκτραρνητικό τό καρβονυλικό ὀξυγόνο.

Ἡ ὑδρόλυση γίνεται κατά τόν μηχανισμό $B_{AC}2$. Ἡ ταχύτητα ὑδρολύσεως αὐξάνεται μέ τήν εἰσαγωγή τοῦ ἁλογόνου καί ἡ ἐνέργεια ἐνεργοποιήσεως ὑφίσταται σημαντική μείωση. Πράγματι ἡ εἰσαγωγή τοῦ +R φαινομένου εὐνοεῖ τήν αὔξηση τῆς ἠλεκτρονικῆς πυκνότητας τοῦ καρβονυλικοῦ δεσμοῦ καί προκαλεῖ ἐξασθένηση τοῦ ἀμιδικοῦ δεσμοῦ. Τοῦτο προκαλεῖ ἐλάττωση τῆς ἐνέργειας ἐνεργοποιήσεως τοῦ συστήματος καί καλύτερη «τακτοποίηση» τοῦ μορίου στήν κατάσταση τοῦ μεταβατικοῦ σταδίου.

Ἐμφανίζεται ἐπίσης σημαντικό ὀρθο-φαινόμενο ἐξ' αἰτίας τοῦ ὁποίου δέν διαπιστώθηκε ὑδρόλυση μέ τίς συνθῆκες συγκεντρώσεων καί θερμοκρασιῶν τοῦ πειράματος, γιά τά ὑδραζίδια τοῦ o-Cl, o-Br καί o-I βενζοϊκοῦ ὀξέος.

Abstract

Study of the hydrolysis of halogen substituted benzoic acid hydrazides

The kinetics of the hydrolysis of halogen ring substituted benzoic acid hydrazides  -CONHNH$_2$ (where X = F, Cl, Br and I in o-, m- and p- position) is studied spectrophotometrically, in alkaline solutions, at a temperature range of 40-60 °C.

There take place the successive reactions of enolization and hydrolysis. The corresponding rate constant values are of the order of 10^{-3} sec^{-1} and 10^{5} mol^{-1}.lit.sec^{-1}, respectively.

The kinetics of the enolization is little affected by the temperature and the substituent. On the other side the temperature as well as the position and the nature of the substituent has a signigicant influence on the reaction rate of the hydrolysis.

Βιβλιογραφία

1. Hammet, L.P.,*Physical Organic Chemistry*, McGraw-Hill, second edition, New York 1970, p. 374.
2. Grekov, A., Chevchenco-Korthenetskaya, I., Malyutenk, S. & Maurenic, O.: *Zh. Org. Khim.*, **6**, (1) 94 (1970).
3. Grekov, A., Chevchenco-Korthenetskaya, I., Malyutenk, S. & Maurenic, O.: *Zh. Org. Khim.*, **6**, (1) 98 (1970).
4. Manoussakis, G.E., Haristos, D.A., & Youri, C.E.: *Can. J. Chem.*, **51**, 811 (1973).
5. Manoussakis, G.E., Haristos, D.A. & Youri, C.E.: *Chim. Chronika*, **1**, 182 (1972).
6. Meites, L.: *Handbook of analytical Chemistry*, McGraw-Hill, New York 1963 p. 3-68.
7. Yatsimirski, K.B., *Kinetic methods of analysis*, Pergamon Press, Glascow 1966, p. 31.
8. Emanuel, N. & Knorre, D.: *Cinetic Chimique, Traduction Francaise, Edition Mir, Moscou*, 1975, p. 189.
9. Pilling, M.J., *Reaction kinetics*, Clarendon Press, Oxford 1975, p. 70.
10. Buckincham, D.A., Francis, D.J. & Sargenson, A.M.: *Inorg. Chem.*, **13**, 2630, (1974).
11. Dunn, A.S.: *J. Chem. Soc.*, 4687 (1957).
12. Steinmetz, W.E., Robinson, D.H. & Ackermann, M.N.: *Inorg. Chem.*, **14**, 421, (1971).
13. Fay, D.F., Nichols, A.R., Jr. & Sutin, N.: *Inorg. Chem.*, **10**, 2096 (1971).
14. Nonoyama, N., Stomita, S. & Yamasaki, K.: *Inorg. Chim. Acta*, **12**, 33, (1975).

Chimika Chronika, New Series, 10, 175-184 (1981)

KINETIC STUDY OF THE OXIDATION OF BENZOIC ACID HYDRAZIDE BY COPPER(II) CHLORIDE.

DEMETRIUS A. HARISTOS and GEORGE E. MANOUSSAKIS.
Laboratory of Inorganic Chemistry, Aristotelian University of Thessaloniki, Greece.

(Received January 10, 1980; Revised December 4, 1980)

Summary

The kinetics of the oxidation of benzoic acid hydrazide (HBAH) by copper (II) chloride is studied at different temperatures, in different acid consentrations and in several ionic strength values in the absence of oxygen.

The reaction rate is first order for each reactant and decreases linearly with the increase of the acid consentration at the pH range 4,4-5,6.

There is also a small dependence on the ionic strength showing a partly ionic character due to the reaction between the polar structure of the HBAH and the Cu(II) ion.

The mechanism of the main reaction is that of one electron's. The electron is transferred from the C-N bond to the Cu(II) by the π^* antibonding orbital of the C-O bond.

Key words: benzoic acid hydrazide, copper(II) chloride, oxidation, reduction, optical density, ionic strength, reaction rate, order and mechanism of reaction.

Abbreviations: HBAH: benzoic acid hydrazide.

Introduction

This paper deals with the redox system of benzoic acid hydrazide-copper (II) chloride and especially refers to the stoichiometry, the order and the mechanism of the reaction.

The oxidation of hydrazides in the presence of copper (II) salts is already known[1,8]. These oxidations were first observed during the preparations of several hydrazide-copper (II) complexes. In these cases various oxidation products were determined while part of the copper (II) ions could possibly have undergone reduction to the monovalent state.

Experimental

Reagents and instruments

The benzoic acid hydrazide (abbreviated as HBAH) was prepared by adding hydrazine hydrate in benzoic acid ethylester[9].

The HBAH standard solutions were prepared by dissolving accurately weighted amounts of it in triple distilled water deairated by continuous bubbling of argon. The used $CuCl_2 2H_2O$ was recrystallized from water. The stock solutions were checked iodometrically.

The buffer solutions (pH range 3.8 to 5.6) were prepared[10] by mixing the appropriate quantity of CH_3COOH and KOH solutions. The CH_3COOH became free of reductive agents by distillation in the presence of $KMnO_4$. The pH measurements were carried out in a Beckmann Research pH-meter.

The constant ionic strength was achieved with analytical grade KCl. The rate of the reaction was followed with a Carl Zeiss RMQ II spectrophotometer equipped with a temperature standardizing system.

The measurements of optical density vs time at constant wave lengths were scanned between 260 and 240 nm which is the $\pi-\pi^*$ excitation state[11-12] of the system (fig. 1).

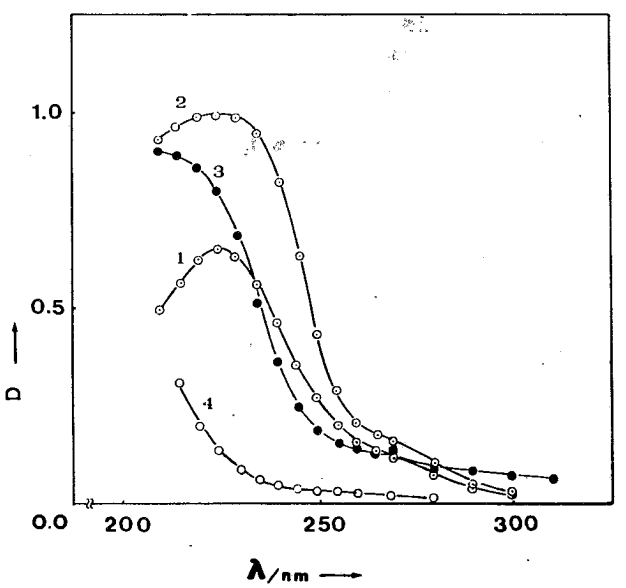

FIG. 1. *Optical density plots vs λ at T=6° C, pH=4.80±0.02 and I=1.25.10⁻² M for the solutions : (1) HBAH (C=8.10⁻⁵ M), (2) mixture of HBAH (C=8.10⁻⁵M) and $CuCl_2$ (C=4.10⁻⁴M) before the reaction (3) the same mixture after the reaction and (4) $CuCl_2$ (C=4.10⁻⁴ M).*

Measurements were also carried out using the stopped flow spectrophotometer, equipped with a Durrum logarithmic amplifier Model D 131.

The idendification and the determination of the reaction products were carried out in solutions of the following initial concentrations; $|CuCl_2|=1.10^{-2} \div 1.10^{-3}$ M and $|HBAH|=1.10^{-3}$–1.10^{-4} M. A gas burret equipped with a temperature standardized system was used to measure nitrogen. Ammonia was detected with Nessler reagent in the distillation products.

The Cu(I) was calculated by determining iodometrically the non reacted Cu(II) after the end of the reaction, in solutions containing an excess of $CuCl_2$.

The determination of the reaction rate was followed by several methods[13-15] at constant ionic strength. The concentrations of the solutions were held constant either for the HBAH or for the $CuCl_2$ while the concentration of the other reagent was changed. The standard solutions of the HBAH were practically unchanged under the conditions of the experiment. This has been checked from the kinetic study of the HBAH hydrolysis[16-17].

Results and discussion

The results of the determination of the reaction products between HBAH and $CuCl_2$ are given in the tables I and II. In these tables are also given the calculated values of the reaction products according to the equation:

$$C_6H_5CONHNH_2 + CuCl_2 + H_2O \rightarrow C_6H_5COOH + 1/2N_2 + NH_4Cl + CuCl \quad (1)$$

TABLE I: *Quantities of N_2 and NH_3 as resulted from the reaction between HBAH ($C=1.10^{-3}$ M) and $CuCl_2$ ($C=1.10^{-2}$ M) in solutions of various initial stoichiometric ratio.*

Stoichiometric ratio of HBAH and $CuCl_2$	N_2/cm³			NH_3/mmol		
	Calcd.	Found	% Diff.	Calcd.	Found	% Diff.
0.40:0.20 (2:1)	2.24	2.32	+3.6	0.200	0.180	—10.0
0.15:0.10 (1.5:1)	1.12	1.16	+3.6	0.100	0.086	—14.0
0.15:0.15 (1:1)	1.68	1.73	+3.0	0.150	0.135	—10.0
0.20:0.30 (0.67:1)	2.24	2.28	+1.8	0.200	0.188	— 6.0
0.10:0.20 (0.5:1)	1.12	1.15	+2.7	0.100	0.092	— 8.0

TABLE II: *Quantities of Cu(I) as calculated from the reaction between HBAH ($C=1.10^{-3}M$) and $CuCl_2$ ($C=1.10^{-2}$ M) in solutions of various initial stoichiometric ratio.*

Stoichiometric ratio of HBAH and $CuCl_2$	Cu(I)/mmol		
	Calcd.	Found	% Diff.
0.80:0.20 (4:1)	0.200	2.215	+ 7.5
0.30:0.15 (2:1)	0.150	0.158	+ 5.3
0.16:0.10 (1.6:1)	0.100	0.112	+12.0

As concluded from tables I and II the reaction is satisfactorily given by the equation (I). Although a small part of the reaction seems to follow the four electron reaction according to the equation:

$$C_6H_5CONHNH_2 + 4CuCl_2 + H_2O \rightarrow C_6H_5COOH + N_2 + 4HCl + 4CuCl \quad (2)$$

Nevertheless, the four electron's reaction for the hydrazine was found to have taken place in strong acidic solutions[18,19]. The quantitative conversion of the hydrazine nitrogen of the hydrazides into elemental nitrogen was found to have taken place during oxidation in the presence of oxygen. This reaction is catalysed by Cu(II) and Cu(I) salts but no quantitative change of the Cu(II) ion is reported[8].

The study of the reaction between HBAH and $CuCl_2$ at higher temperatures (80-100°C) proved an increase of the ratio N_2:NH_3 in the products, and that Cu(I) tends more towards the value as estimated from equation (2).

The increase of the ratio N_2:NH_3 with the temperature could be explained by the following reactions[20,21]:

$$N_4H_6 \underset{\text{heating}}{\rightleftharpoons} 2N_2H_3$$
$$\downarrow \qquad\qquad \downarrow$$
$$N_2 + 2NH_3 \qquad 2N_2 + 6H^+ + 6e$$

As it is shown in fig. 2 and 3 the reaction is one of first order either for the HBAH or for the $CuCl_2$, and the overall reaction was found to follow the kinetics of the second order reaction.

As illustrated in fig. 3 there is a very good linear correlation (r=0.994) between the k_{obs} values and the $CuCl_2$ concentrations. The calculated k value is 16.4 mol $^{-1}$ l s $^{-1}$. On the other hand, for a constant concentration of $CuCl_2$ (4.10^{-4} M) and various concentrations of HBAH ($0.32\text{-}1.28.10^{-4}$ M) at pH = 5.16± 0.02, I = $1.25.10^{-2}$ M and T = 50 °C, k value was 17.1 ± 0.8 mol $^{-1}$ l s $^{-1}$. These two values coincide well, considering also the small difference in pH value.

Applying the data of fig. 4 to equation (3), which is a slightly modified form of the second-order reactions integrated rate expression the calculated k value is 16,5

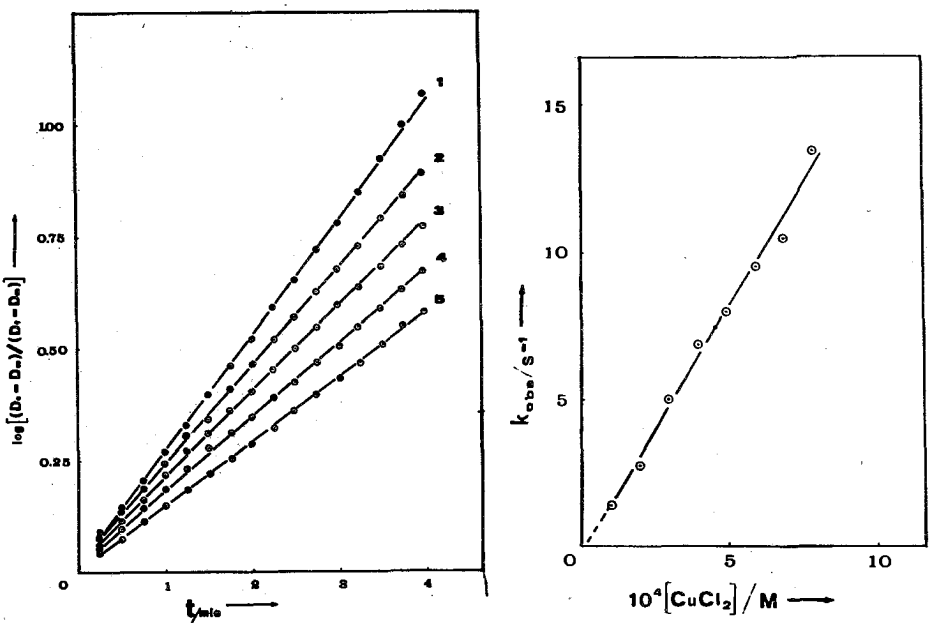

FIG. 2. *First order plots at pH=5.10 + 0.02, I=1.25.10⁻² M, T=50°C with initial |HBAH|=8.10⁻⁵ M and |CuCl₂| are as follows: (1)8.10⁻⁴ M, (2)7.10⁻⁴ M, (3)6.10⁻⁴ M, (4)5.10⁻⁴ M and (5)4.10⁻⁴ M.*

FIG. 3. *Dependence of kobs on |CuCl₂| at pH=5.10 + 0.02, I=1.25.10⁻² M, T=50° C with constant |HBAH|= 8.10⁻⁵ M.*

± 1.3 mol^{-1} $l.s^{-1}$.

In this equation |HBAH| and |$CuCl_2$| are the initial concentrations, Do, Dt and D∞ the optical densities of the system at the beginning of the reaction, at time t. and at the end of the reaction.

$$k = \frac{2.303}{t(|HBAH| - |CuCl_2|)} \log \frac{|CuCl_2|}{|HBAH|} \left\{ \frac{|HBAH| - |HBAH|\left(\frac{D_o - D_t}{D_o - D_\infty}\right)}{|CuCl_2| - |HBAH|\left(\frac{D_o - D_t}{D_o - D_\infty}\right)} \right\} \quad mol^{-1} l\ s^{-1} \qquad (3)$$

Also, by applying the half life method, (under equal initial concentrations from 0.80.10 ⁻⁴ to 2.40.10 ⁻⁴ M at pH values 4.75, 5.00 and 5.24) the resulting average order of the reaction is 2.03.

Influence of acid concentration

In figure 4 is shown the effect of acidity on the oxidation rate of HBAH by $CuCl_2$, studied at constant ionic strength.

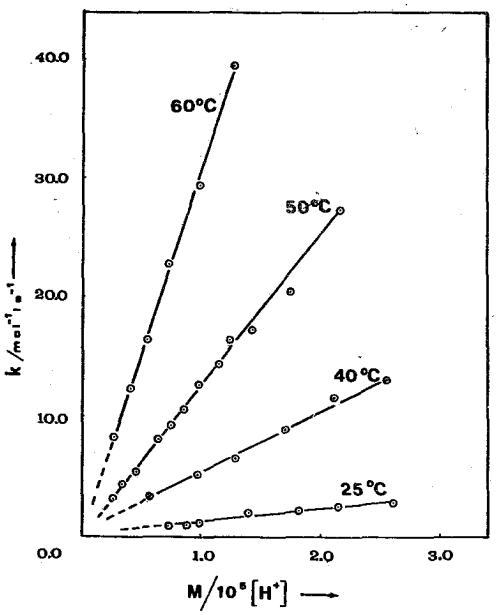

FIG. 4. *Plots of k as a function of* $|H+|^{-1}$ *at different temperatures and I=1.25.10⁻² M for* $|HBAH|=8.10^{-5}$ *M and* $|CuCl_2|=4.10^{-4}$ *M.*

The results showed that the rates decreased linearly with an increase of acid concentration.

The order obtained from the slope of the plot of k vs $|H+|^{-1}$ was -1. Generally, at pH < 4.4 the reaction rate decreases quickly. At pH < 4.0 the k values are very small and the corresponding deviations become large. For pH>5.4 the reaction rate increases quickly but the k values also show large deviations. Under these conditions the overall rate law becomes:

$$\text{Rate} = k \frac{|HBAH|_{tot}}{1 + \frac{|H^+|}{K_{ion}}} |CuCl_2| \qquad (4)$$

where: $k = k' + ka\,|H+|^{-1}$

$|HBAH|_{tot.}$ is the total concentration of the hydradine and Kion is the ionization constant of the protonated form of the hydrazide[12,22]. No evidence has been found for an acid independent path.

The ka values are: ka = (31.0 ± 0.4). 10^{-5} s^{-1} at T=60°C, ka=(12.4±0.6).10^{-5} s^{-1} at 50°C, ka=(5.2 ± 0.3).10^{-5} s^{-1} at 40° C and ka=(1.1 ± 0.1).10^{-5} s^{-1} at 25° C.

The influence of the hydrogen ion could be explained as follows[23,25]: the H+

ion possibly attacks the carbonyl oxygen and thus prevent the donor ability of this group in forming complex compound with the Cu(II) ion.

Influence of ionic strength

The influence of ionic strength was studied in the range of $0.75.10^{-2}$ to $1.625.10^{-1}$ M with KCl[26,27]. Reaction rate measurements were carried out at temperatures of 25, 40, 50 and 60° C and a pH range of 4.75-5.25. As we can see in the plot of log ka vs $I^{1/2}/(1 + I^{1/2})$ (fig. 5) a partly ionic reaction takes place which can be attributed to a reaction between hydrated Cu(II) ions and other possible kinetically active species of Cu(II) hydrolysis, on one side and the polar structure of the hydrazide on the other.

The application on the Arrhenius equation[28] of the values of fig. 4 gives an activation energy Ea of 79,9+1,7 kJ mol^{-1}.

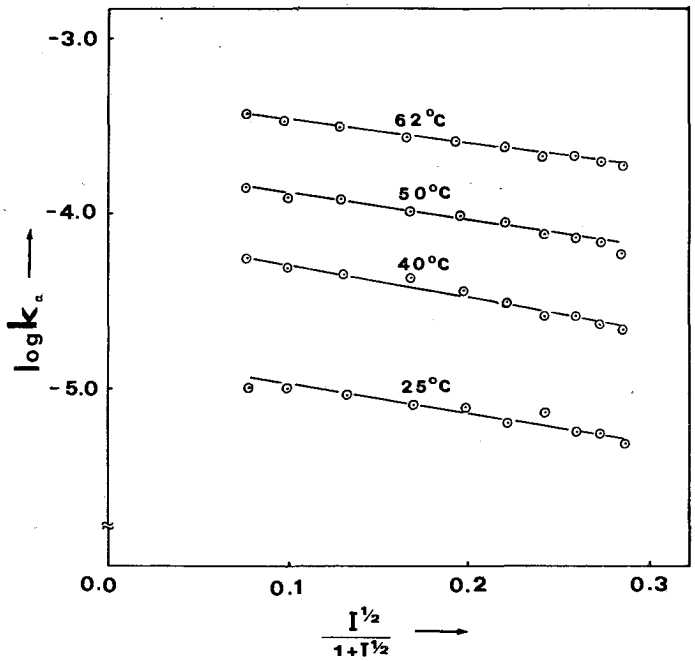

FIG. 5. *Plots of log ka as a function of $I^{1/2}/(1+I^{1/2})$ at different temperatures and a pH range of 4.75-5.25 for $|HBAH|8.10^{-5}$ M and $|CuCl_2|=4.10^{-4}$ M.*

Reaction mechanism

After mixing of the reactants a complex coumpound is formed[29-32]. In this complex the carbonyl oxygen and the aminogroup nitrogen act as donors. More favorable is the oxygen-copper (II) bond[33,34].

The presence of the Cu(II) in the form of the hydrated ion is mainly expected

in this pH and concentration range. Possible forms in very small amounts are also CuOH+, $Cu(CH_3COO)+$ and CuCl+ [35-39]. In the light of the above experimental observations, the following reaction scheme may be suggested:

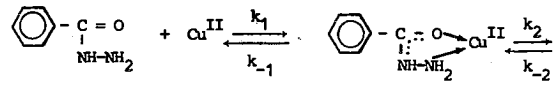

I II

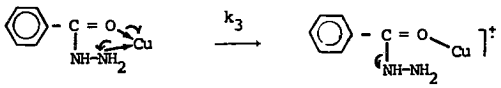

III IV

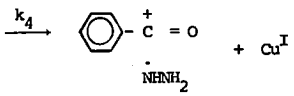

V

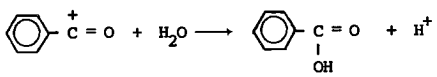

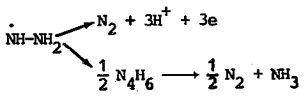

The electron transfer step, is the rate determining slow step of the reaction. The whole reaction takes place with a more complicated mechanism with a possible contribution of the species CuOH+, $Cu(CH_3COO)+$ and CuCl+.

By application of the steady state approximation to the complex (III), the ka of the equation (4) becomes:

$$k_a = K \frac{k_2 k_3}{K_{-2} + k_3}$$

where $K = \frac{k_1}{k_{-1}}$

The electron may be transfered from the amide bond, by the π^*-antibonding orbital of the carbonyl, to the Cu(II) ion. The square planar dsp^2 hybridization of Cu(II) is changed to the tetrahedral sp^3 in Cu(I).

This change in its stereochemistry causes the breaking off of the complex before any rearrangement take place.

Περίληψη

Κινητική μελέτη τῆς ὀξειδώσεως τοῦ ὑδραζιδίου τοῦ βενζοϊκοῦ ὀξέος ἀπό χλωριοῦχο χαλκό (II).

Μελετήθηκε μέ τή μέθοδο τῆς φασματοφωτομετρίας ἡ κινητική τῆς ὀξειδώσεως τοῦ ὑδραζιδίου τοῦ βενζοϊκοῦ ὀξέος ἀπό χλωριοῦχο χαλκό (II).

Ἡ μελέτη ἔγινε σέ διαφορετικές θερμοκρασίες, συγκεντρώσεις ὀξέος καί τιμές ἰονικῆς ἰσχύος, ἀπουσία ὀξυγόνου. Τά προϊόντα τῆς ἀντιδράσεως εἶναι βενζοϊκό ὀξύ, ἄζωτο, ἀμμωνία καί χαλκός (I).

Βρέθηκε ὅτι ἡ ἀντίδραση εἶναι διμοριακή καί πρώτης τάξεως γιά τό καθένα ἀπό τά ἀντιδραστήρια (HBAH καί $CuCl_2$). Ἡ ταχύτητα τῆς ἀντιδράσεως ἐλαττώνεται γραμμικά μέ τήν αὔξηση τῆς συγκεντρώσεως τοῦ ὀξέος γιά περιοχή pH 4,4 ἕως 5,6.

Παρατηρήθηκε ἐπίσης σχετικά μικρή ἐξάρτηση τῆς ταχύτητας τῆς ἀντιδράσεως ἀπό τήν ἰονική ἰσχύ. Ἡ ἐξάρτηση αὐτή μπορεῖ νά ἀποδοθεῖ σέ ἀντίδραση μερικῶς ἰονικοῦ χαρακτήρα μεταξύ τῆς πολικῆς μορφῆς τοῦ HBAH καί τοῦ ἰόντος Cu(II).

Γιά τήν κυρία ἀντίδραση προτείνεται ὁ μηχανισμός μεταφορᾶς ἑνός ἠλεκτρονίου. Δευτερεύουσα ἀντίδραση λαμβάνει χώραν κατά τόν μηχανισμό μεταφορᾶς τεσσάρων ἠλεκτρονίων ὁ ὁποῖος καί εὐνοεῖται ἀπό τήν αὔξηση τῆς θερμοκρασίας.

Τό ἠλεκτρόνιο κατά πάσα πιθανότητα μεταφέρεται ἀπό τόν ἀμιδικό δεσμό σέ κενό τροχιακό τοῦ χαλκοῦ (II) μέσω π* ἀντιδεσμικοῦ τροχιακοῦ τῆς καρβονυλικῆς ὁμάδας ἡ ὁποία δρᾶ σάν γέφυρα γιά τή μεταφορά τοῦ ἠλεκτρονίου.

References and Notes

1. Dutta, A., Manhal, P.K. & Chaudhuri, N.R.: *J. Inorg. Nucl. Chem.* **28**, 2951 (1966).
2. Ahmed, A.D. & Chaudhuri, N.R.: *J. Inorg. Nucl. Chem.* **31**, 2545 (1969).
3. El Sayed, L. & Iskander, M.F.: *J. Inorg. Nucl. Chem.* **33**, 435 (1971).
4. Iskander, M.F., Zayen, S.E., Khalifa, M.A. & El Sayed, L.: *J. Inorg. Nucl. Chem.* **36**, 551 (1974).
5. Miller, J.D. & Morton, D.S.: *Inorg. Nucl. Chem. Lett* **11**, 1 (1975).
6. Baker, R.J., Nyburg, S.C. & Szymanski, J.S.: *J. Inorg. Chem.* **10** 138 (1971).
7. Alcock, J.F., Baker, R.J. & Diamantis, A.A.: *Aust. J. Chem.* **25**, (2), 289, (1972). *Chem. Abstr.* **76**, 67563 g (1972).
8. Tsuji, J., Hayakawa, S. & Takayanagi H.: *Chem. Lett.* **5** 437 (1975).
9. Beilstein: *Handbuch der Organischem Chemie*, Verlag Springer, Berlin **9**, 319.
10. Britton, H.T.S., *Hydrogen Ions*, p. 220 Chapman and Hall Ltd. London 1932.
11. Grammaticakis, P.: *Bull. Soc. Chim. Fr.* 993 (1970).
12. Manoussakis, G.E., Haristos, D.A. & Youri, C.E.: *Can. J. Chem.* **51**, 811 (1973).
13. Yatsimirskii, K.B.: *Kinetic Methods of Analysis*, p. 31 Pergamon Press, Glascow 1966.
14. Weston, K.B., Jr. & Schwarz, H.A.: *Chemical Kinetics*, p. 7 Prentice Hall, New Jersey 1972.

15. Pilling, M.J.: *Reaction Kinetics*, p. 69 Clarendon Press, Oxford, 1975.
16. Manoussakis, G.E., Haristos, D.A. & Tzavellas, L.C.: *Chim. Chronika*, in press.
17. Grekov, A., Shevchenko-Korzhenetskaya, I., Malyutenko, S. & Maurenik, O.: *Zh. Org. Khim.* **6**, 94 (1970). Ibid. 98.
18. Desmarquest, J.P. & Boch, O.: *Electrochimica Acta* **13**, 1109 (1968).
19. Pennenman, R.A. & Audrieth, L.F.: *Anal. Chem.* **20**, 1058 (1948).
20. Higginson, W.C.E., Wright, P.: *J. Chem. Soc.* 1551 (1955).
21. Cahn, S.W., Powel, R.E.: *J. Am. Chem. Soc.* **76**, 2568 (1954).
22. Titov, E., Korzhenevskaya, N. & Rybachenco, V.: *Ukr. Khim. Zh.* 34 (12), 1253 (1968).
23. Mentasti, E., Pelizzeti, E., Pramanto, E. & Giraudi, G.: *Inorg. Chim. Acta* **12**, 61 (1975).
24. Haraguchi, K., Yamada, K. & Saburo, Ito: *J. Inorg. Nucl. Chem.* **36**, 1611 (1974).
25. Toppen, D.L. & Linck, R.C.: *Inorg. Chem.* **10**, 2635 (1971).
26. Robinson, B. & Stokes, R.: *Electrolyte Solutions*, p. 142 Butterworths Scientifig Publ. London 1959.
27. Weston, K.B., Jr. & Schwarz, H.A.: *Chemical Kinetics*, p. 168 Prentice Hall, New Jersey 1972.
28. Emanuel, N. & Knorre, D.: *Cinétique Chimique*, p. 52. Editions mir, Moscou 1975.
29. Issa, R.M., El Shazly, M.F. & Iskander, M.F.: *Z. Anorg. allg. Chem.* **354**, 90 (1967).
30. Albert, A.: *Nature* **177**, 525 (1956).
31. Gogorishvili, P., Karkarashvili, M. & Kalendarishvili, D.: *Zh. Neorg. Khim.* **14**, 1516 (1969). *Chem. Abstr.* **71**, 66805 p (1969).
32. Butsko, S. & Shmańko, P.: *Zh. Neorg. Khim.* **19**, 449 (1974).
33. Steinhaus, R.K. & Barsuhn, C.L.: *Inorg. Chem.* **13**, 2922 (1974).
34. Swaroop, R. & Gupta, Y.K.: *J. Inorg. Nucl. Chem.* **36**, 169 (1974).
35. Nonoyama, M., Tomita, S. & Yamasaki, K.: *Inorg. Chim. Acta* **12**, 33 (1975).
36. Paul, R.C. & Chadha, S.L.: *Spectrochimica Acta* **23A**, 1249 (1967).
37. Sunanda, Aditya: *J. Inorg. Nucl. Chem.* **29**, 1901 (1967).
38. McConnel, H. & Davidson, N.: *J. Am. Chem. Soc.* **72**, 3164 (1950).
39. Perrin, D.D.: *J. Chem. Soc.* 3189 (1960).

Chimika Chronika, New Series, 10, 185-191 (1981)

THE REACTION OF PHENYLIODINE DITRIFLUOROACETATE WITH DIAZOCOMPOUNDS

B. AXIOTIS, S. SPYROUDIS and A. VARVOGLIS
Laboratory of Organic Chemistry, University of Thessaloniki Thessaloniki, Greece.

(Received June 3, 1980)

Summary

Phenyliodine ditrifluoroacetate reacts with aryldiazomethanes and 1-aryl-1-diazoethanes in a complex manner. The main products are esters of trifluoroacetic acid, resulting from an intermolecular hydrogen transfer of a novel type. Other products are benzylic alcohols and carbonyl compounds, while the 4-nitrosubstituted diazocompounds afford also 4,4'-dinitrostilbene and 4-nitrostyrene.

Introduction

The action of polyvalent iodine compounds on diazocompounds has scarcely been investigated. The only relevant studies which could be traced in the literature are the reactions between phenyliodine dichloride (or phenyliodoso dichloride, $C_6H_5ICl_2$) and certain α-keto and α-carbalkoxydiazocompounds leading to 1,1-dichloroderivatives[1,2].

In connection with our continuing study[3] on the reactivity of phenyliodine ditrifluoroacetate[4] (PIT, 1) we have examined its action on three aryldiazomethanes, 2a-c, and three 1-aryl-1-diazoethanes, 3a-c.

Results and Discussion

Most reactions were carried out in dichloromethane solution at 0 °C. Upon mixing of equimolecular quantities of the diazocompounds 2 or 3 with PIT (1), both in CH_2Cl_2, a steady evolution of gas was observed, which lasted for a few minutes. After the end of the reaction the solvent was evaporated and the residue was chromatographed in a silica gel column, using solvents of increasing polarity. Besides iodobenzene, two or up to four products were obtained, as summarized in Table I.

TABLE I: *Reaction Products from PIT and Diazocompounds.*[a]

Diazocompound	*Ester b* (*Ir, νCO cm* $^{-1}$; nmr, δ)	*Alcohol*	*Carbonyl Compound*	*Other Compounds*
2a	4-$NO_2C_6H_4CH_2OCOCF_3$(25) (1782; 5.51s)	4-$NO_2C_6H_4CH_2OH$(5)	4-$NO_2C_6H_4CHO$(17)	$(4\text{-}NO_2C_6H_4CH)_2$(5)
2b	3-$NO_2C_6H_4CH_2OCOCF_3$(20) (1785; 5.55s)	3-$NO_2C_6H_4CH_2OH$(2)	3-$NO_2C_6H_4CHO$(20)	———
2c	2.6-di$ClC_6H_3CH_2OCOCF_3$(20) (1787; 5.72s)	2.6-di$ClC_6H_3CH_2OH$(5)	2.6-diClC_6H_3CHO(15)	———
3a	4-$BrC_6H_4CH(CH_3)OCOCF_3$40 (1782; 1.63d, 5.93q)	———	4-$BrC_6H_4COCH_3$(20)	———
3b	4-$NO_2C_6H_4CH(CH_3)OCOCF_3$(37) (1785; 1.72d, 6.19q)	———	4-$NO_2C_6H_4COCH_3$(24	4-$NO_2C_6H_4CH{=}CH_2$(8)
3c	$C_6H_5CH(OCOCF_3)CH_2C_6H_5$(33) (1785; 3.07d, 3.19d, 5.95t)	$C_6H_5CHOHCH_2C_6H_5$10	$C_6H_5COCH_2C_6H_5$(12)	$(C_6H_5CH)_2$(trace)

a The yields mentioned after the formulas are in some cases approximate, since the effort was on obtaining pure products rather than achieving complete recovery of them.

b The first number in brackets is the carbonyl absorption of the ir spectrum, in cm^{-1}, for neat liquids; the other number refers to ppm values (δ) for the non-aromatic protons in the nmr spectra (s=singlet, d=doublet, t=triplet, q=quartet).

The main product in all reactions was the trifluoroacetate ester of substituted benzyl alcohol 4a-c or 1-arylethanol 5a-c, while considerable quantities of benzaldehyde 6a-c or acetophenone 7a-c were also formed, together with some benzyl alcohol, $ArCH_2OH$, in the case of aryldiazomethanes. An alcohol was also obtained from 3c, while 2a gave in addition 4,4 -dinitrostilbene and 3b gave 4-nitrostyrene. A considerable amount of polymeric material was always retained inside the column; this could be eluted only with methanol and it was not possible to be further characterised. The general course of the reaction may grossly be formulated as follows:

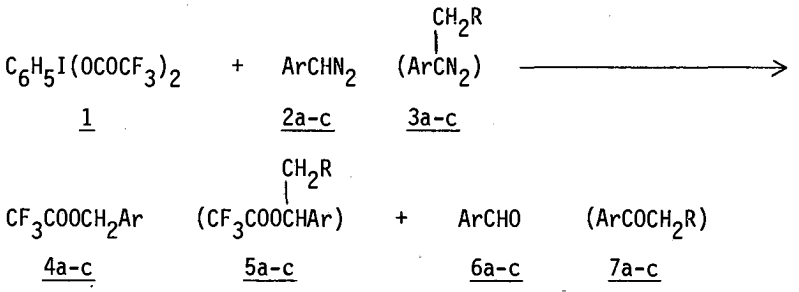

2,4,6a:Ar = 4-nitrophenyl

2,4,6b:Ar = 3-nitrophenyl

2,4,6c:Ar = 2,6-dichlorophenyl

3,5,7a:Ar = 4-bromophenyl, R=H

3,5,7b:Ar = 4-nitrophenyl, R=H

3,5,7c:Ar = phenyl, R=phenyl

The structure of these products, most of which are known compounds, was established using nmr, ir and mass spectroscopy; in many cases a direct comparison

with authentic samples was also possible.

The formation of the major products, i.e. the trifluoroacetate esters 4 and 5, was rather unexpected, since some complex diazocompounds with phenyliodine dichloride give 1,1-dichloroderivatives[1,2] ($RCHCl_2$), while lead tetraacetate, which largely reacts similarly with PIT[5], gives 1,1-diacetoxyderivatives[6] ($R_2C(OCOCH_3)_2$).

Initially it was thought that the presence of moisture or of some trifluoroacetic acid from PIT, which is made by exchange of phenyliodine diacetate with trifluoroacetic acid[3a], were responsible for the formation of the esters. Therefore, the reactions were carried out using carefully dried diazocompounds and solvents, with acid-free PIT. No change was observed in the rate of the reaction as well as in the percentage amounts of the products. Thus the possibility that water or trifluoroacetic acid were responsible for the formation of the esters was ruled out; the only alternative plausible explanation is that the esters are the products of an intermolecular reaction, involving a hydrogen transfer from one molecule of 2 or 3 (or more probably of an intermediate of them with PIT) to another molecule of 2 or 3. In order to confirm the above hypothesis and also to exclude the possibility that hydrogen is provided by the solvent* (a process known to occur in some other reactions of diazocompounds[7]) we have prepared 2,2,2-trideuterio-1(4′-nitrophenyl)-1-diazoethane and allowed it to react with PIT. Although we have prepared 100% deuterated 4-nitroacetophenone, its diazoderivative was only 50% deuterated, because of exchange during the preparation of the hydrazone, which was subsequently oxidised to the diazocompound. The isolated 5b from the reaction of partially deuterated 3b with PIT was examined by mass spectroscopy and it was found that the ratio of D:H transfer was approximately 1:2, instead of the expected 1:1. This apparent anomaly can be attributed to the isotope effect and the uncertaintly about the actually deuterated species of 3b (see experimental for details). Anyway, even this reduced but significant D transfer confirms the intermolecular character of the reaction. Concerning its mechanism, several possibilities have been considered, but we feel that our evidence is quite insufficient to propose any meaningful mechanism. In the case of esters 4a-c, again an intermolecular mechanism must take place, although quite distinct from that responsible for the formation of esters 5a-c.

The isolation of benzylalcohols without doubt is due to hydrolysis of the esters during the chromatographic work-up. The lack of their characteristic peaks in the nmr spectr (at 4.5 δ) before the work-up and similar behaviour of other trifluoroacetate esters[8],[3c] are considered as good evidence for their formation from the esters.

The aldehydes 6a-c and acetophenones 7a-c that are invariably isolated in considerable quantities must also be secondary products, since they are not detected by nmr among the initial reaction products. Their formation may be attributed to hydrolysis of 1,1-ditrifluoroacetoxyaryl methanes and ethanes, which

* Several reactions were run in $CDCl_3$ and monitored by nmr, without any noticeable decrease of the ester, which also rules out any participation of the solvent.

are the expected products from the reaction of diazocompounds with PIT. Such compounds have not been described in the literature, although their 1,1-acetoxy analogues are well-known: it is reasonable to assume that once formed, they are easily hydrolysed to the carbonyl compounds during the work-up, because of the lability of the -O-$COCF_3$ bond:

It is worth mentioning that the methinic proton in the aldehyde derivatives, $ArCH(OCOCF_3)_2$, is not detected in the nmr spectra, because it has been estimated to fall in the region of the aromatic protons. Indeed, the compound $CF_3CH(OCOCF_3)_2$ has recently been found[9] to display a quartet for the methinic proton at 7.2 δ.

Among the reaction products of 2a is also found 4,4′-dinitrostilbene, mainly as the trans-isomer. Stilbenes are oxidation products of diazocompounds with iodine[6], ceric ammonium nitrate[10] and tetrachloro-p-quinone[11]. Several mechanisms may explain the formation of 4,4′-dinitrostilbene, including generation of 4-nitrophenylcarbene, which is attacked by another molecule of 2a. An attempt was made to trap this carbene by adding cyclohexene to the reaction mixture. Unfortunately, cyclohexene reacts with PIT[5], so that no addition product could be detected.

The formation of 4-nitrostyrene from 3b is also possible to proceed through a carbene, since it is known that methylphenylcarbene, generated photochemically from 1-phenyl-1-diazoethane, isomerises to styrene[12]. Another possibility, i.e. the dehydration of 1-(4-nitrophenyl) ethanol, which is not found among the products, seems unlikely under the experimental conditions used.

The catalytic role of PIT in the decomposition of the diazocompounds may be attributed to its character as a Lewis acid, because of its dissociation to $C_6H_5I^+$–$OCOCF_3$ and CF_3COO^-. Attack of iodine from the carbanionic carbon of the diazocompound would give a diazonium salt of the type $C_6H_5I(OCOCF_3)CH(Ar)N_2^+$ CF_3COO^-, decomposing to ArCH and N_2, with regeneration of PIT. The acylals $ArCH(OCOCF_3)_2$ mentioned above, which are thought to hydrolyse to carbonyl compounds, is possible to be formed from carbenes and PIT. A similar proposal has been made by Hensel[6] for the formation of $(C_6H_5)_2C(OCOCH_3)_2$ from diphenyldiazomethane and lead tetraacetate.

That an intermediate between PIT and diazocompounds is really formed has been proved in its reaction with diazoacetic ethylester. In this case no gas is evolved upon mixing of the reagents, but a downfield shift in the nmr spectrum of the methinic proton of the ester is observed (from 4.78 to 4.83 δ). The two diferent signals coexist for some time, until that of the diazoacetic ester disappears. This is taken as a proof that the shift is not due to a solvent effect. When the reaction mixture is passed through the chromatographic column, gas evolution is observed and among the numerous products obtained only the aldehyde-ester, OHC-

$COOC_2H_5$, has been detected with certainty.

Conclusion

The reaction between PIT and diazocompounds is a complex one and apparently two at least main pathways are available to account for the products isolated:

1. The first inolves reaction of the diazocompounds with PIT and further reaction of the resulting reactive intermediates with an intact molecule of diazocompound. The main products are the esters.
2. The second is probably a PIT catalysed decomposition of the diazocompounds to carbenes, which react further mainly with PIT to the unstable acylals, while it is also possible to give some stilbene or styrene.

Experimental

Measurements. Melting points have been obtained on a Kofler hot stage apparatus and they are uncorrected. Ir spectra were obtained from neat liquids or nujol mulls with a Perkin-Elr - Model 257 spectrophotometer.[1] H nmr spectra were recorded on a Varian A-60A spectrometer in $CDCl_3$, with TMS as an internal standard. The mass spectra were obtained with a Hitachi-Perkin-Elmer Model RMU-6L spectrometer with ionisation energy 70 eV.

Materials. Phenyliodine ditrifluoroacetate (PIT) was prepared as previously described[3a]. The diazocompounds were prepared by oxidation of the hydrazones of substituted bezaldehydes and acetophenones with activated MnO_2, according to the method of Goh and Gian[13], which was found to be superior to older methods. Their purification was based on repeated extraction with hexane; the combined extracts were evaporated to a small volume until the diazocompounds crystallised. Further purification may be effected by recrystallisation from acetone-water. The purity of these compounds was always checked by tlc, ir and nmr just before use. Compounds 2a, 2b and 3b were stable for a long time in the dark at -10°C. Compounds 2c and 3a decomposed slightly after 2-3 days, while 3c decomposed fairly quickly to stilbene. The diazocompounds had the following characteristics:

2a: Mp 79-80° C; ir 2050 cm $^{-1}$; nmr 5.16(s), 7.02(d), 8.21(d) δ. Yield 72%.

2b: Mp 77-78° C; ir 2055 cm $^{-1}$; nmr 5.08(s), 7.02-7.25(m), 8.15-8.25(m) δ. Yield 45%.

2c: Mp 45-50° C; ir 2060 cm $^{-1}$; nmr 5.34(s), 7.08-7.20(m), δ. Yield 54%.

3a: Mp 30° C; ir 2020 cm $^{-1}$; nmr 2.07(s), 6.76(d), 7.43(d) δ. Yield 40%.

3b: Mp 83-85° C; ir 2035 cm $^{-1}$; nmr 2.25(s), 7.00(d), 8.23(d) δ. Yield 82%.

3c: Liquid; ir 2030 cm $^{-1}$; nmr 3.73(s), 7.21(s), 7.24(s) δ. Yield 35%.

General procedure. The diazocompound (0.08 mole) is dissolved in dry CH_2Cl_2 (20 ml) at 0°C, in an atmosphere of nitrogen, and 0.08 mole of PIT in CH_2Cl_2 (20 ml) is added with stirring to the first solution dropwise during 5-10 min. The dark

coloured solution becomes progressively lighter in colour, while gas evolution is observed. In the case of 3b the reaction was carried out at 15-20° C. When gas is no longer evolved, the reaction mixture is condensed in a rotary evaporator and applied into a chromatographic column packed with silica gel. The column is eluted with mixtures of hexane-chloroform of increasing polarity, until pure chloroform is used. The products appear in the following order: iodobenzene, ester, carbonyl compound, alcohol. Styrene or stilbene, if any, are eluted after iodobenzene, while some unreacted PIT may be collected in some cases after the alcohol.

Products identification. All esters were liquids and they have been identified from their ir, nmr and mass spectra. It is worth mentioning that the esters show in their mass spectrum a prominent molecular ion, while the base peak corresponds to a M-CF_3COOH^+ fragment; also a M-CF_3COO^+ fragment of high relative abundance is always observed, while esters 5a-c have also a fairly abundant M-CH_3^+ fragment. The ir and nmr spectra of the esters appear in the Table. In addition, the esters were hydrolysed with alkali to the corresponding alcohols, which are solids and known compounds. Some esters, notably 3b, were also independently prepared from the diazocompounds and trifluoroacetic acid; they were in all respects identical to those isolated from the reaction products.

The alcohols, the carbonyl compounds, 4,4′-dinitrostilbene and 4-nitrostyrene were all known compounds and they have been obtained crystalline; they were identified from spectral data and their melting points.

Preparation and reaction of deuterated 3b. 4-Nitroacetophenone (3g) was refluxed for 1 hr in a mixture of D_2O (15 ml) and dioxane (10 ml) containing a catalytic amount of NaOH. On cooling fully deuterated in the methyl group 4-nitroacetophenone (shown by nmr) was obtained (2.45 g). The deuterated compound (4-$NO_2C_6H_4COCD_3$, 2g) was refluxed for 2.5 hr in a mixture of aqueous 98% hydrazine (7 ml) and C_2H_5OD (15 ml). The deuterated ethanol was prepared by an adaptation of the method of Swain et al.[14], used originally for the preparation of CH_3OD. On cooling and after the addition of a little D_2O, the hydrazone crystallised (1.8 g). The nmr spectrum of the hydrazone showed that a mixture of partially deuterated species had been formed. This was oxidised to the diazocompound 3b in the usual manner. The nmr spectrum of deuterated 3b showed a ratio of aromatic to methylic protons 8:3, indicative of a 50% deuteration of the methyl group. Statistically but not actually this means that 3b is a mixture of the following composition: 25% $ArCN_2CH_3$, 25% $ArCN_2CH_2D$, 25% $ArCN_2CHD_2$ and 25% $ArCN_2CD_3$.

The isolated ester 5b from the reaction of 3b with PIT was examined by mass spectrometry. Its molecular ion consisted of a cluster of five peaks ranging from m/e 263 (non-deuterated) to 267 (fully deuterated). Since it was not easy to deduce the abundance of the deuterated ester from the molecular ion, the fragment M-15$^+$ (M-CH_3) was judged to represent better the extent of deuterium migration. Thus the ratio of fragments m/e ArCD-$OCOCF_3^+$ (249) to ArCH-$OCOCF_3^+$ (248) was found to be 9:21, which means that, allowing for the natural isotope content of the non-deuterated fragment, approximately 25% of the ester was formed by D transfer.

Περίληψη

Ἡ Ἀντίδραση Διτριφθορακετοξυ-ιωδοβενζολίου μέ Διαζω-ενώσεις.

Στήν ἐργασία αὐτή ἐξετάζεται ἡ ἀντίδραση μερικῶν ἀρυλοδιαζωμεθανίων καί 1-ἀρυλο-1-διαζωαιθανίων μέ τό παράγωγο τοῦ τρισθενοῦς ἰωδίου διτριφθορακετοξυ-ιωδοβενζόλιο, $C_6H_5I(OCOCF_3)_2$. Τό κύριο προϊόν πού σχηματίζεται εἶναι οἱ τριφθορακετοξικοί ἐστέρες τῆς ἀρυλομεθανόλης ἤ τῆς 1-ἀρυλοαἰθανόλης-1, τοῦ τύπου $ArCH_2OCOCF_3$ ἤ $ArCH(CH)_3OCOCF_3$, ἐνῶ σέ σημαντικά ποσά ἀπομονώνονται καί ὑποκατεστημένες βενζαλδεῦδες ἤ ἀκετοφαινόνες. Ἄλλα προϊόντα εἶναι ἀρυλομεθανόλες καί ἀπό τά 4-νιτροϋποκατεστημένα διαζωπαράγωγα τό 4,4′-δινιτροστιλβένιο ἤ τό 4-νιτροστυρόλιο.

Τά παραπάνω προϊόντα πρέπει νά προέρχονται ἀπό δύο τουλάχιστο διαφορετικές ἀντιδράσεις. Κατά τήν πρώτη πιθανότατα σχηματίζεται ἀρχικά ἕνα δραστικό ἐνδιάμεσο προϊόν μεταξύ διαζωενώσεως καί διτριφθορακετοξυιωδοβενζολίου, πού ἀντιδρᾶ μέ ἀναλλοίωτη διαζωένωση καί δίνει τελικά τόν ἐστέρα, μέ ἕνα μηχανισμό πού παραμένει ἄγνωστος. Κατά τή δεύτερη οἱ διαζωενώσεις διασπῶνται καταλυτικά ἀπό τό διτριφθορακετοξυιωδοβενζόλιο, πιθανότατα πρός καρβένια, ἀπό τά ὁποῖα προκύπτουν μέσω τῶν ἀσταθῶν 1,1-διτριφθορακετοξυπαραγώγων τους οἱ βενζλδεῦδες ἤ οἱ ἀκετοφαινόνες, καθώς καί τό δινιτροστιλβένιο ἤ τό νιτροστυρόλιο. Οἱ ἀλκοόλες εἶναι προϊόντα ὑδρολύσεως τῶν ἐστέρων, πού προκύπτουν κατά τή διαδικασία τῆς ἀπομονώσεως μέ χρωματογραφία στήλης.

References and Notes

1. Roedig, A. & Kloss, R.: *Justus Liebigs Ann. Chem.* **612**, 1 (1958).
2. Roedig, A., Aman, H. & Fahr, E.: *Justus Liebigs Ann. Chem.* **675**, 47 (1964).
3. a. Spyroudis, S. & Varvoglis, A.: *Synthesis 445* (1975).
   b. Spyroudis, S. & Varvoglis, A.: *Synthesis 837* (1976).
   c. Spyroudis, S. & Varvoglis, A.: *J. Chem. Soc. Chem. Comm.*, 615 (1979).
4. This is the current Chemical Abstracts name; other names are ditrifluoroacetoxy iodobenzene or bis (trifluoroacetoxy) iodobenzene and iodobenzene ditrifluoroacetate or phenyliodoso trifluoroacetate.
5. Spyroudis, S.: *Ph. D. Thesis*, University of Thessaloniki (1981).
6. Hensel, H.R.: *Chem. Ber.*, **88**, 527 (1955).
7. Parham, W.E. & Hasek W.R: *J. Am. Chem. Soc.*, **76**, 935 (1954).
8. Hollbert, G.H. & Ganem B.: *J. Chem. Soc. Chem. Comm.*, 248 (1978).
9. Schreiber, S.L.: *Tetrahedron Letters*, 1027 (1980).
10. Trahanovsky, W.S., Robbins M.D. & Smick D.: *J. Am. Chem. Soc.*, **93** 2086 (1971).
11. Oshima, T. & Nagai, T.: *Tetrahedron Letters*, 2789 (1979).
12. Overberger, C.G. & Anselme, J.P.: *J. Org. Chem.*, **29**, 1188 (1964).
13. Goh, S.H. & Gian H.L.: *J. Chem. Soc. Perkin I*, 1625 (1979).
14. Swain, C.G., McKnight J.T. & Kreiter, V.P.: *J. Am. Chem. Soc.*, **79**, 1088 (1957).

Chimika Chronika, New Series, 10, 193-201 (1981)

ELECTROCHEMICAL BEHAVIOR OF NITROBENZENE AND RELATED COMPOUNDS IN METHANOL

GEORGE KOKKINIDIS, PANTELIS KARABINAS and DIMITRIOS JANNAKOUDAKIS
Laboratory of Physical Chemistry, University of Thessaloniki, Thessaloniki, Greece.

(Received December 17, 1980)

Summary

The electrochemical behavior of nitrobenzene, nitrosobenzene and phenylhydroxylamine in methanol was investigated by employing cyclic voltammetry, d.c. polarography and controlled potendial electrolysis. The oxidation-reduction couple peak due to the reversible redox system C_6H_5NHOH - C_6H_5NO appears in the cyclic voltammogram of nitrobenzene. Phenylhydroxylamine in the presence of CH_3O^- ions, both formed during the reduction of nitrobenzene or nitrosobenzene, undergoes oxidation at less positive potenials than phenylhydroxylamine diffusing from the solution. The influence of added proton donors upon the oxidation reduction couple peak appearing in the cyclic voltammograms of nitrobenzene and nitrosobenzene was also examined. The solutions of nitrobenzene after exhaustive electrolysis were found to exhibit the same electrochemical behavior with that of solutions containing phenylhydroxylamine and CH_3ONa.

Key words: Polarography, Cyclic voltametry, Control potential electrolysis, Nitrosobenzene, Phenylhydroxylamine.

Introduction

Phenylhydroxylamine is reported to be the electroreduction product of nitrobenzene both in protic[1-4] and aprotic[5,6] solvents. The same compound is also the product of the electroreduction of nitrobenzene in protic solvents[7-10], while in aprotic solvents azoxybenzene is obtained by coupling reaction of the intermediate nitrosobenzene radical anion[11-13]. In alkaline protic solutions the reduction of nitrosobenzene gives phenylhydroxylamine, which reacts with unreduced nitrosobenzene yielding azoxybenzene[7,14]). The system of nitrosobenzene-phenylhydroxylamine behaves resersibly and this reversibility was investigated over a large range of pH both at the d.m.e.[9] and at the graphite electrode[10].

Since the reversible redox system of C_6H_5NO-C_6H_5NHOH appears in the cyclic voltammogram of nitrobenzene at the h.m.d.e. in methanol[15], it was thought

useful to study the behavior of all these compounds under similar conditions. Cyclic voltammetric and potentiostatic experiments were carried out in pure methanol in the absence and in the presnece of proton donors.

Experimental

Cyclic voltammetric i-E curves at a h.m.d.e. and d.c. polarographic curves were obtained as described previously[16]. Controlled potendial electrolysis at a mercury pool cathode was carried out using the same potentiostat of reference 16. The quantity of electricity passed trhough the cell was determined either by integration of the i-t curves or by a silver coulometer. The potential values were taken in reference to the aqueous calomel electrode (SCE) saturated with NaCl. The experiments were carried out at constant temperature 25±0.1°C.

The reagents methanol and lithium perchlorate were as reported previously[16]. The other substances were of high grades obtained commercially, except phenylhydroxylamine and nitrosobenzene which were prepared following vogel[17]. Phenylhydroxylamine was recrystallized from benzene and nitrosobenzene from ethanol. Their purity was established by thin layer chromatography, NMR and infrared spectral data.

Results and Discussion

Cyclic Voltammetry

In the cyclic voltammogram of nitrobenzene in methanol at the h.m.d.e. we observe the peak due to the reduction of nitro group and two couples of peaks at less negative and positive potendials respectively (Fig. 1A). The peaks at positive potentials (IIIa and III_b) were examined previously[15] and found to describe the polarization and depolarization of the mercury electrode by the CH_3O^- ions formed during the non reversible reduction of nitro group. The second couple of peaks (IIa and II_b) is apparently due to the reversible redox couple of C_6H_5NHOH - C_6H_5NO. Phenylhydroxylamine, the reduction product of nitrobenzene, is oxidized to give nitrosobenzene, which in turn is reduced to yield again phenylhydroxylamine. A similar oxidation-reduction couple peak was found in the case of o- and m-trifluoromethylnitrobenzene in N,N-dimethylformamide under voltammetric conditions[18].

In order to make precise identification of this couple peak appearing in the cyclic voltammogram of nitrobenzene, the cyclic voltammograms of authentic solutions of phenylhydroxylamine and nitrosobenzene were obtained under the same conditions (Fig. 1C, B). As it can be seen the oxidation-reduction couple peak of the reversible redox system C_6H_5NHOH - C_6H_5NO appears at different potentials in the cyclic voltammograms of each compound. When nitrosobenzene and phenylhydroxylamine are in the same solution, two oxidation-reduction couple peaks at the same potentials are also obtained (Fig. 2). Besides, the oxidation-reduction couple peak of C_6H_5NHOH - C_6H_5NO appearing in the cyclic voltammogram of nitrobenzene is identified with that of nitrosobenzene and not with that of phenylhydroxylamine.

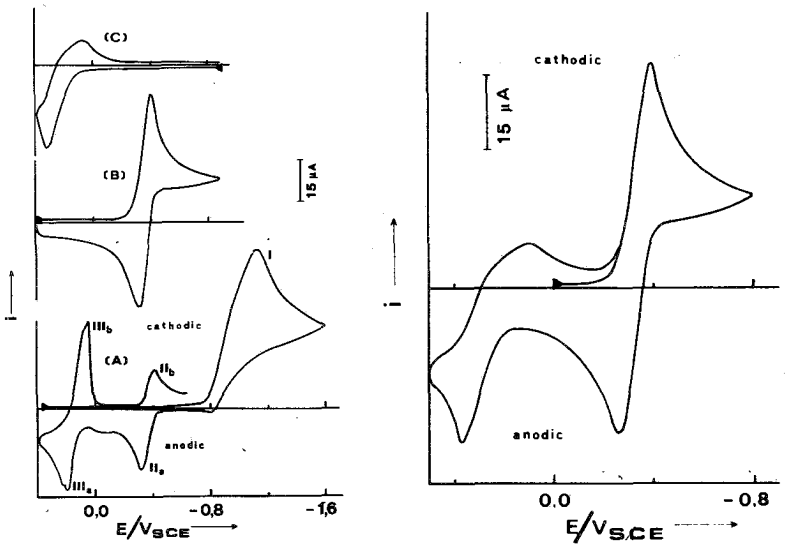

FIG. 1 *Cyclic voltammograms of 10-3 M nitrobenzene (A), 10-3 M nitrosobenzene (B) and 10-3 M phenlhydroxylamine (C) in methanol. Supporting electrolyte 0,1 M $LiClO_4$.v = 200 mV/sec.*

FIG. 2. *Cyclic voltammogram obtained from a methanolic solution containig 10-3 M nitrosobenzene and 10-3 M phenylhydroxylamine. Supporting electrolyte 0,1 M $LiClO_4$.u = 200 mV/sec.*

The above experimental data show that phenylhydroxylamine,which is formed during the reduction of nitrosobenzene or nitrobenzene, is oxidized at less positive potentials than phenylhydroxylamine diffusing from the solution towards the electrode. On the contrary, nitrosobenzene formed during the oxidation of phenylhydroxylamine is reduced at less negative potential than nitrosobenzene diffusing from the solution. This behavior can be understood accepting that the oxidation of phenylhydroxylamine in the presence of CH_3O^- ions, both formed during the reduction of nitrosobenzene, occurs at the same negative potential, where the nitrosobenzene is reduced.

$$C_6H_5NO + 2e^- + 2CH_3OH \rightarrow C_6H_5NHOH + 2CH_3O^- \text{ cathodic}$$
$$C_6H_5NHOH + 2CH_3O^- \rightarrow C_6H_5NO + 2e^- + 2CH_3OH \text{ anodic} \qquad (I)$$

On the other hand, the reduction of nitrosobenzene in the presence of $CH_3OH_2^+$ ions, both formed during the oxidation of phenylhydroxylamine, takes place at the same positive potential, where the phenylhydroxylamine is oxidized.

$$C_6H_5NHOH + 2CH_3OH \rightarrow C_6H_5NO + 2e^- + 2CH_3OH_2^+ \text{ anodic}$$
$$C_6H_5NO + 2e^- + 2CH_3OH_2^+ \rightarrow C_6H_5NHOH + 2CH_3OH \text{ cathodic} \qquad (II)$$

This can be confirmed by the fact that the reduction potential of nitrosobenzene under polarographic conditions in the presence of strong acids (H_2SO_4, p-CH_3-C_6H_4-SO_3H) is identical with that of nitrosobenzene, formed during the oxidation of phenylhydroxylamine under voltammetric conditions. Similarly, the oxidation potential of phenylhydroxylamine in the presence of CH_3ONa is identical with that of phenylhydroxylamine, formed by the reduction of nitrosobenzene.

The reduction of nitrobenzene implies the formation of a quatramolecular amount of CH_3O^- ions. Since the moiety of these ions are neutralized by the protons released during the oxidation of phenylhydroxylamine, an excess of CH_3O^- ions continues to exist on the electrode surface causing the anodic dissolution of the mercury electrode[15] (Fig. 1A). A quantity of phenylhydroxylamine, possibly existing in the solution, could be oxitized at the same potential with phenylhydroxylamine formed by the reduction of nitro group in the presence of the excess of the CH_3O^- ions. In Fig. 3 the cyclic voltammograms of nitrobenzene in the presence of varying amounts of phenylhydroxylamine are given.

It is apparent (Fig. 3) that increasing the concentration of phenylhydroxylamine the height of current peak IIa increases until it approaches a maximum value, which is twice higher than the initial height. On the other hand, the polarization and depolarization peak of the mercury electrode completely disappears, when the concentration of the added phenylhydroxylamine becomes equal to that of nitrobenzene. It is obvious that the oxidation of phenylhydroxylamine, which diffuses towards the electrode, also occurs in the presence of CH_3O- ions and as a result neutralization of the excess of these ions is observed. In higher concetrations of phenylhydroxylamine than that of nitrosobenzene, the excess of phenylhydroxylamine undergoes oxidation at the same potential with that of phenylhydroxylamine in the absence of CH_3O^- ions. In this case the cyclic voltammogram shows the corresponding oxidation-reduction couple peak at positive potentials (Fig. 3, curve 4).

Effect of proton donors. In the presence of proton donors the reduction -

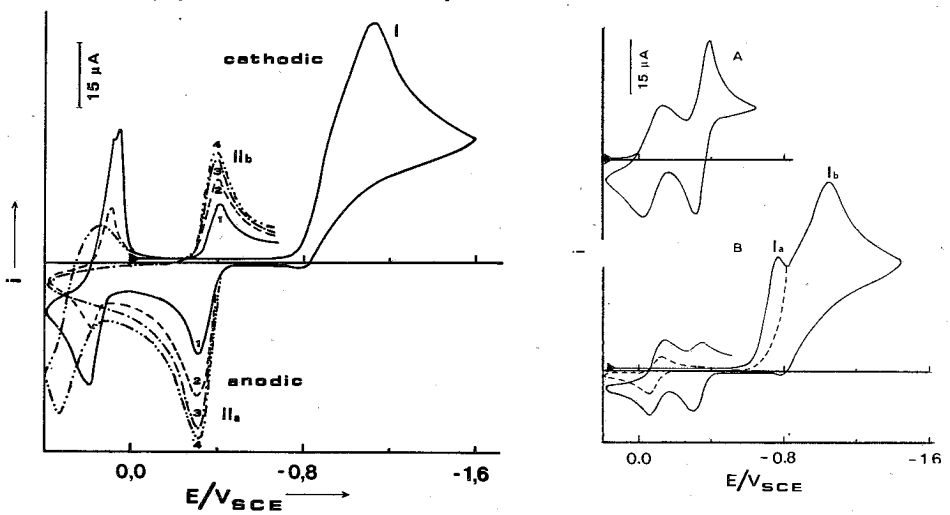

FIG. 3 *Cyclic voltammograms of $10^{-3}M$ nitrobenzene in the presence of varying amounts of phenylhydroxylamine in methanol. 1) without C_6H_5NHOH, 2) $5.10^{-4}M$, 3) $10^{-3}M$ and 4) $2.10^{-3}M$ C_6H_5NHOH. Supporting electrolyte 0,1 M $LiClO_4$. $v=200$ mV/sec.*

FIG. 4 *Cyclic voltammograms of $10^{-3}M$ nitrosobenzene in the presence of $10^{-3}M$ CH_3COOH (A) and $10^{-3}M$ nitrobenzene in the presence of $2.10^{-3}M$ CH_3COOH (B) in methanol. Supporting electrolyte 0,1 M $LiClO_4$. $v=200$ mV/sec.*

oxidation couple peak of the reversible redox system C_6H_5NO - C_6H_5NHOH appears at less negative potentials both in the cyclic voltammograms of nitrosobenzene and nitrobenzene. Typical cyclic voltammograms of nitrosobenzene and nitrobenzene in the presence of CH_3COOH are shown in Fig. 4.

When the molar ratio of C_6H_5NO - CH_3COOH is 1:1. two reduction - oxidation couple peaks are observed. This happens because the half quantity of nitrosobenzene undergoes reduction at less negatice potential and the formed phenylhydroxylamine is oxidized in the presence of the less basic CH_3COO^- ions at the same potential.

$$1/2C_6H_5NO + 1e^- + CH_3COOH \underset{\text{anodic}}{\overset{\text{cathodic}}{\rightleftharpoons}} 1/2\ C_6N_5NHOH + CH_3COO \qquad \text{(III)}$$

Nitrobenzene exhibits similar cyclic voltammetric behavior concerning the reversible redox couple of C_6H_5NO - C_6H_5NHOH, when the molar ratio of $C_6H_5NO_2$ - CH_3COOH is 1:2 When, however, potentials of scan reversal between peaks Ia and Ib (Fig. 4B) - reduction of nitro group in the presence and in the absence of CH_3COOH - are taken, one can observe that only the oxidation - reduction couple peak at less negative potentials appears. The same occurs, independelty of the potential of scan reversal, when the molar ratio of $C_6H_5NO_2$ - CH_3COOH is 1:4. In the case of nitrosobenzene analogous behavior occus, when the molar ratio of C_6H_5NO - CH_3COOH is 1:2.

As far as it is concerned the shift of the potential of the reduction-oxidation couple peak of C_6H_5NO - C_6H_5NHOH towards positive values has been found to depend on the strength of the acids used.For stronger acids, the reduction-oxidation couple peak is shifted to more positive potentials. The interpretation must be analogous to that concerning the influence of proton donors upon the reduction potential of organic compounds in methanol[2,19].

The following general conclusion can be drawn from the described experimental data. The ions of the solvent molecules or ions of the acids used, which are formed during the elecrochemical reduction of nitrosobenzene or nitrobenzene, determine the oxidation potential of phenylhydroxylamine under voltammetric conditions. These ions cause local changes in the pH on electrode surface, due to the lack of buffer. As it will be shown the CH_3O^- ions also influence the chemical behavior of phenylhydroxylamine formed in methanol under potentiostatic conditions.

Controlled potential electrolysis

Controlled potential electrolysis of nitrobenzene in methanol was carried out at a mercury pool electrode at potentials corresponding to the plateau of the polarographic wave. Polarograms were taken at intermediate stages during the reduction in the same cell in order to avoid exposure of the solution to atmospheric oxygen. Typical polarographic curves of nitrobenzen before and after reduction are presented in Fig. 5.

Two anodic waves appear after electrolysis of the nitrobenzene. The first wave

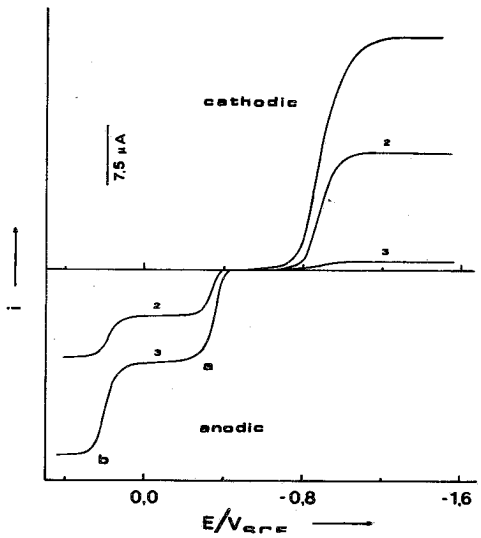

FIG. 5 *Polarograms of 10^{-3}M nitrobenzene at different stages during electrolysis in methanol. 1) Before electrolysis, 2) after electrolysis at -1,2V, 3) after exhaustive electrolysis at -1,2 V. Supporting electrolyte 0,1 M $LiClO_4$.*

(a) corresponds to the oxidation of phenylhydroxylamine in the presence of CH_3O^- ions, while the second wave (b) is due to the anodic dissolution of the mercury electrode by the excess of the CH_3O^- ions[15]). In all these experiments the number of electrons consumed per molecule of nitrobenzene were found to be equal to 3.9 - 4.1.

Further confirmation that the product of controlled potential electrolysis of nitrobenzene is phenylhydroxylamine can be concluded by comparison of the polarographic behavior of a solution of nitrobenzene (10^{-3} M) after exhaustive electrolysis with that of a solution containing 10^{-3} M phenylhydroxylamine and 4.10^{-3} M CH_3ONa. In both cases, the solutions exhibit the same polarographic behavior. In deaerated solutions the height of the reduction wave of phenylhydroxylamine decreases slowly over a period of hours and three new waves appear in the polarogram (waves c, d, e in Fig. 6). From these waves the cathodic wave c is obviously due to the reduction of the formed nitrosobenzene. Identification of the other waves will appear below. Exposure of the solutions to the air (oxygen) for a few minutes and then oxygen removal by passing nitrogen through the cell gives polarograms having the form of curve 4 (Fig. 6). In this curve the wave due to the oxidation of phenylhydroxylamine is completely disappeared.

In deaerated basic solutions phenylhydroxylamine is slowly oxidized by traces of oxygen to give nitrosobenzene[10], which reacts with residual phenylhydroxylamine to from azoxybenzene. On the contrary, in aerated solutions the same reaction leads to the formation of nitrosobenzene as a final product[10]. The kinetics of the autoxidation of phenylhydroxylamine to azoxybenzene[20] as well as the kinetics and the mechanism of the condensation reaction between nitrosobenzene and phenylhydroxylamine has been studied both in acidic[21,22] and in basic [23,24] media. The condensation reaction of nitrosobenzene with phenylhydroxylamine

has also been studied electrochemically[14]. In basic solutions this condensation reaction proceeds via formation of the indermediate nitrosobenzene radical anion ($C_6H_5NO^{\cdot-}$), which couples to give azoxybenzene[24]. The electroreduction of nitrosobenzene to azoxybenzene in aprotic solvents[12,13] also proceeds with the same mechanism.

The oxidation of phenylhydroxylamine in aerated solutions (presence of oxygen) gives nitrosobenzene as was mentioned above. However, the polarographic behavior shows the formation of an other product except of nitrosobenzene (waves d and e in curve 4 in Fig. 6). In order to identify these waves cyclic voltammetry was employed. The cyclic voltammogram corresponding to the polarographic curve 4 of Fig. 6 and the cyclic voltammogram presenting the reduction of oxygen in methanol are compared (Fig. 7).

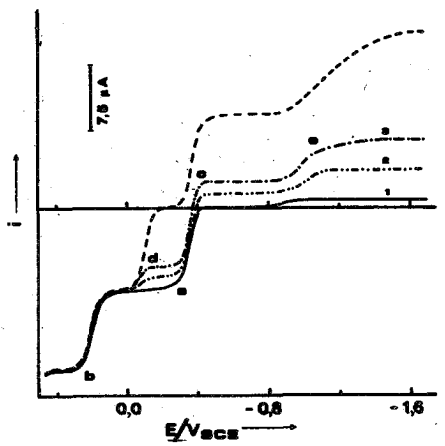

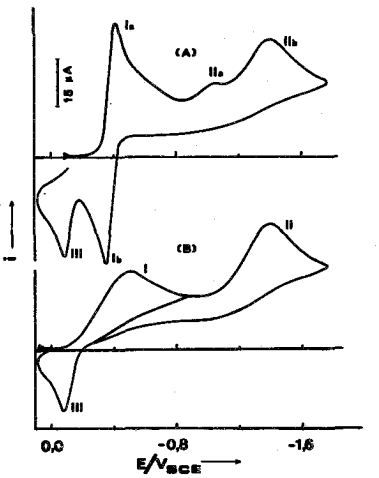

FIG. 6 *Polarograms obtained from a methanolic solution of 10^{-3}M nitrobenzene after exhaustive electrolysis at -1,2 V. 1) immediately after electrolysis, 2,3) 40 and 80 min after the electrolysis, 4) after exposure the solution to air for 10 min. Similar polarograms were obtained from a methanolic solution of 10^{-3}M phenylhydroxylamine in the presence of 4.10^{-3}M CH_3ONa under the same conditions. Supporting electrolyte 0,1 M $LiClO_4$.*

FIG. 7 *A) Cyclic voltammogram obtained from a methanolic solution of 10^{-3}M nirobenzene after exhaustive electrolysis at -1,2 V and exposure to air for 10 min. A similar cyclic voltammogram was also obtained from a methanolic solution containing 10^{-3}M phenylhydroxylamine and 4.10^{-3}M CH_3ONa after exposure to air for 10 min. B) Cyclic voltammogram of oxygen in methanol. Supporting electrolyte 0,1 M $LiClO_4$, v=200 mV/sec.*

Two peaks (IIa and IIb, Fig. 7A) appear in the region where the cathodic wave e is formed in the corresponding polarographic curve. The fact that the potential of peak IIa is identical with that of azoxybenzene proves that this small peak is due to the reduction of a small amount of formed azoxybenzene. Peaks IIb and III are identified to the peaks II and III (Fig. 7B) appearing in the cyclic voltammogram of oxygen. The above peaks II and III correspond to the reduction and oxidation of hydrogen peroxide formed during the first step of the reduction of oxygen. It is well known[25-27], that the reduction of oxygen occurs in two steps: the first represents the

reversible reduction of oxygen to hydrogen peroxide and the second the irreversible reduction of hydrogen peroxide to water.

This comparison leads to the unambiguous conclusion that hydrogen peroxide is formed, when phenylhydroxylamine is oxidized to nitrosobenzene (in methanol , in the presence of CH_3O- ions and oxygen). Therefore, we are obliged to accept the following stoichiometric equation:

$$C_6H_5NHOH + O_2 \xrightarrow{CH_3O} C_6H_5NO + H_2O_2 \qquad (IV)$$

No attempt was made to elucidate the mechanism of this reactions. This will probably consist the objective of a further investigation.

Coulometric experiments of nitrosobenzene were carried out under the same conditions. A wave due to the reduction of azoxybenzene appears in the polarograms taken immediately after the electrolysis. The formed phenylhydroxylamine reacts in the presence of CH_3O- ions with unreduced nitrosobenzene to yield azoxybenzene. The number of electrons cosmumed per molecule of nitrosobenzene has been found less than the stoichiometric value of 2. When, however, the reduction of nitrosobenzene occurs in the presence of CH_3COOH, the number of electrons consumed is 2 and the wave due to the reduction of azoxybenzene does not appear in the polarograms taken after the electrolysis.

Περίληψη

Ἠλεκτροχημική Συμπεριφορά Νιτροβενζολίου καί Σχετικῶν Ἑνώσεων σέ Μεθανόλη.

Ἡ ἠλεκτροχημική συμπεριφορά τοῦ νιτροβενζολίου, νιτρωδοβενζολίου καί τῆς φαινυλυδροξυλαμίνης σέ καθαρή μεθανόλη μελετᾶται μέ τή βοήθεια τῆς κυκλικῆς βολταμετρίας, τῆς d.c. πολαρογραφίας καί τῆς ἠλεκτρολύσεως σέ σταθερό δυναμικό. Κατά τήν ἠλεκτροχημική ἀναγωγή τοῦ νιτροβενζολίου στή μεθανόλη ἐμφανίζεται ἕνα ζεῦγος ἀντιστρεπτοῦ ὀξειδοαναγωγικοῦ peak πού ὀφείλεται στό σύστημα φαινυλοδροξυλαμίνη - νιτρωδοβενζόλιο (Σχ. 1A, peaks IIa καί IIb). Ἡ φαινυλυδροξυλαμίνη παρουσία ἰόντων CH_3O-, τά ὁποῖα σχηματίζονται κατά τήν ἀναγωγή τοῦ νιτρο-ἤ νιτρωδοβενζολίου, ἐμφανίζει στό κυκλικό βολταμογράφημα κύμα ὀξειδώσεως σέ λιγότερο θετικά δυναμικά ἀπ' ὅτι ἀπουσία αὐτῶν (Σχ. 2 καί 3). Μελετᾶται ἐπίσης ἡ ἐπίδραση δοτῶν πρωτονίων στό ὀξειδοαναγωνικό σύστημα φαινυλοδροξυλαμίνης - νιτροδοβενζολίου (Σχ. 4). Μεθανολικά διαλύματα νιτροβενζολίου μετά ἀπό ἐξαντλητική ἠλεκτρόλυση σέ ἠλεκτρόδιο Hg μεγάλης ἐπιφάνειας παρουσιάζουν τήν ἴδια ἀκριβῶς συμπεριφορά, μέ ἐκείνη διαλυμάτων φαινυλυδροξυλαμίνης καί CH_3ONa γραμμομοριακῆς ἀναλογίας 1:4 (Σχ. 5, καμπ. 3).

References

1. Coopmann R., and Gerischer H. *Ber. Bunsengs. Phys. Chem.*, **70**, 127 (1966).
2. Jannakoudakis D., and Wildenau A., *Z. Naturforsch.*, **22b**, 118 (1967).
3. Vijayalakshamma S.K., and Subrahmanya R.S. *J. Electroanal. Chem.*, **23**, 99 (1969).
4. Sadek A., and Abd-El-Nahey B.A.: *Electrochimica Acta*, **17** 2065 (1972).
5. Cadle S. H., Tice P.R., and Chambers I. Q. *J. Phys. Chem.* **71**, 3517 (1967).
6. Jannakoudakis D., Stalidis G., and Kokkonidis G., *Sci. Ann. Fac. Phys. Math., Univ. Thessaloniki*, **11**, 477 (1971).
7. Vijayalakshamma S.K., and Subrahmanya R.S. *Electrochimica Acta*, **17**, 471 (1972).
8. Scandler R., Will H., and Holleck L.: *Z. Electroch. Ber. Bunsengs. Phys. Chem.*, **63**, 596 (1959).
9. Smith J.W., and Waller J. G. *Trans. Faraday Soc.*, **46**, 290 (1950).
10. Chuang L., Fried I., and Elving P.J. *Anal. Chem.*, **36**, 2426 (1964).
11. Kemula W., and Sioda R. *J. Elecroanal. Chem.*, **6**, 183 (1963).
12. Asirvatham M.R., and Hawley M.D. *J. Electroanal. Chem.*, **57**, 179 (1974).
13. Lipsztajn M., Grygowski T.M., Laren E., and Galus, Z. *J. Elecroanal. Chem.*, **57**, 339 (1974).
14. Laviron E., and Vallat A., *J. Electroanal. Chem.*, **46**, 421 (1973).
15. Karabinas P., Kokkinidis G., and Jannakoudakis D. *J. Electroanal. Chem.*, **98**, 141 (1979).
16. Kokkinidis G., Karabinas P., and Jannakoudakis D. *J. Electroanal. Chem.*, **91**, 265 (1978).
17. Vogel A.I., *A Textbook of Practical Organic Chemistry*, 1st ed., Longmans, Green and Co., London, 1948 pp. 602, 603.
18. Grieg W.N., and Rogers J.W. *J. Am. Chem. Soc.*, **91**, 5495 (1969).
19. Holleck L., Jannakoudakis D., and Wildenau A. *Electrochimica Acta*, **12**, 1523 (1967).
20. Ogata Y., Sawaki Y., Mibae J., and Morimoto T. *J. Am. Chem. Soc.*, **86**, 3854 (1964).
21. Ogata Y., Tsuchida M., and Tagagi Y. *J. Am. Chem. Soc.*, **79**, 3397 (1957).
22. Moinet C. and Peltier D. *Bull. Soc. Chim. Fr.*, 4850 (1972).
23. Russell G.A. and Geels E.J. *J.Am. Chem. Soc.*, **87**, 122 (1965).
24. Russell G.A. Geels E.J. Smentowski F.J. Chang K-Y., Reynolds J., and Kaupp G. *J. Am. Chem. Soc.*, **89**, 3821 (1967).
25. Bagotsky V.S., and Yablokova I.J. *Zh. Fiz. Khim.*, **27**, 1663 (1953).
26. Kuta J., and Koryta J. *Polarography 1964*, Proc. Third. Inter. Congress, Southampton, ed. Hills G.J. Interscience, New York 1966 p. 447.
27. Bockris J.O.M., and Oldfield L.F. *Trans. Faraday Soc.*, **51**, 249 (1955).

Short Papers

Chimika Chronika, New Series, 10, 203-204 (1981)

GLYCERYL-ETHER OXIDIZING EXOENZYME FROM T. PYRIFORMIS.

V.M. KAPOULAS, G.N. ATHANASIOU, C.A. DEMOPOULOS.
Department of Biochemistry, University of Ioannina.
Department of Food Chemistry, University of Athens

Exoenzymes, released to their surroundings by protozoa and other unicellular organisms, seem to be of significant importance for the nutrient procurement by these organisms via extracellular digestion of large molecules. The interest of biological research in the study of these exoenzymes was recently renewed for two main reasons: First, phagocytotic organisms, like Tetrahymena, possessing the possibility to ingest particulate material from their surrounding, would not be expected to depend on extracellular digestion for their nutrient procurement. Second, the source of some of the exoenzymes excreted by certain flagellates is the flagellar pocket (1) and not their lysosomes.

Tetrahymena pyriformis was reported to excrete, in 5 hours, 20% of its α-glycosidase, β- glycosidase, β-N-acetylglucosaminidase and amylase intracellular activities and 33% of its intracellular deoxyribonuclease and phosphatase activities (2). Reported here are our findings on the release by Tetrahymena of another exoenzyme, able to degrade glycerylethers.

In preliminary experiments we found that 5% of radioactive glyceryl ether is degraded by the exoenzymes of Tetrahymena pyriformis according to the following technique: Tetrahymena pyriformis, strain W, was grown as previously described (3). The log-phase cells were harvested by centrifugation (3) and resuspended for 2h in an equal volume of Wagner's solution. Then, the cells were centrifuged off (500 g, 10 min) and 0.2 ml of the clear supernatant was tested as previously described (3) except that the substrate concentration was 2γ (plus 10^5 cpm) of tritiated batyl alcohol per ml.

Further study of the exoenzyme was carried out on enriched enzyme preparations isolated according to scheme 1. Assays of these enriched enzyme preparations by the above test procedure yielded 13-17% degradation of the substrate to degradation products identified as α-0-alkyldihydroxyacetone (12.5%) and fatty acid (4.5%).

Optimization of conditions yielded the following results: Optimum time of

CULTURE OF T. PYRIFORMIS (log-phase)
1. Harvesting (500 g, 10 min).
2. Washing with 0.008 phosphate buffer, pH 7.6
3. Centrifugation (500 g, 10 min).

PACKED CELLS
1. Resuspension in 0.5 vol. of Wagner's solution.
2. Two hours
3. Centrifugation (500 g, 10 min).

SUPERNATANT
1. Addition of ammonium sulphate (65% saturation)
2. Centrifugation (7000 g, 20 min, 4°)

PELLET
1. Suspension in 1ml Wagner's solution

ENRICHED ENZYME PREPARATION

Scheme 1: *Isolation of glyceryl ether degrading exoenzyme from T. pyriformis.*

highest concentration of excreted exo-etherase, 2h; optimum range of ammonium-sulphate concentration for precipitating the enzyme, 65-75% of saturation; optimum pH, 7.6-8.2.

These findings, apart from their general biological interest (see above), support our previous evidence that the biodegradation of glycerylether **via** α-0-dihydroxyacetone is an alternative degradative pathway in protozoa (4).

Abstract

Tetrahymena pyriformis excretes an exoenzyme, able to degrade glyceryl-ethers into α-0-alkyldihydroxyacetone and fatty acid. Highest concentration of the enzyme is detected after 2h in inorganic medium. It is precipitated by ammonium sulfate (65-75% of saturation) and its pH optimum is in the range 7.6-8.2.

Περίληψη

Ἐξωένζυμο Ὀξειδώσεως Γλυκερυλαιθέρων ἀπό T. pyriformis.

Τό πρωτόζωο T. pyriformis ἐκκρίνει στό περιβάλλον του ἕνα ἐξωένζυμο, ἱκανό νά ἀποικοδομεῖ τούς γλυκερυλαιθέρες πρός α-0-διϋδροξυακετόνη καί λιπαρά ὀξέα. Μέγιστη συγκέντρωση τοῦ ἐνζύμου βρίσκεται μετά παραμονή 2 ὡρῶν σέ ἀνόργανο μέσο ἀνάπτυξης. Τό ἔνζυμο καταβυθίζεται μέ θειϊκό ἀμμώνιο (65-75% κορεσμοῦ) καί ἔχει μέγιστη δραστικότητα σέ περιοχή pH 7,6-8,2.

References

1. Steiger R.F., Hoof F.V., Bontemps J., Nyssens-Jadin M. & Druetz J.E.: *Acta Tropica* **36**, 335-341 (1979).
2. Rothstein T.L. & Blum J.J.: *The journal of Cell Biology* **57**, 630-641 (1973).
3. Kapoulas V.M., Thompson G.A., Jr. & Hanahan D.J.: *Biochim. Biophys. Acta*, **176**, 237 (1969).
4. Kapoulas V.M.: *Biochem. Biophys. News-Letter*, **3**, 4 (1972).